THE COMMERCIAL VIABILITY OF DIRECT POWDER ROLLED TITANIUM:

A SYSTEMATIC REVIEW AND MARKET ANALYSIS

Centre for Materials Engineering, University of Cape Town

Dissertation submitted for the degree of Master of Science
in Engineering

Student: Megan Steytler

Supervisor: Prof. R.D. Knutsen

14-02-2018

University of Cape Town

The copyright of this thesis vests in the author. No quotation from it or information derived from it is to be published without full acknowledgement of the source. The thesis is to be used for private study or non-commercial research purposes only.

Published by the University of Cape Town (UCT) in terms of the non-exclusive license granted to UCT by the author.

University of Cape Town

Plagiarism Declaration

I know the meaning of plagiarism and declare that all the work in the document, save for that which is properly acknowledged, is my own. This thesis/dissertation has been submitted to the Turnitin module (or equivalent similarity and originality checking software) and I confirm that my supervisor has seen my report and any concerns revealed by such have been resolved with my supervisor

Signature: Signed by candidate Date: 14-02-2018

Abstract

Direct powder rolling (DPR) is thought to be a more cost-effective, more direct route to producing flat product of near final thickness. It is a particularly attractive route for titanium given that the existing wrought method of melting titanium sponge to ingot followed by rolling to slab to plate and finally to thin gauge product is an energy and capital-intensive process. There are several studies that have investigated the operational parameters of DPR, but there has been little assessment of the realization of DPR as a fully operational process producing a commercially viable product. The commercial viability of DPR is a particularly pertinent question for South Africa given the investment, by the Council for Scientific and Industrial Research and the Department of Science and Technology, in the development of an innovative powder manufacturing technology, as well as complementary powder metallurgy methods.

A commercial viability assessment of DPR was structured around three analyses: 1.) whether a supply-side market exists to support a commercial enterprise, 2.) how the performance of DPR product compares to the performance of product produced via the conventional wrought route, and 3.) what range of potential product applications could be suitable for DPR product. A systematic review of published research was conducted by extracting and consolidating performance and process data, and a market analysis was conducted by sourcing price points from powder suppliers and wrought product suppliers.

The performance of DPR product, in terms of elongation and ultimate tensile strength, was found to be comparable to the typical properties of ASTM grade 3 and 4 wrought product, which contain higher oxygen and are the least ductile of the commercially pure titanium grades. Due to the particulate nature of the starting stock and titanium's affinity for oxygen, oxidation was found to be the single greatest problem in powder metallurgy. The upper and lower bounds of the oxygen range were identified, and the consolidation of data showed that an oxygen content of less than 0.2 wt% is not commonly achieved for non-hydride derived product. The possibility of producing a weldable product via DPR was found to be low, due to the unacceptable degree of chlorine content, which is typically greater than 0.02 wt% in low-cost (non-melt) commercially available powders, as well as the fact that weldability has not been reliably demonstrated for powder metallurgy product made from these powders. The existing powder market was also found to be inadequately geared towards supporting a commercial enterprise due to the small size of the market and the lack of availability of low-cost quality powders. The comparison of powder prices to wrought product prices showed that the potential for commercial viability is likely to exist only for thin gauge strip of less than 1mm thickness, as this is where cost savings can be attained through direct route processing.

Based on the DPR product profile identified, the range of potential product applications was found to be greatly limited. The inability to reliably meet the typical properties of the "workhorse", grade 2, excludes the largest proportion of applications for which pure titanium in strip form is used (heat exchangers and tubing). Furthermore, the lack of evidence of adequate weldability further restricts the usage of DPR product to applications where welding is not a critical requirement. For these reasons, it was concluded that DPR is not a commercially viable process.

Acknowledgments

The author would like to acknowledge and thank the following people and entities:

- My Supervisor, Professor Robert Knutsen, for his guidance, expertise and support throughout the past two years.
- The Centre for Materials Engineering at the university of Cape Town for affording me the opportunity to complete my Masters.
- My parents, for their wholehearted support of all my endeavours, as well as the educational opportunities they have afforded me.
- Tom, for your encouragement, patience and continuous support.

Table of Contents

List of Figures and Tables

Figures

Tables

List of Acronyms and Abbreviations

IM	Ingot Metallurgy
PM	Powder Metallurgy
DPR	Direct Powder Rolling
CP	Commercially Pure
CIP	Cold Isostatic Pressing
HRD	Hot Roll Densification
HIP	Hot Isostatic Pressing
NNS	Near Net Shape
HDH	Hydride-Dehydride
Wt%	Weight percent
BE	Blended Elemental
PA	Prealloyed

1 Introduction

1.1 Building a Titanium Industry in South Africa – A National Strategy

Titanium is known for its high strength-to-weight ratio and good chemical and corrosion resistance but it has seen limited use, outside of the aerospace industry, due to high processing and fabrication costs. In light of this, there has been much interest in the use of powder metallurgy (PM) as a viable, cost reduction alternative to conventional ingot metallurgy (IM), which is energy and capital intensive.

South Africa has the fourth largest recoverable titanium ore reserves, and in 2016, mined the largest quantity of the mineral concentrate, ilmenite [1]. However, most of it is exported in its raw, unbeneficiated form [2]. The fact that there is no local, primary titanium metal industry is lost economic opportunity. In addition, when it comes to downstream processing of titanium, the South African manufacturing industry has limited fabrication capacity. There are only some minor operations producing final products [2].

Due to the lack of beneficiation of local titanium resources, the Department of Science and Technology (DST) and the Department of Mineral Resources (DMR) identified the titanium metals industry as a key growth area for South Africa [3]. The Titanium Centre of Competence (TiCoC) was subsequently established to coordinate research and development efforts and ensure close collaboration with industry. The TiCoC's focus is on value addition in both primary and downstream titanium metal processing, as shown in Figure 1 below. The proposed industry plan is reliant on the development and commercialisation of a proprietary and cost-effective titanium powder production technology [4], the objective being to establish a competitive advantage through innovation. The Council for Scientific and Industrial Research (CSIR) has patented a continuous metallothermic reduction process that converts titanium tetrachloride directly to titanium powder in a medium of molten salt. The product is expected to be commercially pure (CP) grade 1 (the purest of the ASTM grades) [5]. A pilot plant has been built to test the technology, and a commercial-scale plant, producing titanium powder at a lower cost than imported feedstock, is envisaged for 2020 - 2023 [6]. Several powder applications have been identified, as seen in Figure 1. The direct powder rolling route (highlighted in orange) has been identified as a potential route for the production of flat product.

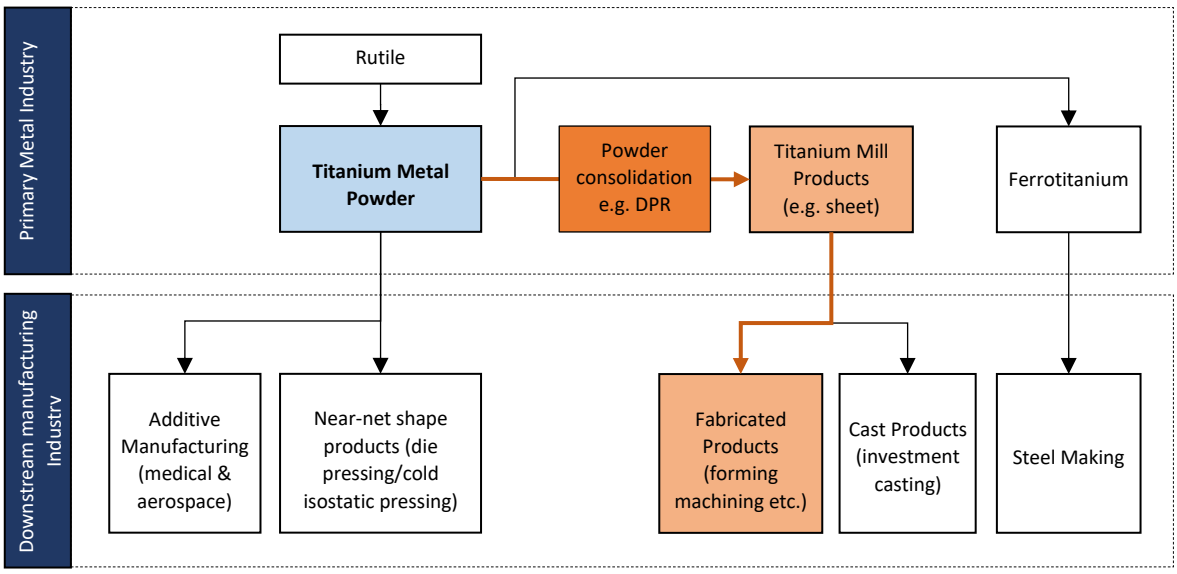

Figure 1: The proposed South African titanium metal industry. Diagram adapted from Du Preez [6].

1.2 Direct Powder Rolling

In its simplest form, direct powder rolling involves the following:

1. The feeding of metal powder, from a hopper, into a rolling mill where it is cold compacted (Figure 2) producing a green strip that possesses a certain degree of porosity.
2. The strip is fed continuously, or placed in batches, into a furnace where it is sintered in a vacuum or an inert atmosphere. Strength and ductility are improved and alloys are chemically homogenized.
3. Subsequent operations include thickness reduction via cold/hot rolling and annealing to close remaining porosity and refine the grain structure.

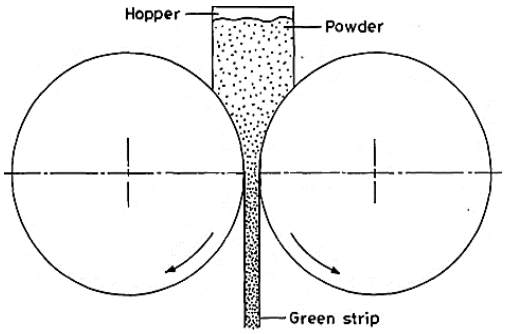

Figure 2: Roll compaction of metal powder (adapted from Dube [7]).

DPR is one of the most direct methods of producing flat product of near final thickness [8]. This is important when considering that the cost of sheet is predominantly due to mill processing, with the reduction of ingot to ~25 mm (1 inch) plate accounting for 47% of the total cost (Figure 3) [9]. Figure 4 compares the conventional ingot metallurgy route to the direct powder rolling route. In the DPR route, the reduced number of rolling and annealing cycles to produce thin gauge product is a cost advantage. Furthermore, the use of powder feedstock derived from sponge or an earlier precursor (e.g. $TiCl_4$ in the CSIR powder process) bypasses the melting to ingot step, which accounts for 15% of plate manufacturing costs.

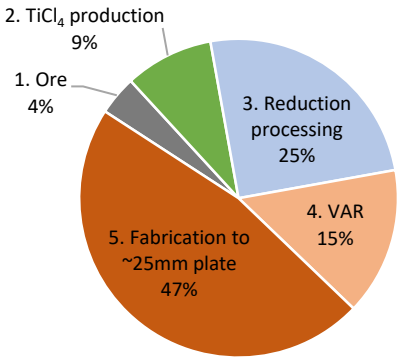

Figure 3: Cost contribution of various titanium production steps [9].

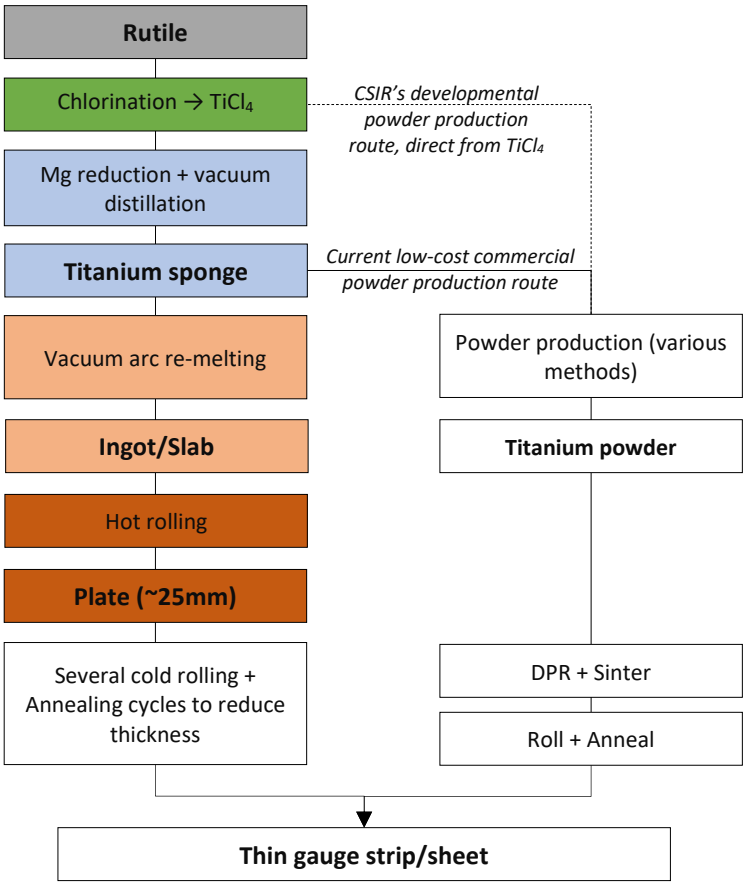

Figure 4: Conventional ingot metallurgy route versus the direct powder rolling route.

In a manufacturing market evaluation conducted by the US Department of Energy in 2007, thin gauge titanium sheet via PM methods was one of two product areas identified as having the greatest price and energy reduction benefits (the report was not made public but key findings were reported by Peter *et al* [10]). Due to the commercial potential of DPR, a number of processing routes are being investigated by the following entities:

1. **The CSIRO in Australia** (another titanium resource rich country also developing a proprietary powder production process called the TiRO process) is pursuing commercialization of a continuous roll compaction process. Their innovation involves the feeding of green strip into a furnace where it is pre-heated rapidly in an argon atmosphere for a few minutes before undergoing hot roll densification (HRD). They claim that commercially pure titanium and its alloys can be manufactured to thin gauge sheet (<1mm) in one or two HRD passes.

2. **The US company ADMA Products Inc.** has patented a roll compaction process that uses two horizontal rollers of different diameters [12]. This asymmetric rolling results in bending deformation and improved densification. The strip is then fed directly into a second rolling mill with rollers of equal diameters rotating at different rates, promoting shear deformation and additional densification. Subsequent cold rolling produces a strip of almost 100% relative density[1]. The final operation is sintering.

3. **Ametek Specialty Metal Products** has extensive experience in producing metal strip via powder roll compaction (50 years of rolling nickel sheet), and has been collaborating with Oak Ridge National Laboratory (ORNL) to develop roll compaction technology for titanium and Ti-6Al-4V. In 2011, efforts to commercialize the product were reported to be ongoing [14].

4. **The CSIR, the University of Cape Town and the University of Kwazulu-Natal.** Parallel to the development of a proprietary and commercially scalable titanium powder production process in South Africa, several local research entities are investigating the technical feasibility of DPR.

DPR product produced by CSIRO, ADMA and Ametek are shown in Figure 5. ADMA is the most commercially advanced entity. Their direct powder rolled product, as well as other PM products, were made available for purchase only very recently (2017), but the size of their operation and success of their commercialisation is unknown. As of 2014, the CSIRO were optimizing their DPR process, and investigating factors that significantly affect the ability to form the sheet into useful parts. [15]. They have been actively "seeking industry engagement" as far back as 2010 to expand the process from pilot plant to commercial operation [16]. There has been little information on progress since. In South Africa, DPR research efforts have not yet progressed beyond lab-scale work. Before investing heavily in continued development, it is an imperative that the commercial viability of the process be assessed.

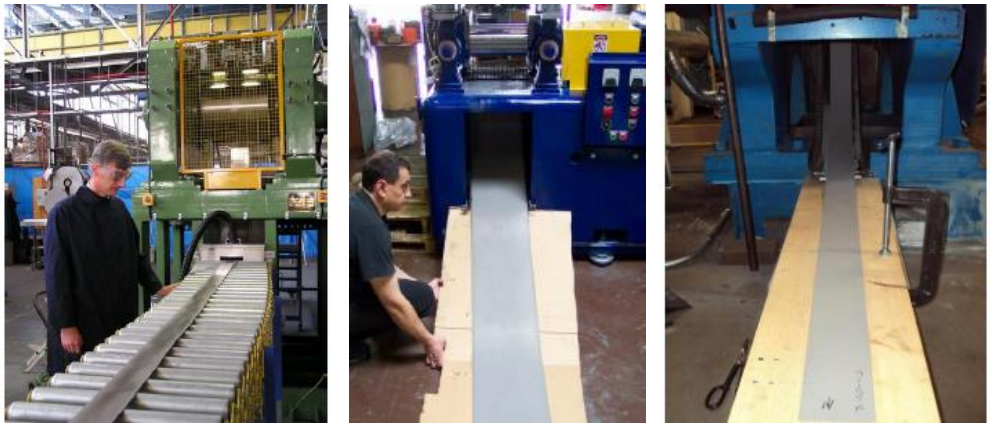

Figure 5: Direct powder rolled titanium produced by CSIRO [11] (left), ADMA [13] (middle) and Ametek [14] (right).

[1] Relative density in powder metallurgy is the ratio of the density of the compact to the density of the metal without porosity.

1.3 Research Problem, Aim and Objectives

Several studies have investigated the operational parameters of DPR, but there has been little assessment of the realization of DPR as a fully operational process producing a commercially viable product. This is particularly pertinent research for South Africa given the investment, by the Council for Scientific and Industrial Research and the Department of Science and Technology, in the development of a Ti powder metallurgy industry.

The aim of this research is to determine whether commercially viable titanium product is producible via the direct powder rolling process.

The objectives of this research are:

1. Using consolidated data from literature, to identify the prospective profile of DPR product, in terms of the typical, upper and lower bounds of performance, as well as the dimensional range of the product.
2. Using consolidated data from literature, to compare the typical performance of DPR product to the typical performance of wrought product.
3. To compare the price of wrought product to cost estimates for DPR product, and hence determine if/where a margin of profit exists.
4. To identify potential product applications, and respective fabricability and performance requirements, for which the DPR product could be suitable.

2 Research Framework

2.1 Commercial Viability

The end-to-end system in which any commercial enterprise exists can be represented as:

Figure 6: SIPOC diagram.

Although conventionally used as an analysis tool in process improvement initiatives, the SIPOC diagram offers a high-level view of the process elements, from end to end, that enable the delivery of a service or product to a customer. The adaption of this framework for the direct powder rolling process is shown in Figure 7. Based on this framework, three key analyses have been identified regarding the viability of a commercial DPR operation. These include: 1.) whether a supply-side market exists to support a commercial enterprise, 2.) whether the process produces product equivalent to that produced via the conventional wrought route (i.e. it must demonstrate technical feasibility), and 3.) whether an end-market exists in which the product generates reasonable demand.

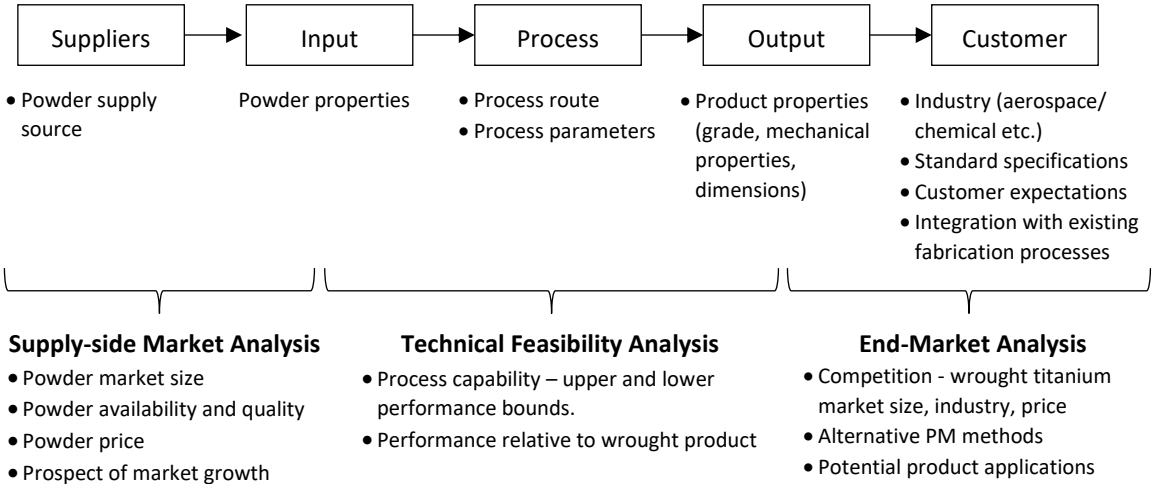

Figure 7: Structured frame - SIPOC diagram adapted for the direct powder rolling process.

A market analysis is one of three stages in the feasibility phase of a technology commercialization model [17], shown in Table 1 below. The second stage is a technical feasibility analysis. In this context, this is the capability of the process/technology using available inputs to manufacture a product with properties comparable to or better than competing product on the market. The third stage in the commercialization model is the economic feasibility of the technology. This involves the development of a financial model which is beyond the scope of this dissertation, but a high-level assessment of costs and pricing will be conducted. The market analysis and technical feasibility analysis will be used to assess the commercial viability of direct powder rolled titanium.

Table 1: Technology commercialization model (the first 3 phases: investigation to development)

	TECHNICAL	MARKET	BUSINESS
1. Concept phase	Technical Analysis	Market needs assessment	Venture assessment
2. Feasibility	Technical feasibility	Market study	Economic feasibility
3. Development	Engineering prototype (in this case pilot plant)	Strategic market plan	Strategic business plan

3 Technical Feasibility

3.1 Green Density and Strip Thickness

The final density attained in a powder metallurgy (PM) part is critical for achieving good static and fatigue properties. Static properties (elongation, yield and ultimate tensile strength) have been shown to increase linearly with increasing relative density [18], hence the final density of the product greatly affects the ability to form the sheet into suitable components [10]. In PM, achieving static properties comparable to wrought product commonly requires hot consolidation techniques, or additional post processing operations that add to the overall cost. Sintered DPR sheet usually contains some porosity and further operations, i.e. hot/cold rolling and annealing cycles, are required to improve densification. The density of the un-sintered strip (termed the green density) is a critical intermediate property as it determines the degree of downstream processing required to attain full density. Likewise, the range of strip thickness producible is a key consideration for the range of potential product applications.

For a given roller diameter, thicker strip is produced by increasing throughput. This is done by simultaneously increasing roll speed, feeding rate and the size of the roll gap. However, to produce any significant changes in strip thickness, a larger roll diameter is required. Increasing the roll diameter increases the arc of contact between powder and roller surface, thereby increasing the size of the compaction area as well as the time during which the powder mass is subjected to pressure [19]. To maintain a certain densification ratio for a larger roll diameter, a larger volume of powder needs to be gripped by the roller's surface area and fed into a wider roll gap. A thickness-to-diameter proportionality is cited as a general rule, with a variety of ranges seen in literature. A 0.6-2% thickness-to-diameter ratio is reported necessary for rolling [20]. The **maximum** thickness of powder-rolled strip is said to vary from 0.33-1% of the roll diameter, depending on the material [7].

In terms of green density, there is little information on the upper limits that can be achieved. Katrus [21] found that for various metals rolled to between 0.1 and 3mm thickness, the upper limit of relative green density at which the strip retains its shape without disintegrating is between 85% and 90%. Araci *et al*. [22] reported that 75–80% relative green density for 1.5mm thick titanium strip could be achieved under optimized rolling conditions. For nickel, cobalt and iron-nickel alloy powders, 72-82% is typically achieved [23], but with no specifics on thickness. For copper strip, Tundermann *et al*. [24] noted that the maximum relative green density possible, before strip splitting and edge cracks were observed, was >90.8% (for a strip thickness of <1mm). These strip defects are shown in Figure 8, the cause of which was attributed to overloading, or more specifically, internal strains in the green strip.

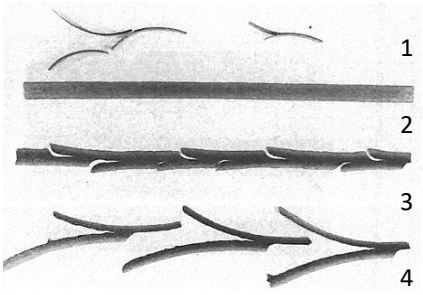

Strips rolled from electrolytic copper powder:

1. Edge view showing lamellae. Strip thickness: 1.295mm
2. Surface view. 0.762mm
3. Surface view. 0.597mm
4. Surface view. 0.521mm

Figure 8: Strip defects observed in the rolling of copper powder [24].

In the rolling of titanium powder, Hong *et al*. [25] observed edge cracks at a roll gap of 0.1mm and density of >90%. In the rolling of iron powder, Musikhin [26] observed over-pressing and axial splitting of strip rolled to 87% relative density on the 0mm roll setting (possible because of roller push-back). Dube [7] points out that the minimum roll gap setting is not "well defined" and that it is generally taken as the point at which the green strip starts exhibiting defects such as cracking. Although high densities of over 85% have proved possible for metal powders, the above studies rolled powder to within a limited range of very thin strip thicknesses.

The literature on DPR does not specifically define the boundaries of the feasible thickness range for titanium green strip. Hence, an attempt has been made to determine this by consolidating research data from individual experiments. This is presented in Figure 9. The data collected was extracted from figures, graphs and reported results from the earliest records of DPR titanium (1962), up until the most recent efforts in 2016 (17 sources in total). Data for porous strip was excluded as researchers would not have been aiming for high densities. The data is from vertical, gravity fed operations only (i.e. no horizontal rolling or screw feeding). To the best of the author's knowledge, this is the first comparison of all available titanium data from literature.

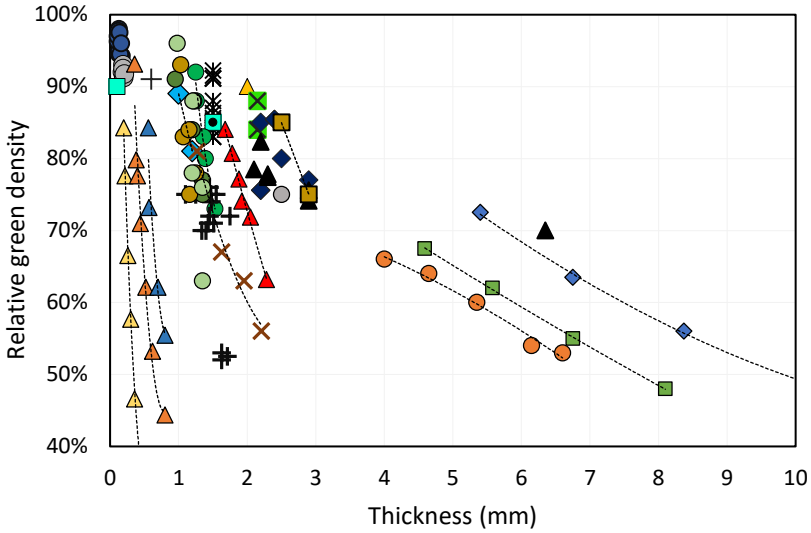

Figure 9: Green density and thickness for DPR titanium and Ti-6Al-4V strip. Data from 17 sources (10, 22, 25 and 27-39).

For any given study in Figure 9, the density is seen to increase as the strips are rolled thinner. The addition of roll dimensions in Figure 10 below shows that for the rolling of thicker strip, larger roll diameters are used to accommodate the increased volume flow rate required for a larger roll gap. However, the most notable result is that increasing the strip thickness (by increasing roll diameter) appears to be at the expense of the maximum attainable density. Assuming that researchers adjusted rolling parameters within reasonable operating limits with the objective being to achieve high green densities, then there appears to be a limit or upper boundary, with a distinct slope.

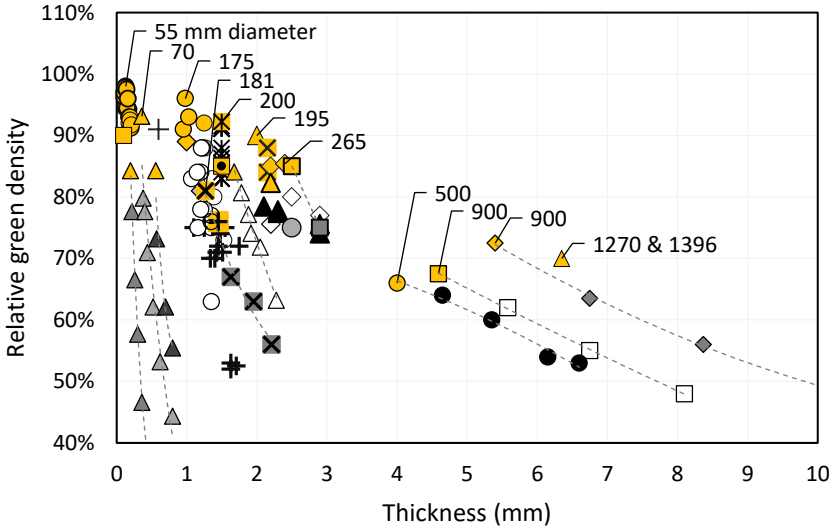

Figure 10: Green density and thickness for titanium strip produced using various roll diameters. Highest densities for discrete experiments are highlighted in colour.

The thickness-to-diameter ratios (S/D) were calculated to confirm that diameters in Figure 10 were selected proportionally to the strip thickness i.e. if too small a diameter is chosen for a selected thickness range, the densification ratio will not be sufficient to compact to full density. The highest density in each primary source was selected for this calculation. Figure 11 shows that the ratios are within the range cited in literature - 0.33-1% [7].

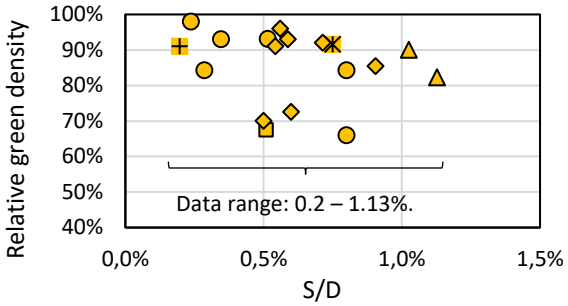

Figure 11: Relative green density of DPR strip versus thickness-to-roll diameter ratios (S/D).

Few researchers have compared the influence of different roll diameters, and of those that have, they have not observed a similar thickness-dependent density limit, as seen in the consolidated data from literature. However, the parameter ranges tested in these studies were narrow, hence the limit would not have been observable. For example, the maximum density limit in Figure 10 is observable over a wide range of thickness (~0.5 - 8.5mm) for a wide range of roll diameters (55-1270mm), whereas Katashinskii [40] rolled iron and nickel powder to only 0.65-1.5mm strip thickness on diameter rolls that were not greatly different in size (89mm and 174mm). Similarly, Lozhechnikov *et al*. [41] rolled iron strip of only 0.54 to 1.36mm thickness to a target relative density of 70% (which is well within the range of DPR compactibility capabilities and thus would not have tested the upper limit) and once again using only a narrow range of roll diameters (60 - 160mm). Neither of these studies observed a thickness dependent density limit. Hence, to the best of the authors knowledge, the thickness dependent density limit has not been observed directly in the experimental investigations of different rolling scales, and no review has encapsulated as wide a range of strip thicknesses in a single investigation. Rowe *et al*. [42] and Reynolds *et al*. [43] claim that there have been few comparisons of rolling operations at different scales. Due to cost constraints, experimental work is often limited to single, small-scale pilot mills, with a focus on optimizing parameters for a set roll diameter. Large designs of experiments involve large investments, which are magnified during process scale-up [42].

3.1.1 DPR Modelling – Early Reference Point Method

The following section looks to determine whether theoretical modelling of powder roll compaction accounts for the thickness-dependent density limit seen in the consolidated data.

Early research conducted by the Ukrainian Academy of Sciences in the 1960's [39] used a reference point method to determine the density of strip for a given thickness using the following equation:

$$\frac{H}{h_s} = 1 + \frac{D}{h_s}(1 - cos\ \alpha') \qquad [1]$$

H is the distance between the rolls at the angle α' shown in Figure 12 and h_s is the strip thickness. α' is the angle at which powder is gripped by the rolls (also known as the nip angle). The compactibility coefficient (H/hs) is proportional to the relative green density for a given bulk density of powder (defined as mass/volume). For a rolling mill of set diameter (D), a family of curves corresponding to different values of α' can be constructed for strip density versus thickness, as seen in Figure 13.

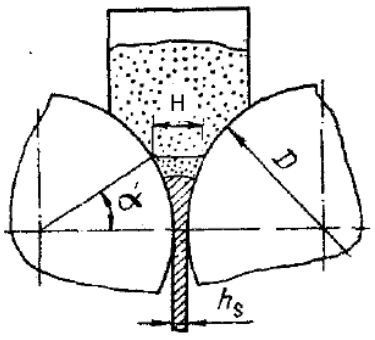

Figure 12: Compaction parameters H, hs, diameter (D) and angle α' [39].

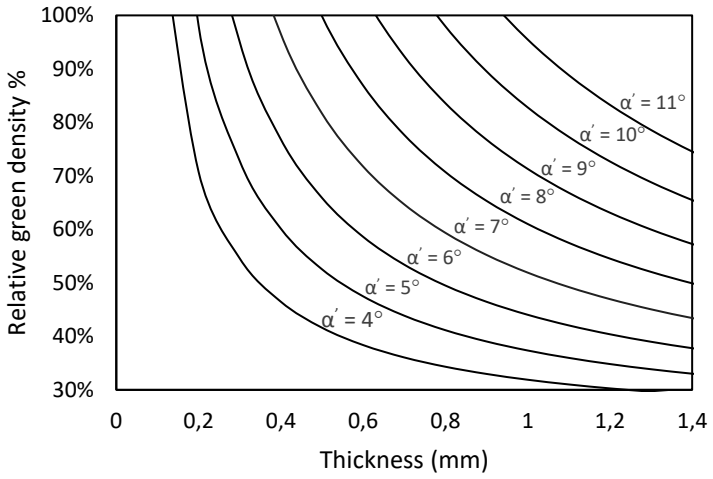

Figure 13: Relative green density and strip thickness for 180 mm diameter rolls and various α' values.

Using the family of curves in figure [13] and a single density-thickness reference point, that has been determined experimentally, it is possible to determine the density of any other thickness for the same set of rolling conditions. This method is valid only when strip thickness is altered by changing the roll gap or feed hopper width while keeping all other parameters constant.

A second method was subsequently proposed for which the relationship between the strip thickness h_s and the strip density y_s was defined as:

$$y_s = 0.5\frac{C^2}{h_s} \qquad [2]$$

Where C is an empirical coefficient that represents the combined effect of the complex interdependencies of all geometrical and physicomechanical parameters. Once again, a single reference point allows for the determination of C, and subsequently the density for any other strip thickness. Vinogradov [39] validated the reference point method by gathering data from literature for various metal powders and plotting density curves (Figure 14).

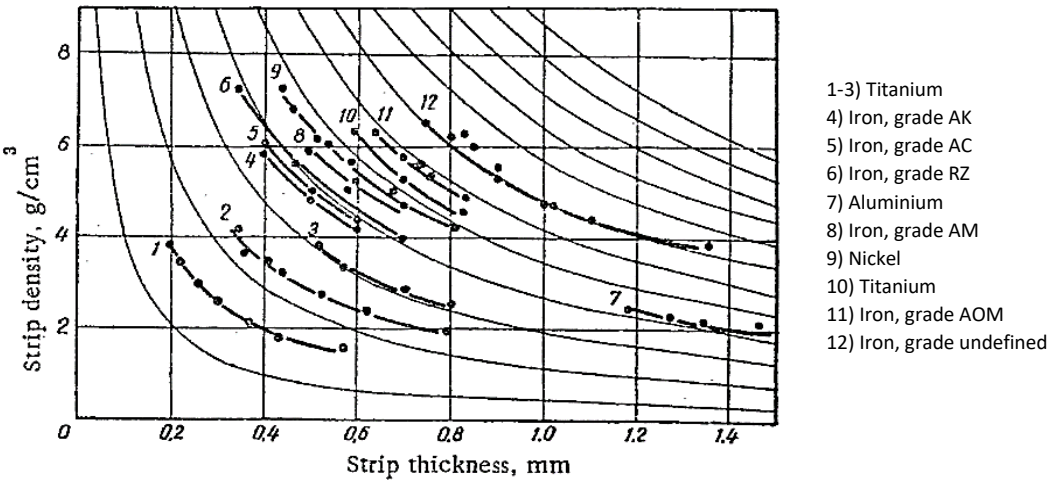

Figure 14: Density curves for metal powders rolled to different strip widths using different roll diameters and rolling speeds [39].

Vinogradov found that uniaxial hyperbolic curves conformed well to the data, with most experimental points deviating by less than 5%. However, the limitation of Vinogradov's validation was the narrow thickness range - between only 0.2 and 1.4 mm, in which almost all powders attained high relative densities of over 90%. Whether high densities could be rolled for thicker strip was not established, and the hyperbolic density-thickness relationship was not validated beyond 1.4mm.

The reference point method was applied to selected studies from the data consolidated from literature, specifically those that changed only the roll gap while holding all other parameters constant. Figure 15 shows that the method conforms well for thin strips (as Vinogradov found) but that for thicker strip there is evidence of deviation from the hyperbolic curves.

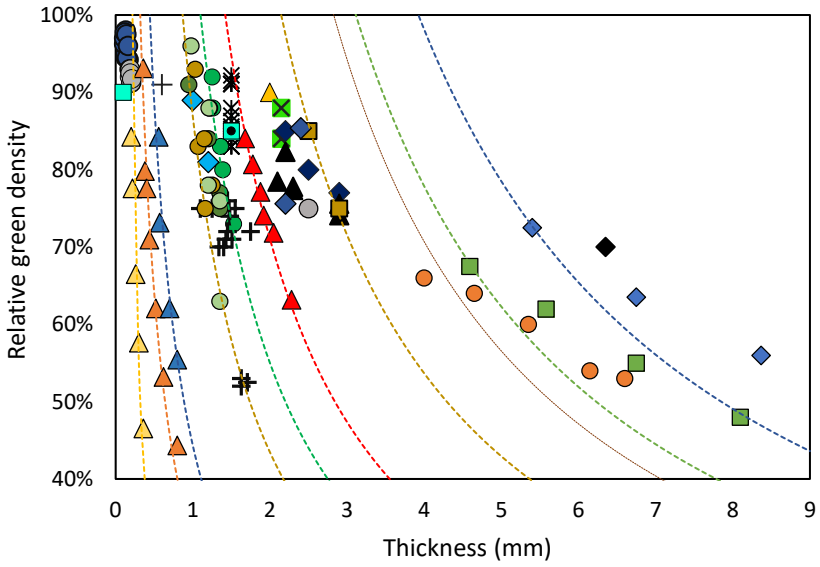

Figure 15: Compaction curves calculated via the reference point method.

3.1.2 Johanson's Model

Johanson's model for powder roll compaction, developed in parallel to the Ukrainian research, is a one-dimensional analytical model that predicts the roll force, roll torque, roll gap and feed pressure required to achieve a certain maximum pressure [44]. As one of the earliest complex models, it provided a valuable understanding of the explicit relationships between many of the rolling parameters. Since most of the model inputs are easily determined (roller dimensions, powder properties and surface conditions), Johanson's model is still used today. The assumptions made by Johanson include the following [45]:

- The particulate material being rolled is isotropic, frictional and cohesive
- The powder is subject to continuous shear deformation
- The rollers are rigid and do not deform during rolling
- There is continuous plane-strain deformation

Johanson identified two regions: the feed region, where slipping occurs between the roll surface and the powder; and the nip region, where the powder is gripped by the rolls. The boundary line demarcating these two regions is defined by the nip angle α, as shown in Figure 16.

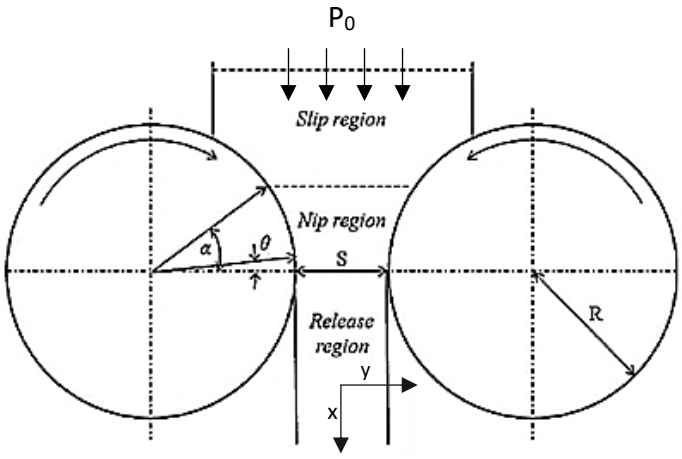

Figure 16: The slip and nip region and the nip angle α.

The slip region begins where the powder initially makes contact with the roll surface, at an angle known as the entry angle. Some particle rearrangement occurs in the slip region, but the pressure exerted on the powder is small, the dominant stress being the feed pressure P_0, and there is only a small degree of densification [46]. In the slip region, Johanson assumed steady state powder particle flow and used the Jenike and Shield effective yield criterion to determine the effective internal angle of friction δ, which dictates the shear and normal stress at the roll surface in this region. Then, for a given roll diameter (D) and roll gap (S), the normal stress gradient on the roll surface in the slip region is expressed as:

$$\left(\frac{d\sigma}{dx}\right)_{slip} = \frac{4\sigma\left(\frac{\pi}{2} - \theta - v\right)tan\delta}{\frac{D}{2}\left[1 + \frac{S}{D} - cos\theta\right]\left[\cot(A-\mu) - \cot(A+\mu)\right]} \quad [3]$$

Where:

$$\mu = \frac{\frac{\pi}{4} - \frac{\delta}{2}}{2} \quad [4]$$

$$\mathrm{A} = \frac{\theta + v + \pi/2}{2} \quad [5]$$

$$v = \frac{\pi - \arcsin\left(\frac{sin\Phi}{sin\delta}\right)}{2} \quad [6]$$

θ is the angular position on the roll, with θ = 0 at the minimum roll gap S and θ = α at the transition between the slip and nip region. The effective angle of wall friction, Φ, and the effective angle of internal friction, δ, are attained through shear tests**.**

For the non-slip region, the powder is trapped between the rolls and assumed to be compressed into a strip with a thickness equal to the roll gap. The pressure gradient in this region is given by:

$$\left(\frac{d\sigma}{dx}\right)_{no\ slip} = \frac{K\sigma_\theta\left(2cos\theta - 1 - \frac{S}{D}\right)tan\theta}{\frac{D}{2}\left(1 + \frac{S}{D} - cos\theta\right)cos\theta} \quad [7]$$

Where:

- K is the powder specific compressibility factor attained from the slope of a density-pressure logarithmic plot, derived from uniaxial compression tests [47] .
- σ_θ is the stress at the nip angle

Johanson proposed that the pressure gradients in the slip and no slip (nip) region are equal at the nip angle α, as shown in Figure 17.

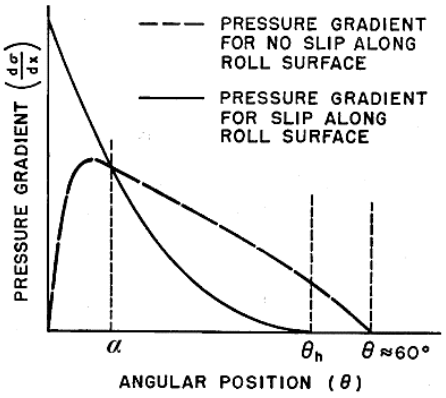

Figure 17: The nip angle at the intersection of the slip and nip pressure gradients [47].

The nip angle α can therefore be determined by equating the two pressure gradients:

$$(\frac{d\sigma}{dx})_{slip} = (\frac{d\sigma}{dx})_{no\ slip} \quad [8]$$

Since θ = α at the transition point, the nip and slip pressure gradients convert to:

$$\frac{4\left(\frac{\pi}{2} - \alpha - v\right) tan\delta}{[\cot(A-\mu) - \cot(A+\mu)]} = \frac{K\left(2cos\alpha - 1 - \frac{S}{D}\right) tan\alpha}{cos\alpha} \quad [9]$$

Once α is determined, the maximum or peak horizontal pressure that occurs at the smallest gap between the rolls i.e. where θ = 0, can be calculated. In reality, the maximum pressure occurs slightly before the minimum separation of the rolls [48]. The density of the rolled strip is dependent on the maximum pressure. Using a density-pressure plot (determined experimentally from uniaxial compression tests) and the calculated peak pressure, the corresponding density is predicted.

3.1.3 Assumptions and limitations of the Johanson model

Influence of roll diameter and roll gap

According to Johanson's model, for a given roll gap, a larger diameter results in an increase in the maximum pressure because of an increase in volumetric throughput due to a larger arc of grip, as shown in Figure 18.

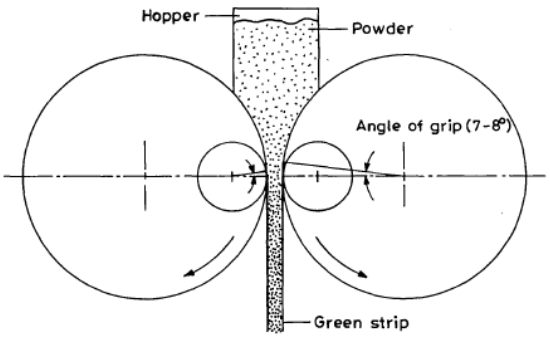

Figure 18: Small and large roll diameter [7].

In the Johanson model, the effect of a larger roll diameter (D) on the nip angle, a critical compaction parameter, is shown in Figure 19.

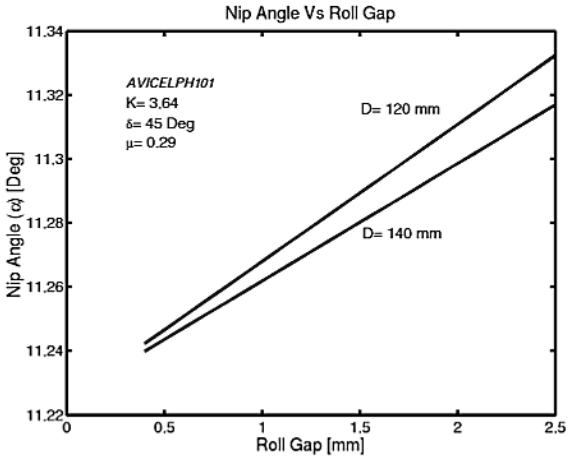

Figure 19: Nip angle versus roll gap for two different roll diameters (powder is a pharmaceutical excipient) [45].

As can be seen by the small increments on the y-axis, both the roll gap and diameter exact a relatively small change in nip angle (only a few tenths of a degree). Furthermore, when the roll gap-to-diameter ratio (S/D) is less than 1, the model predicts that the nip angle depends only on the material properties i.e. the compressibility constant (K), the effective angle of friction (δ), and wall friction (μ) [47]. In the validation of the model, Bindhumadhavan *et al*. [49] observed some deviation from the model prediction, as seen in Figure 20. Nevertheless, Bindhumadhavan *et al*. concluded that the calculated nip angle in the model is a reasonable estimate as the predicted peak pressure was still in agreement with the measured value.

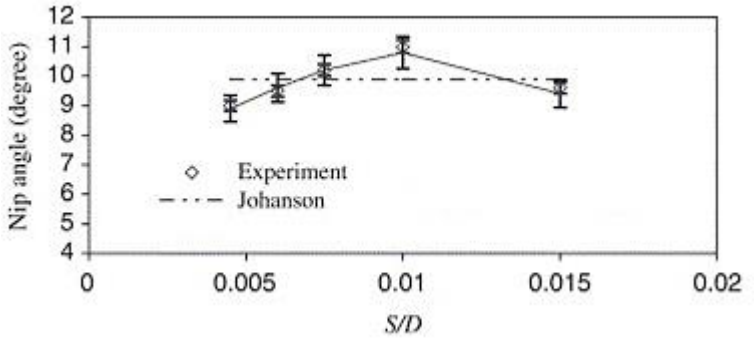

Figure 20: Comparison of predicted and experimental nip angles [49].

Feed pressure

Zhang [35] showed that Johanson model predictions and experimentally determined relative densities compared well for larger roll gaps in the selected range, but diverged significantly for smaller roll gaps where the rate of increase in maximum pressure increased steeply (Figure 21). Where Johanson's model predicted almost 100% relative density, the measured result was only 85%. This inconsistency was seen for both titanium and stainless-steel powder.

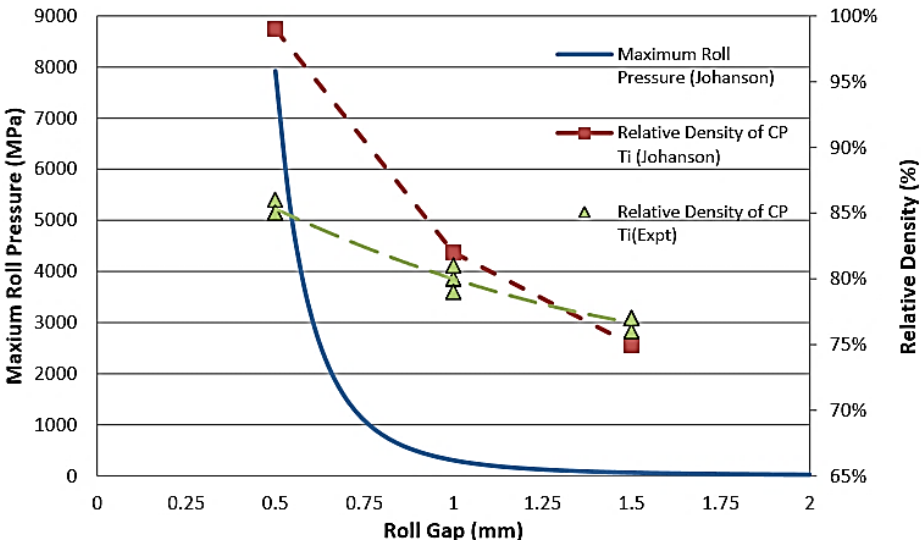

Figure 21: Predicted and experimentally determined relative density versus roll gap [35].

The difference between the predicted and measured pressure was hypothesized to be a result of roll displacement due to the higher rolling pressure at smaller gaps, as well as the use of estimated feed pressures instead of experimentally determined pressures, which are difficult to measure due to the need for a pressure sensor. This is problematic given that the Johanson model has been criticized for being sensitive to changes in feed stress, as the maximum stress in the roll gap is directly proportional to the stress at the feed point [50]. A larger feed stress increases pre-densification, and a higher initial density in the feed zone ultimately results in a higher final density [51] [52]. However, Rowe *et al*. [42] caution that increased powder densification in the feed zone could result in a greater probability of jamming or overloading. The Johanson model has been criticized for not satisfactorily accounting for effects in the feeding zone, e.g. the degree of initial material densification or how efficiently the material is passing through the rolls [42]. Modelling this is difficult because the powder undergoes significant evolution in properties as it moves from the feed region to the nip region [51].

Roll speed

In the rolling of a pharmaceutical excipient, Bindhumadhavan *et al*. [49] found that the faster the roll speed, the greater the inaccuracy of the predicted maximum pressure in the Johanson model (Figure 22). The reduction in peak pressure was attributed to the fact that that the nip pressure decreases with increasing roll speed. Secondly, increased air entrapment was identified as a possibility (air is ejected back through the powder mass, fluidising the feed and reducing the feed pressure and volumetric throughput of the powder [53]. Bindhumadhavan *et al*. [49] found that the predicted pressure discrepancy was more severe at a smaller roll gap particularly in combination with a greater rolling speed (seen in Figure 22). In addition to powder fluidisation, increasing the roll speed has been found to reduce the nip angle, which would decrease the pressure due to less powder being pulled into the gap. Evidence of this was observed by Yu [44], who determined the nip angle directly from a measured pressure profile and found that for increasing roll speed, the nip angle decreased, particularly for cohesive powder with poor flowability. Mansa [54] made similar observations, concluding that the decrease in nip angle, with increasing roll speed, was less severe for powders exhibiting better flowability.

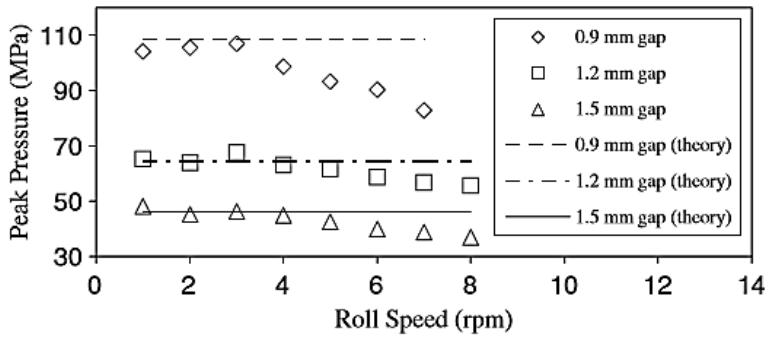

Figure 22: The effect of roll speed on the peak pressure at different roll gaps [49].

Use of uniaxial compression data

Uniaxial compression data, gathered experimentally, is used to predict the relative density for a given, predicted peak pressure. However, uniaxial compression is not identical to the compaction mechanism that occurs during rolling. Roll compaction comprises a greater element of shear stress, which enhances consolidation, and a greater uniaxial pressure is therefore required to achieve the same level of densification seen in roll compaction with an equivalent normal pressure element [55][56]. In the rolling of various metal powders to densities of between 60% and 90%, Mal'tsev [37] found that the measured maximum pressure for roll compaction was 20-30% less than the uniaxial compaction pressure required to produce compacts of the same density. This pressure difference was found to increase with increasing strip density. Mal'tsev attributed the pressure difference to better particle stacking in roll compaction due to relative particle displacement in the zone preceding intense densification.

Non-uniform pressure distribution across the roll width

In the Johanson model, the peak pressure is assumed to be a uniform, average response across the width of the strip [55]. In actuality, the peak pressure is a distribution, with the maximum pressure occurring at the centre of the strip width. This is due to the existence of friction between the edges of the strip and the side cheek plates (used to prevent leakage). The Johanson model does not account for this pressure distribution. Patel *et al* [57] claim that the measured peak pressure can be 40% greater than the mean pressure across the rolls.

Effect of the release region – actual thickness versus roll gap

In the Johanson model it is assumed that the strip thickness equals the roll gap. In reality, the strip thickness is slightly larger than the roll gap for two reasons. Firstly, under load, the roll gap changes because of clearance in the roll shaft bearings and frame members [52]. Secondly, once the strip clears the roll and the pressure is released, the strip expands due to elastic recovery as well as the expansion of compressed air trapped in the pores of the strip [52] [24]. The Young's modulus and Poisson's ratio affect the level of expansion, although it is cautioned that these properties change depending on the degree of powder densification [51]. The influence of elastic recovery is diminished with increasing density because the proportion of plastic deformation in the strip is greater. At higher pressures, the elastic compression of the mill rolls has more influence on the discrepancy between the initial unloaded roll gap and the final thickness of the green strip [58].

Material properties

DPR process parameters have a strong dependence on the properties of the powder [59]. Powder properties have an especially dominant influence on the nip angle when the roll gap-to-diameter is much less than 1, and the rolls are smooth [47]. The nip angle is influenced by the compressibility, flowability and frictional properties of the powder. Powders with poor compressibility lead to a decrease in the nip angle, and the opposite is true for powders exhibiting good compressibility [46]. Increased powder flowability improves the efficiency of the powder feeding system, which increases the pressure in the nip region [46]. In terms of frictional properties,

increases in the friction and wall coefficient have been found to result in an increase in the nip angle and maximum pressure when other parameters are kept constant [46][48].

Given the wide range of powder properties, and their dominant influence, the Johanson model is limited in its ability to accurately account for all these conditions. For example, the model has shown good agreement between measured and predicted force values for granular materials that have a high powder-to-wall coefficient of friction, and average or low compressibility (i.e. higher values of the compressibility constant, K). However, discrepancies (sometimes over 50%) have arisen when very compressible powders (low values of K) are subjected to high pressures [60] (but Roman *et al*. [60] did not quantitatively define "high" and "low"). Yu *et al*. [46] have stressed the importance of accurate measurement of frictional properties and powder compressibility because of the critical dependence of the nip angle on these parameters. The problem is that powder properties are not measured under relevant rolling conditions [51]. The frictional properties, measured initially, are likely to change, since the volume and density of the material mass is changing between the rolls [56][51]. Yu *et al*. [46] conclude that it is still unclear how the two dominating compression parameters (compaction pressure and the nip angle) depend upon the properties of the feed powder.

Given the critical influence of material properties on the roll compaction process, it is important to note that much of the roll compaction research has arisen due to an interest in dry granulation of pharmaceutical excipients. In fact, the Johanson model was originally applied to non-metallic particulates [45]. These powders are difficult to consolidate directly into tablets due to poor flowability and segregation (regions of coarse and fine powder or chemical inhomogeneity) [57]. Hence, the purpose of roll compacting pharmaceutical excipients is to increase bulk density, and improve flowability and uniformity of blended formulations [46]. Dry granulation is therefore an intermediate process, the objective being to merely increase the size of the granules in preparation for final compaction into tablets. Given that the target relative density of granulated pharmaceutical material is said to be generally less than 75% [56], application of the Johanson model may not be entirely suitable for metal powders roll compacted to densities over 75%. A review of pharmaceutical literature (Table 2) gives an indication of the narrow range of parameters for the rolling of pharmaceutical excipients. For example, roll diameters range from 100 to 250mm (compared to 55 to 1270 mm for titanium powder), roll gaps from 0.4 to 4mm (compared to 0.16 to 8mm thick titanium strip) and densities from 50 to 80% (whereas titanium green densities are from 50 up to 98%).

Table 2: Rolling parameters and properties of pharmaceutical excipients

Source	Diameter	Material	Gap (mm)	Rel. Dens.
[54]	200 mm	5 different formulations	0.4-1.4	Undefined (U)
[61]	130 mm	Solids hydrargilitte (SH100), salt, and lactose	0.9-1.4	U
[62]	200 mm	Quartz and calcite	U	U
[63]	250 mm	Microcrystalline cellulose	3	U
[64]	120 mm	Microcrystalline cellulose	1.75-2.5	~0.5-0.65
[55]	120 mm Screw feed	15% paracetamol, 55.3% mannitol, 23.7% microcrystalline cellulose	1.43-3.54	0.65-0.75
[43]	120 mm	Immediate release development formulation	1.6-2.4	0.74 – 0.78
[42]	120 mm	Various blends using microcrystalline cellulose PH102 and croscarmellose sodium, anhydrous lactose, colloidal silicon dioxide, magnesium stearate	2-3.3	U
[45]	130 mm Screw feed	Monohydrate lactose	1-1.5	U
[59]	100 mm Screw feed	Microcrystalline cellulose	2	U
[57]	200 mm	Microcrystalline cellulose	0.9-1.8	U
[56]	250 mm	AMG 009	1.5-3.5	U
[46]	200 mm	Microcrystalline cellulose (MCC) and di-calcium phosphate dihydrate (DCPD).	1	U
[65]	U	microcrystalline cellulose and 0.75% magnesium stearate	2-4	0.5-0.8
[66]	120 mm	Several blends	1.7-2.1	U

Assumption of mass continuity

In FEM simulations conducted by Muliadi *et al*. [67] and Michrafy *et al*. [59], the material is seen to remain in a state of slip in the no-slip region, whereas the Johanson model assumes a complete transition across the theoretical line drawn at the nip angle (Figure 23) and therefore does not account for a velocity gradient. The powder in contact with the roll surface rotates at the same speed as the roller, but powder closer to the centreline of the gap, Y=0, moves at a slower speed. Consequently, not all the powder in the slip region is conveyed in its entirety to the roll gap [57]. Cunningham [48] also demonstrated significant variation in stress, strain and velocity in the span-wise direction. Johanson's mass continuity simplification results in an over-prediction of the amount of powder that is delivered to the nip region, and therefore an over-prediction of the peak pressure and relative density [67].

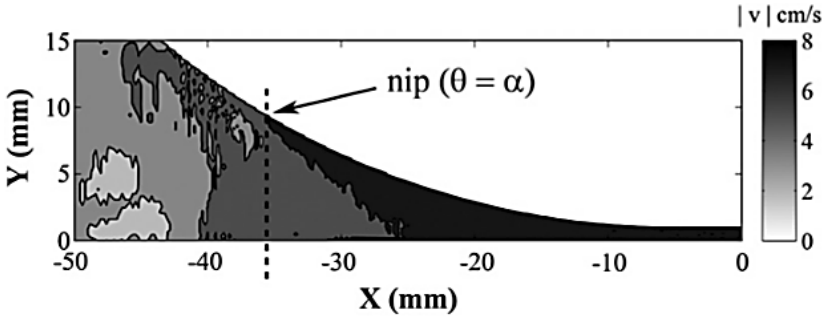

Figure 23: FEM material velocity field for rolling speed of 8 cm/s. Dashed line indicates where the slip region becomes the nip region in the Johanson model [67].

3.1.4 2-D and 3-D models

The review of DPR modelling has focused mainly on the Johanson model due to its widespread use and ease of application, as it is a computationally economical model [67]. Subsequent advancements in modelling have included more complex 2-D and 3-D FEM models, where, for example, the powder is seen to behave as a single phase porous medium [59]. The main advantages of FEM models include fewer modelling assumptions and the ability to account for more complex roll geometries and material properties [67]. However, the application of these models is not suitable for real-time process control because of long computational times. There are also validation problems and limitations i.e. parameters that are difficult to measure directly (tangential force along the arc of contact between the powder and roll [59], the operating roll surface pressure which requires special instrumentation [49], the need to revert to simplifications (using a uniform feed load to approximate the feed system for a 2-D FEM model [59]), not being able to account for the effect of air pressure in the compacting powder [59], and the need for accurate measurement of material properties that change gradually depending on the density of the material [60] [59]). Roman *et al*. [60] claim that the greatest challenge in implementing FEM modelling is the need for adequate input data. As with the Johanson model, FEM models require the inlet pressure and initial material properties such as bulk density [67]. Another limitation pertinent to modelling in general is the need for large experimental data sets. Rowe *et al*. [42] claim that rigorous testing of both observed experimental trends and proposed models has been conducted under limited conditions and that in many studies, different results have been obtained when tested outside the original experimental conditions.

The difficulty in modelling the direct powder rolling process has been noted by several researchers. Yu *et al*. [46] attribute the process's complexity to the large variety of controlling factors and material properties. Cantin *et al*. [53] and Reynolds [43] ascribe modelling challenges to the complex behaviour of particulate materials in the feeding and compaction zones. In these zones, the powder becomes distorted in "an almost unpredictable way" while passing between the rolls [49]. Yu *et al*. [46] identify the need for a better understanding of how the properties of the particulate material influence the dominating compression parameters (compaction pressure and nip angle). The mechanism of roll compaction is still not completely understood [46], [49] and [53].

3.1.5 In Summary

The review of the Johanson model has identified several reasons as to why the model does not consistently describe the direct powder rolling process accurately. In summary, it is a 1-dimensional model that is limited by the requirement for several assumptions. Under or over-predictions of density in the model may be due to the following aspects not accounted for in the model:

- Non-uniform feed pressure.
- Non-uniform velocity gradient for the powder moving from feed to nip region.
- The dynamic properties of the powder as it moves through various stress states between the rolls.
- The additional densification from shear stresses which are neglected due to the use of the uniaxial compression data.
- The influence of roll speed on nip angle and powder fluidisation.
- Non-uniform pressure distribution across the strip width.
- Compression and push-back of the rolls.
- Elastic unloading of compact.

The above limitations are applicable to the rolling of powders in general. However, this review has highlighted that a significant limitation in the modelling of metal powders using the Johanson model is that the original application was for the rolling of non-ductile pharmaceutical excipients, to a target density of 75% or less, whereas metal powders are generally rolled to densities greater than 75%. The Johanson model has not demonstrated acceptable performance predictability for this density range.

It is evident that the powder roll compaction process is still not entirely understood. While there has been increased interest in the use of more complex 2-D and 3-D modelling, these more complex models are limited by the following challenges, which are characteristic of DPR modelling in general [51]:

- The dynamic behaviour of the powder i.e. frictional conditions that are process-time dependent and that evolve depending on the stress state during rolling.
- Process sensitivity to input parameters that are difficult to measure under process relevant conditions.
- The difficulty in experimentally measuring the actual process to validate the models.

3.2 Rolling Mill Operating Limits

The above review of the Johanson model has identified several possible reasons for disagreement between predicted and actual maximum pressure (both under and over predictions). Most of the discrepancies are due to assumptions and simplifications, and none single-handedly explain the sloping density limit seen in the consolidated DPR data (Figure 24 below). The Johanson model is ultimately a theoretical model for calculating the roll force, torque, diameter, gap, and feed pressure necessary to achieve a certain maximum pressure. The question is whether the calculated operating parameters required to attain high density are feasible or within the specification ranges of rolling mills available today. According to Johanson's model, for a given roll gap, and a larger diameter, the maximum pressure increases because of an increase in volumetric throughput due to a larger arc of grip (as seen by the red line in Figure 25). Likewise, for a larger roll gap, the model predicts that it is possible to achieve the **same** maximum pressure by using a larger roll diameter (green line in Figure 24). The density of the rolled strip is dependent on the maximum pressure, regardless of the strip thickness [68]. It is evident that the pressure curve tends asymptotically for both the small and large diameters, and consequently full density would, theoretically, be possible for both.

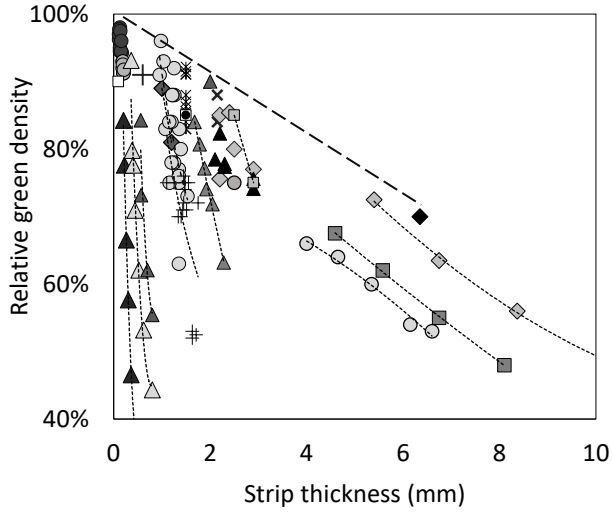

Figure 24: Green density and thickness for DPR titanium and Ti-6Al-4V strip.

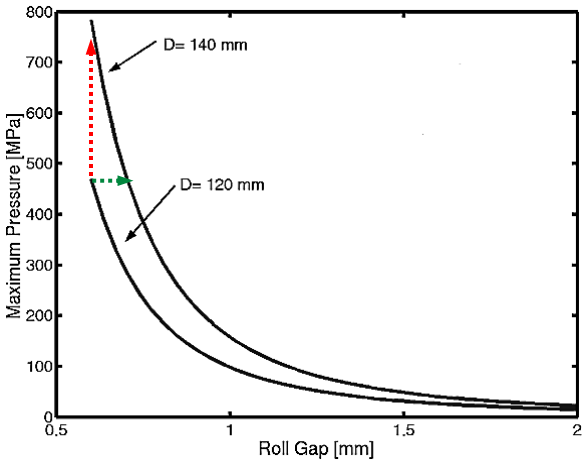

Figure 25: Maximum pressure versus roll gap for two different roller diameters. Johanson model [45].

However, in attaining such high densities, the rolling pressures become large, and elastic compression and push-back of the rolls is known to create a discrepancy between the initial unloaded roll gap and the final thickness of the green strip [58]. Larger discrepancies have been observed for smaller roll gaps [35].

3.2.1 Influence of diameter on roll separation force

This section investigates design limitations of rolling mills, particularly the ability to cope with the forces involved in the rolling of thicker strip on larger roll diameters.

The roll separating force is the force exerted on the work roll by the material being compacted between the rolls. In the Johanson model [47], the roll separating force is given by:

$$RF = \int_{\theta=0}^{\theta=\theta_h} \frac{P_\theta W D}{2} cos\theta \, d\theta \qquad [10]$$

Where θ is the angular position on the roll, W is roll width and D is the roll diameter. P_θ is the pressure between the rolls at angular position θ, and is given by:

$P_\theta = \sigma_\theta \ (1 + \sin\delta)$ (δ is the effective angle of internal friction). [11]

Since the pressure in the region where θ > α (i.e. the slip region) is small compared to the nip region, the roll force is approximated by setting the upper limit of integration in equation 10 to α. The result is:

$$RF = \frac{P_m WDF}{2} \quad [12]$$

Where W is the roll width, D is roll diameter, P_m is maximum roll pressure at θ = 0, and F is the roll force factor given by:

$$F = \int_{\theta=0}^{\theta=\alpha} \left[\frac{S/D}{(1 + S/D - cos\theta)cos\theta}\right]^K cos\theta \, d\theta \quad [13]$$

Where K is the compressibility coefficient.

For the specific case of maintaining a certain maximum pressure (P_m) by simultaneously increasing the roll gap and roll diameter (such that S/D is constant), F remains constant if the nip angle, α, remains constant. As discussed in section, the nip angle has been found to be mostly independent of the roll gap and roll diameter (it is influenced predominantly by frictional parameters), and can therefore be assumed constant. If F is constant, and a maximum pressure P_m is maintained, then the roll separating force must be increased to roll thicker strip on a larger roll diameter. In other words, as the diameter increases, the area over which the pressure distribution acts (the arc of grip) is larger, hence the roll separating force must increase if a given maximum pressure is to be maintained. Figure 26 illustrates this relationship, using $\mathrm{RF} = \mathrm{Pm\ WD}F/2$ and the following input parameters:

- P_m is estimated using uniaxial compression data for HDH titanium powder from 15 sources from literature (data shown in Figure 29 in section 3.2.2).
- *F* is calculated using an S/D ratio of 0.65% (which is the median value for the consolidated titanium DPR data set, shown in Figure 30 in section 3.2.2), and a compressibility factor of 6.34, determined by Zhang [35] for -100 mesh (<149 μm) HDH Ti powder.
- Roll width and Diameter (WxD) is treated as a variable.

From Figure 26 it is evident that the rate of increase in roll separating force is greater the higher the density requirement.

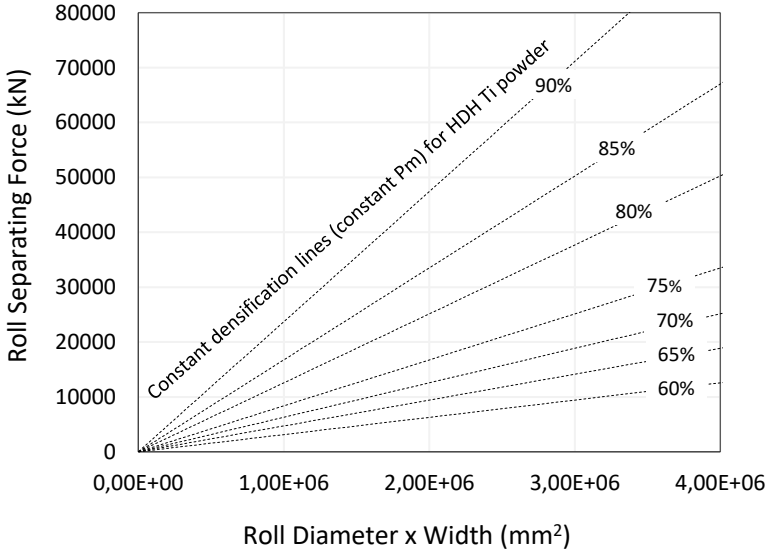

Figure 26: Roll separating force requirements for increasing roll diameter x strip width, for various strip densities.

3.2.2 Rolling mill capabilities

Specifications for 2-high rolling mills (only 2 rolls as opposed to 4 or 6) were obtained from 13 sources from literature and vendors (the details are given in Table 15 in Appendix B). The roller specifications (the maximum roll separating force and roll diameter x maximum sheet width) are presented in Figure 27, and are overlaid on the density lines presented in the previous section. Figure 28 below presents the same data as Figure 27 but shows only mills with roll diameters ≤500mm. The mills are limited to cold rolling, and all are appropriate for the rolling of metals. Only 2-high rolling mills are included in the data set, as there are few reports of DPR on 4-high mills.

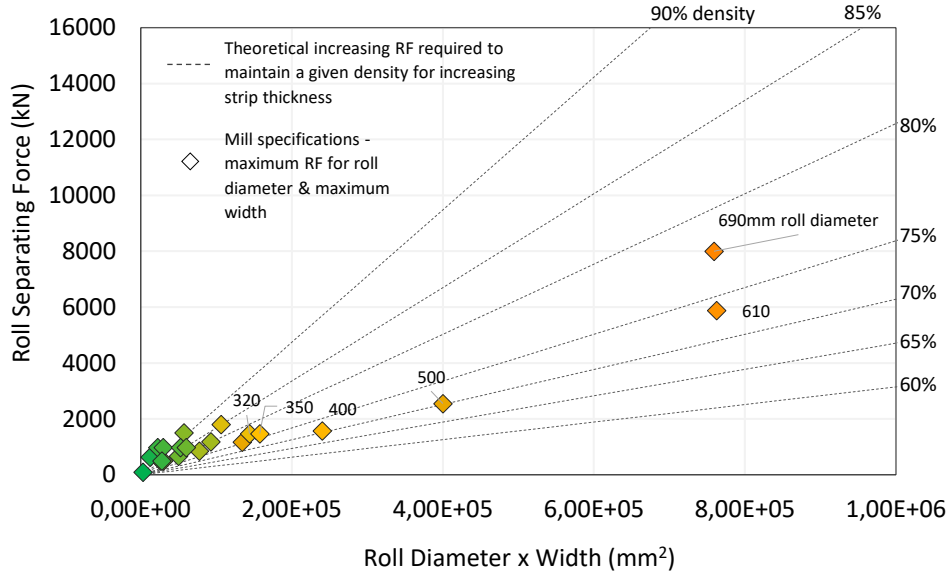

Figure 27: Maximum roll separating force for various 2-high rolling mills. Data point labels and colours indicate the size of the roll diameter. Theoretical lines of constant densifications are for HDH Ti powder, calculated using a compressibility factor = 6.35 and compaction parameter S/D = 0.65%.

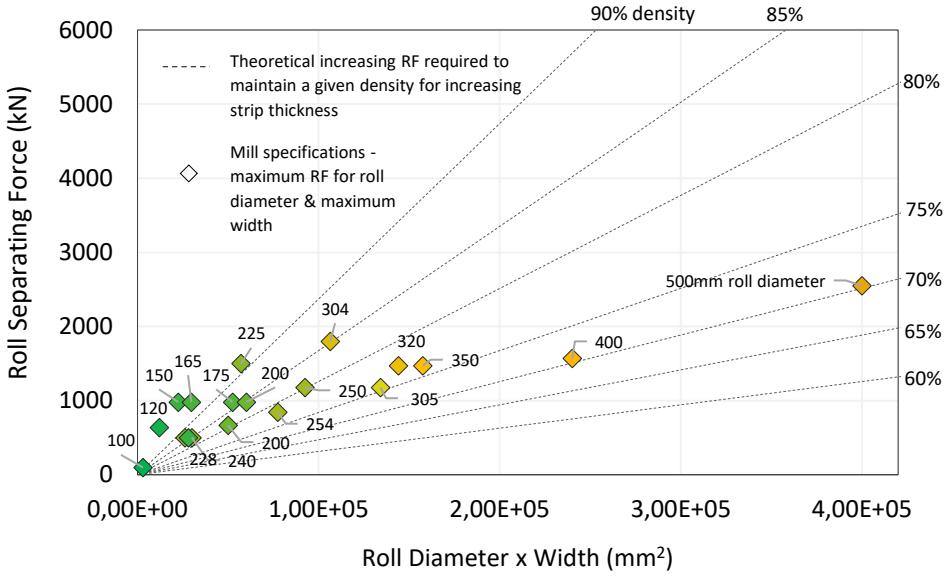

Figure 28: Same data as figure 27 but showing only roll diameters ≤500mm.

Figure 27 and Figure 28 indicate that there is a possibility that the rate of increase of **maximum** roll separating forces for mill specifications cannot meet the gradient required to maintain a constant, high densification for increasing strip thickness rolled on larger diameters. The uncertainty in the strength of this proposition is due to sensitivity to input parameters in $\mathrm{RF} = \mathrm{Pm}\ \mathrm{WD}F/2$. For example, for each DPR densification line in Figure 28, P_m

is estimated using uniaxial compression data from literature shown in Figure 29, where a range of green densities have been achieved for a given pressure. There is also sensitivity to the S/D ratio, selected in this case as 0.65%, but which exists as a range of 0.2 to 1.1%, as shown in Figure 30.

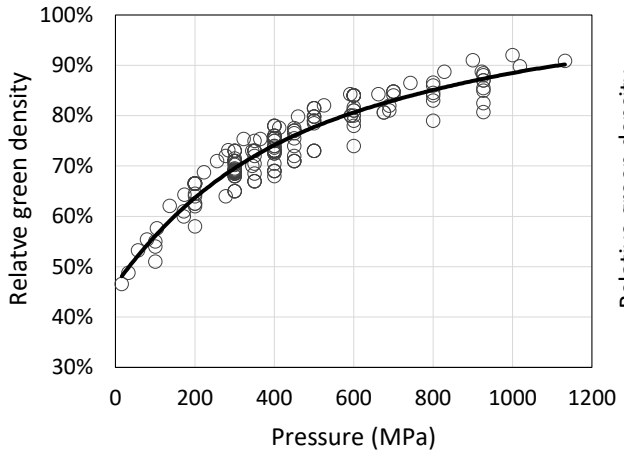

Figure 29: Green density versus compaction pressure for die pressed HDH powder. Fine powders of <45 µm / -325 mesh excluded. Data from 15 sources.

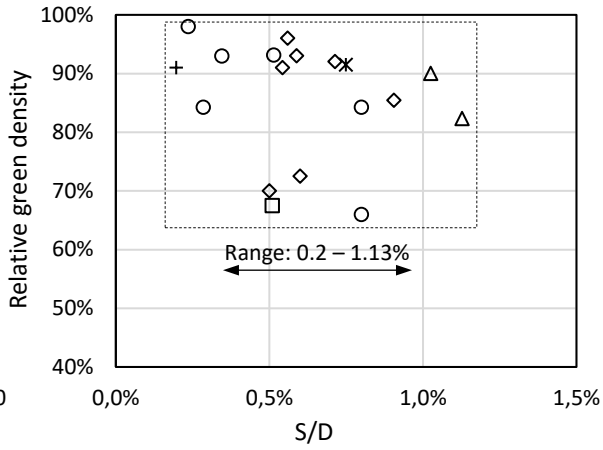

Figure 30: S/D ratios for the highest green density data points from the DPR data set consolidated from literature.

RF is sensitive to the S/D range, as shown in the comparison of the left graph (S/D= 1%) and the right graph (S/D = 0.3%) in Figure 31. Adjusting this parameter to the minimum and maximum value shifts the densification lines up or down, making the roll force gradient more, or less severe. It can be seen that in both S/D cases, as thicker strip is rolled on larger diameters, the same densification cannot be achieved as for thin strip rolled on smaller diameters.

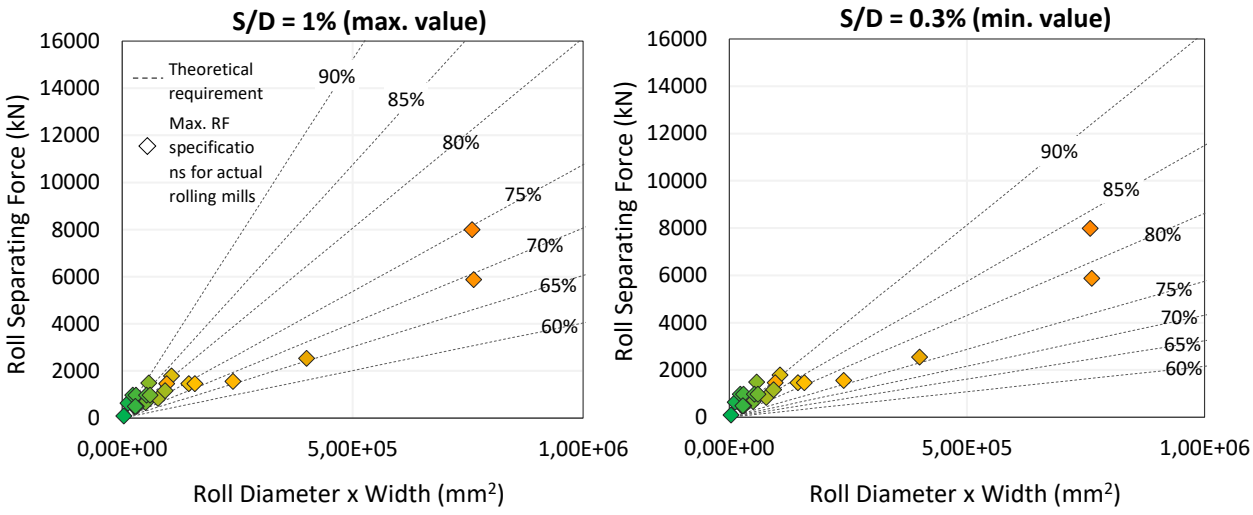

Figure 31: The sensitivity of roll force to the compaction parameter S/D. Maximum S/D = 1% (left graph) and minimum S/D = 0.3% (right graph). Points in colour represent the maximum design specifications for 2-high rolling mills. Lines of constant densifications are for HDH Ti powder with a compressibility factor = 6.35.

3.2.3 Direct Powder Rolling of Other Metals

Further evidence to support the roll force limitation proposition is seen in the comparison of consolidated DPR data for other metals in Figure 33, including aluminium, copper, iron, steel, nickel, stainless steel and molybdenum. A similar density limitation is seen for increasing strip thickness, for some of the metals, particularly for larger data sets such as iron and steel. The roll compacted metals are arranged from 1 to 7 for highest to lowest compressibility. This ordered arrangement is based on UTS and yield strength data sourced from literature, and consolidated in figure 33. UTS and yield strength are used as an indication of compressibility[2].

In Figure 33, it can be seen that the higher green densities are achieved for more compressible powders (almost 100% in the case of aluminium). For less compressible metal powders, a greater pressure would be required to achieve similar high green densities. As seen in

Figure 32, by moving from most to least compressible, the highest green density achieved shifts left, and then down. This could be due to the roll force design limitation discussed in the previous section. Rolling mills are likely to have excess roll force capacity for more compressible metal powders (i.e. because the mill is not being pushed to the operating limit when rolling a 1 mm thick aluminium strip, larger roll diameters can be used to roll thicker strip to as high a density until the forces exerted begin to exceed the design limitations of 2-high rolling mills available on the market, at which point the density attainable will become limited).

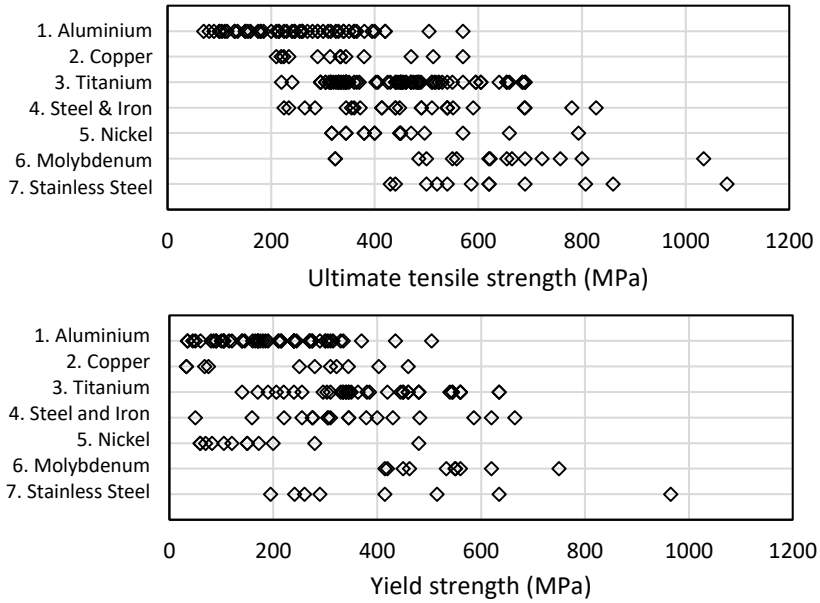

Figure 32: Tensile strength and yield strength ranges for the 7 metals for which DPR densification data exists.

Another limiting factor for powder roll compaction is that the mill size requirement is greater than that required to roll solid metal to a similar thickness. Much larger roll diameters are required for DPR to ensure sufficient feeding of powder to the roll gap, and to make up for powder slipping in the feed zone [69] [70]. Hence, Silins *et al*. [71] argue that very large diameter rolls with large support frames would be necessary to roll compact relatively thick product, and that the cost implications of such equipment have discouraged the use of DPR for thicker product.

[2] Powder compaction is a complex process influenced by several parameters, including particle shape, size and distribution, the presence of non-metallic particulates, the addition of alloying elements and the hardness of the metal [69]. In the first stage of compaction, starting pressures are low and the initial densification is due to particle rearrangement. With increased loading, there is localised plastic deformation and particle fragmentation [7]. Although the tensile and yield strength of the metal are not identified as factors affecting powder compressibility directly, there is a correlation between strength and hardness, with hardness often being 3 times the strength for work-hardened crystalline materials [72]. Since an increase in material hardness is known to reduce compressibility, the use of strength properties to arrange the graphs in Figure 33, in substitution for hardness, is justified.

32

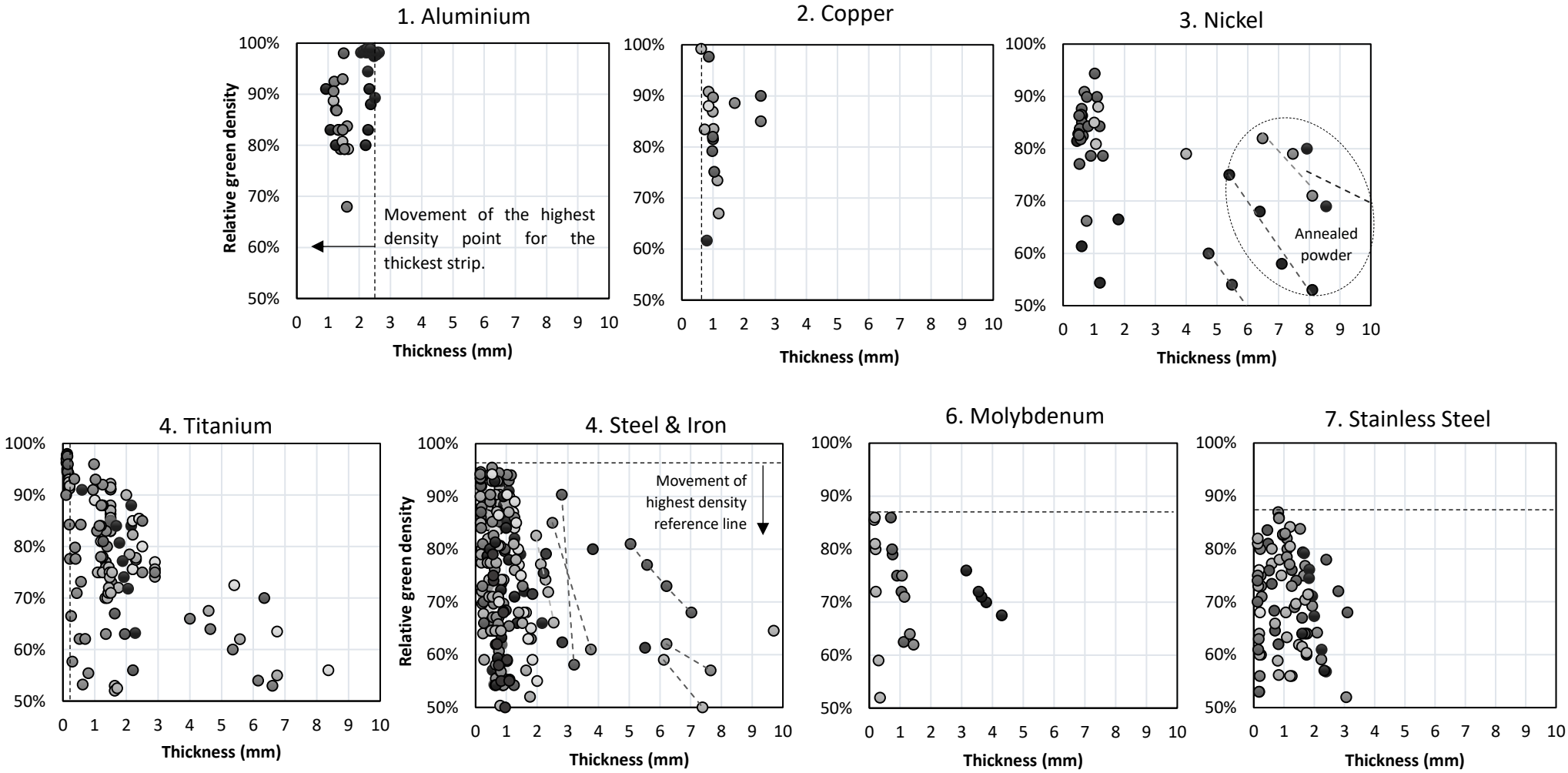

Figure 33: Density data for different powdered metals that have been roll compacted to various strip thicknesses. The attainment of high densities for thicker strip is increasingly limited as the ultimate tensile strength and yield strength generally increase for metals 1 to 7. It is noted that data points may be missing for higher densities, for example in the Nickel data set.

3.2.4 In Summary

The analysis in this section suggests that the current roll force capabilities of 2-high mills cannot meet the roll forces required to produce thicker, high density DPR strip. Experimental research is required to support this. The improvement in rolling mill capabilities, so as to withstand higher forces, is not expected to be economically feasible due to the cost implications.

3.3 Maximum Final Thickness of DPR Product

After sintering, the strip undergoes hot rolling or multiple cold rolling and annealing cycles which closes much of the remaining porosity. This additional processing reduces the thickness of the strip. It is therefore important that the targeted thickness of the final product be considered when selecting for the initial thickness of the green strip. There is little information concerning the level of reduction required to reach full density, as a function of green strip porosity. For the rolling of metal powder in general, Bex *et al*. [73] claim that the green strip thickness must be reduced by 80 to 90% if adequate final density is to be achieved, while Shakespeare [74] reports that no more than a 3:1 (66%) reduction is probably required. For iron powder, Davies *et al*. [75] claim that a thickness reduction of greater than 50% is usually required. For titanium, Cantin *et al*. [53] claim that green strip thickness must be approximately four times the final thickness if mechanical properties similar to wrought metal are to be achieved (i.e. a 75% reduction is required). Cantin *et al*. [53] cite Blore *et al*. [76], who report that during rolling of the sintered sheet, some of the plastic deformation closes the remaining porosity while a proportion of this deformation elongates the product. The greater the elongation, the less efficient the process is in closing porosity. Therefore, a greater degree of of thickness reduction is required than what would be theoretically necessary to close the remaining porosity.

To estimate the degree of thickness reduction required for titanium green strip, rolling reduction data was sourced from literature. Table 3 gives the green, sintered and final density of titanium strip as well as the percentage thickness reduction from green strip (unfortunately, few papers report on the sintered density) to the final rolled strip. All strips have a green density ≥ 70%, and most are above 80%. All but one source report a final density greater than 99%. The reduction in thickness for these cases ranges from 45% to 75%.

Table 3: Percentage thickness reduction of DPR green strip. Data from 7 sources

Titanium/ Alloy	Green density %	Sintered density %	Final density %	% Thickness reduction	Source
Titanium	85	93-94	99.9	**50**	[32]
Titanium	85-76	88-95	98.3-98.8	**50**	[35]
Ti-6Al-4V	84-88	-	99.6	**62-74**	[34]
Titanium	83-92	84-96	>99	**47**	[30]
Titanium	81-89	-	99.9	**50**	[29]
Titanium	75-85	-	Full/near full	**60-66**	[10]
Ti-6Al-4V	70	-	100	**60**	[12]
Titanium	75	-	Full/near full	**45**	[36]
Titanium	81	-	99.9	**50**	[77]
Titanium	89	-	99.5	**59**	[77]

To date, the densest green strip rolled on the largest roll diameter is 6.35 mm, at 70% green density (yellow marker in Figure 34, rolled *by ADMA)*. After several cold rolling and annealing cycles (60% reduction), the final thickness for this strip was 2.5 mm, with a density of 99.7%. This point is assumed to represent the limits of DPR for the following reasons. Firstly, a green density of 70% is nearing the minimum density requirement for green strip coherency. Strip of low green density is at risk of being too week to withstand further handling and processing. In a DPR patent for metal powders, Marlowe *et al*. specify that a green density of at least 65% is preferable [78]. In the rolling of copper, Evans [79] showed that the

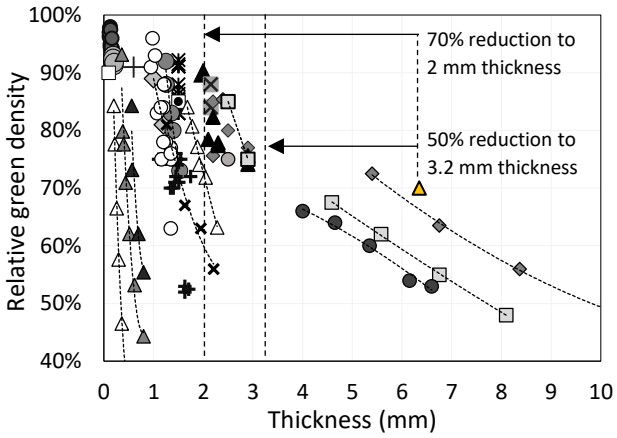

Figure 34: Estimate of the maximum thickness of DPR product.

lowest density for coherent green strip is 62%. Hence, 70% minimum green density is a reasonable assumption for titanium DPR. Secondly, this green strip was rolled on a mill with roll diameters comparable in size to those of large, 2-high plate mills used in industry. Due to cost and density implications discussed in section 4.2, it is assumed that 1270 mm diameter rolls are the limit, and that green strip thicker than 6.35 mm is unlikely. Hence it is assumed that the maximum titanium green strip thickness is 6.35mm.

Based on data in Table 3, applying a 50-70% reduction to the 6.35 mm thick green strip gives a conservative estimate of 2 to 3.2 mm for the maximum thickness of fully processed DPR product, indicated by arrows in Figure 34.

3.4 Chlorine Content

The direct rolling of metal powder is not a new technology. The filing of several patents in the 1950's points to the earliest evidence of an interest in the commercial potential of this method. Patents pertaining to the manufacturing of metal strip from metal powder are detailed in Appendix A. In the late 1950's, Du Pont looked to commercialize a continuous roll compaction process for producing titanium. They manufactured their own feedstock – powder from sodium reduced titanium sponge from the Hunter process – which was particularly suited to DPR due to its morphology and excellent particle interlocking [80]. Initial investigations were deemed commercially promising and the process was scaled up to tonnage quantities. It was reported that the green sheet could reach 90% relative density when particle size distribution was optimal, there was excellent control of the final gauge, and the sheet had high ductility and a superior finish [80]. The rolling of Ti-6Al-4V sheet was also demonstrated [81]. However, in 1962, Du Pont discontinued manufacturing the powder due to unacceptable levels of chlorides, which volatilized during welding and caused a build-up of salt on the welding electrodes. This created an unstable arc which resulted in poor and inconsistent weld quality [8]. The chlorine range in Du Pont's powder was 0.01 – 0.05 wt%. In experiments carried out by Du Pont, chloride levels were lowered by mixing their powder with more expensive, purer powders that had been manufactured via melting to remove residual chlorides. Du Pont concluded that satisfactory welding could be achieved only at levels of **0.005 wt%** or less but this target was deemed impractical or too costly at the time [80].

In the 1970s, Imperial Clevite investigated the use of DPR to manufacture high strength titanium alloy foil for use in honeycomb structures [31], but they too never produced products in volume due to the presence of chlorides, as well as unacceptable porosity [82]. Other factors that contributed to the commercial failure of Du Pont and Imperial Clevite include the high cost of powder, and the lack of high volume domestic powder production [8]. However, the single greatest barrier to the commercialization of Du Pont's operation was reported to be the chlorine problem. Du Pont believed that "marginally weldable product" could not compete with established product on the market [80]. However, Robertson *et al*. [83] believe that had DuPont persevered, their products were likely to have been adequate for some applications.

Following the discontinuation of Du Pont's DPR venture in 1962, residual chlorine continued to be cited as problematic. In the 1980s, the prospect of a low chloride electrolytic sponge garnered attention [84], but efforts were aborted due to engineering or economic issues [85]. Efforts to develop a low cost, electrochemical or alternative non-melt powder process have continued, but the technology remains developmental. These include the Metalysis FFC Cambridge approach, the MER technique, the CSIRO TiRO method, and the Armstrong process [86].

Today, titanium is extracted predominantly via the Kroll process, and most commercially available powders are derived therein [88]. Following improvements to the Kroll process in the 1990's, the Hunter process (the sodium reduction process used by Du Pont in the 1960's) became a less viable alternative [89]. It was more expensive than Kroll [90] and produced a smaller amount of titanium than could be produced by Kroll in a similar sized retort [9]. RMI and Deeside, two major sponge producers using the Hunter process, closed their plants in 1992 and 1993 respectively [88]. The last remaining Hunter plant is operated by Alta Group in Utah, USA and produces only high purity titanium (99.999%) for integrated circuits [89].

The Hunter and Kroll processes are similar in that both reduce $TiCl_4$, the first with sodium and the latter with magnesium, and the resultant sponge in both cases is known for high chloride impurities ($NaCl_2$ and $MgCl_2$ respectively). This means that the chlorine contamination problems faced by Du Pont in the 1960's are still applicable today, as most low-cost powder is derived from Kroll sponge (although powder processing methods have been developed to reduce chlorine levels). Purification of Kroll sponge involves the removal of $MgCl_2$ (and other residuals such as Fe) via vacuum distillation, which is an energy intensive batch operation. It is the most time-consuming and expensive operation in the purification process [91], taking about 4 days, requiring heating to 1000°C [88] and accounting for about 30% of the final cost of ingot [92]. The refined sponge removed from the reaction vessel varies in quality depending on the degree of purification. To produce wrought product, the sponge undergoes double or triple vacuum arc melting, where traces of chlorine are removed completely. As a result, the ASTM B265 specification for wrought titanium does not specify a maximum chlorine content.

Titanium powders are derived from various stages of the refining process described above, depending on quality and application requirements. GA (gas atomization), PA (plasma atomization) and PREP (plasma rotation electrode process) are high quality, expensive powders, produced by the melting and spheroidisation of IM product (i.e. ingot or melt for GA; wire for PA; and titanium bar for PREP [93]). The spherical morphology of these powders (Figure 35) is not suitable for DPR due to poor particle interlocking and low green strength. Although expensive, these powders are characteristically low in chloride impurities because they are ingot derived.

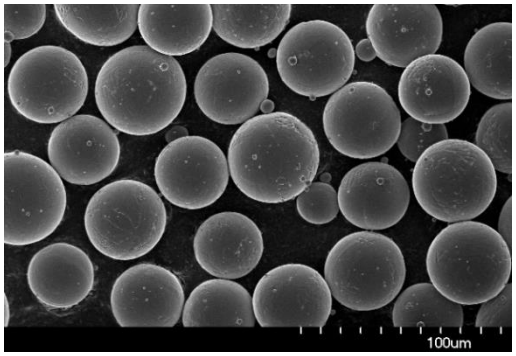

Figure 35: Plasma atomized titanium powder (AP&C).

In the production of inexpensive powders, which are sponge - and not ingot - derived, the process stops short of the melting step, and therefore avoids the associated cost. However, the trade-off is the presence of residual reaction products from the reduction process [94]. The cheaper, meltless powders include following:

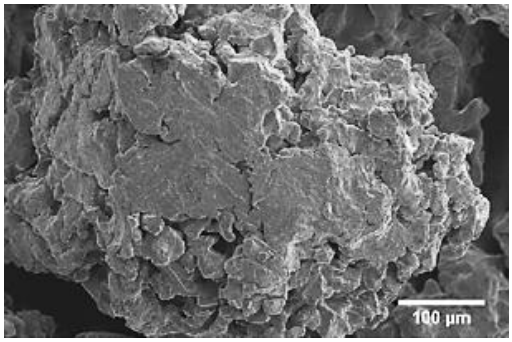

Figure 36: Sponge fines [95].

Sponge fines: Sponge is crushed before vacuum arc melting, and those particles that do not meet the size requirement for further conventional processing are termed "sponge fines" (shown in Figure 36 [95]). Being a by-product, it is a relatively cheap source of elemental titanium [96]. Sponge fines have a coarse particle size (typically 180 – 850µm, as produced [97]) and are limited in application due to the difficulty in grinding the ductile particulates to a finer mesh size [98]. The irregular or sponge-like morphology is an advantage during powder compaction, providing good green strength [96].

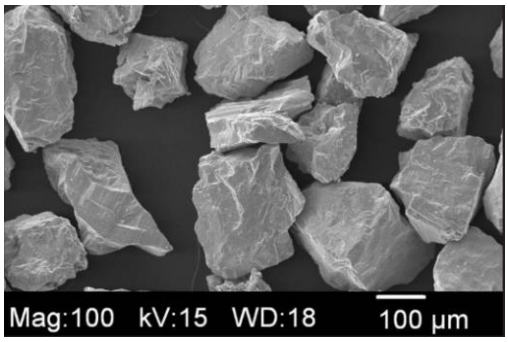

Figure 37: HDH powder (Ametek Specialty Metal Products).

Hydride-dehydride powder (HDH): HDH offers the advantage of controlled particle size. A starting stock of sponge, scrap and/or machine turnings is embrittled by heating in a hydrogen atmosphere, resulting in friable TiH_2, which is subsequently crushed to the desired particle size, and then dehydrogenated via heating in a vacuum [96]. HDH powders contain less residual chlorine than the sponge precursor due to the release of Cl from closed pores during crushing to finer size [99] and because of the cleaning action of hydrogen removal during the dehydrogenation stage [100], but the risk of oxygen pick-up is greater because of the size reduction process [101]. The powder has an angular/irregular morphology (Figure 37). It is also made via the hydrogenation of milled/sliced ingot, making it a much purer [102] albeit more costly powder.

TiH_2: TiH_2 is an intermediate product of the HDH process. It is brittle and therefore not suitable for DPR due to poor particle interlocking, but there is growing interest in compacting TiH_2 preforms via cold isostatic pressing, followed by dehydrogenation of the compact and thermomechanical work (e.g. forging or rolling to plate and possibly sheet). There are several advantages of using this powder which are discussed later in section 4.

Figure 38 shows the various powder production routes and the relative powder purity and price depending on the starting stock (i.e. sponge, ingot, mill product, and/or scrap). HDH powders and atomised powders are the two main commercially available powders today [103].

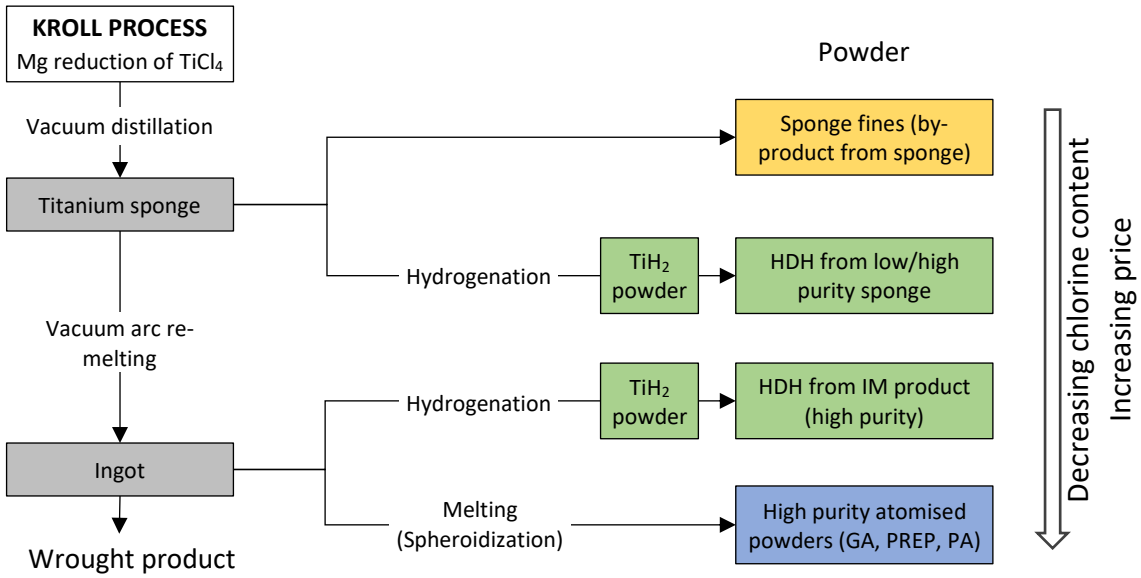

Figure 38: Commercial powder manufacturing routes and relative degrees of chlorine content.

The Adverse Effects of Chloride Impurities

In a review of titanium powder metallurgy, [102] reported that problems arising from chloride impurities have been found to present as macroporosity, microinclusions, grain boundary embrittlement and poor weldability. Regarding macroporosity, Weiss *et al*. [104] suggested that higher residual porosity in compacts made from high chloride powder is due to pressure from chloride gas in the closed pores. No chemical analysis was conducted to support this suggestion, instead they referenced Jackson *et al*. (paper unobtainable[3]), who suggested that chlorine vapor in the pores reacts with titanium, producing $TiCl_2$ or $TiCl_4$, and that at the high processing temperatures used, the resulting vapor pressure prevents pore closure. In the cold isostatic pressing of high chlorine blended elemental Ti-6Al-4V powder, Fan *et al*. [105] did test for chlorine localities. They confirmed the presence of chlorine in the as-sintered microstructure in three forms – 1. as shells of fine NaCl particles in macropores, 2. as NaCl precipitates in the alloy matrix, and 3. as Cl and Na in grain boundaries. Peter *et al*. [94] claim that there is ample evidence to suggest that impurities such as magnesium and sodium chlorides cause porosity, but that how these contaminants directly affect the properties of titanium is still unclear.

Eliminating the porosity is problematic. Weiss *et al*. [104] claim that 100% densification cannot be achieved even with the use of post-sintering forging or hot isostatic pressing and that chlorine as low as 0.018 wt% was sufficient to prevent the attainment of full density. Horiya *et al*. [106] reported on Nippon Steel's success in using a CHIP process (cold followed by hot isostatic pressing) to produce compacts free of internal defects with properties equivalent to wrought product, but this was achieved with the use of extra-low chloride powder (≤0.005wt%). The chloride inclusions also adversely affect fracture toughness [419], although this property is more critical for fatigue related applications.

As discussed above, welding issues have been found to occur due to the volatilization of chlorides which leads to a build-up of salt on the welding electrodes, resulting in inconsistent weld quality [8]. However, subsequent to Du Pont's work, there has been very little research investigating the effect of chloride impurities on welding of titanium PM product. Froes [107] reports that in the 1980 TMS Conference, it was noted that recent work showed that weldability could be improved if chlorine was below 0.015 wt%.

Much of the research into the influence of chloride impurities was conducted in the 1980's and 90's ([101] – 1993; [104] – 1986; [105] – 1996) when commercially available titanium powders at the time (Kroll/Hunter

[3] A.G. Jackson, J. Moteff, and E H. Froes: Metall. Trans. A, 1984, vol. 15A, p. 148.

sponge fines) had a standard chlorine content of 0.15wt% [101]. Following the commercialisation of the HDH process, chloride levels have improved but are still not ideal. Figure 39 presents evidence of problems experienced at different levels of chlorine content, compared on a scale alongside the chlorine content reported for HDH sponge derived powders. Instances of chlorine related problems (highlighted in orange) are seen to occur below the lower end of the chlorine range for low-cost HDH powders. For example, "inexpensive" HDH powder contains >0.02 wt% chlorine, but weldability is reportedly improved only at 0.015 wt% [107]). Purer HDH powders with 0.001 wt% Cl are available, but are expensive, having been derived from IM material.

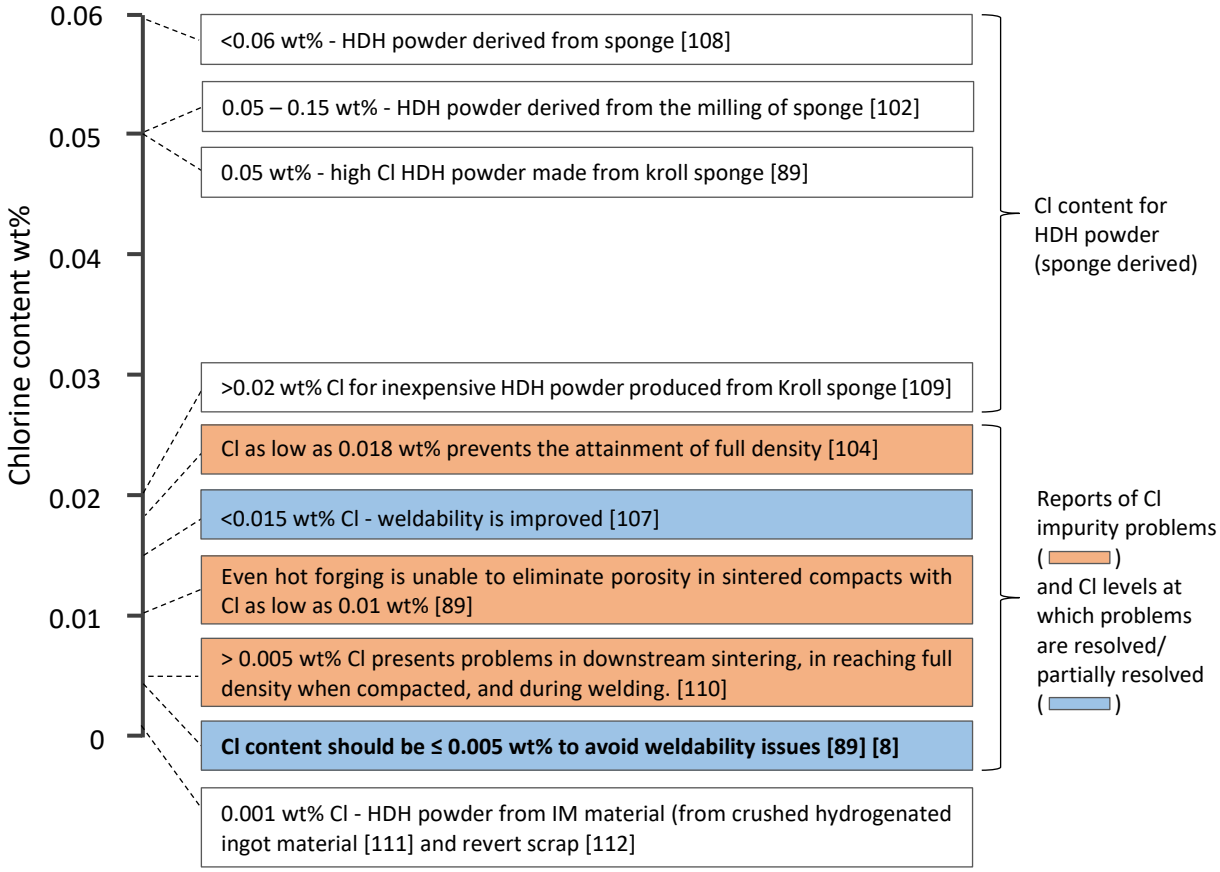

Figure 39: Range of chlorine content reported in literature and compared on a scale.

The chlorine content range for various titanium powders is consolidated in Figure 41 below. As expected, sponge fines have the highest Cl content (0.08 – 0.21 wt%). There are two points that have unusually low Cl, labelled as point 1 and 2. They also have unusually small particle sizes (average of 33μm for point 1 and <45μm for point 2, compared to the typical, as produced size range of 180 – 850μm for sponge fines [97]). The action of crushing to smaller particle sizes and consequent release of chlorine, as discussed earlier, is a likely explanation for the low chlorine level of point 1 and 2. However, the downside of such small particle sizes is the increased risk of oxygen contamination, as will be discussed in a later section. TiH_2 powder has the second highest range of Cl (0.05 – 0.12 wt%), and as expected, the HDH powder range (0.002 – 0.08 wt% Cl) is lower due to Cl removal during powder dehydrogenation. The HDH powder could not be separated into that derived from ingot material and that derived from sponge, as most sources did not specify the production method. The lowest chlorine content reported for sponge derived HDH powders is 0.02 wt% [109] [113] and 0.023 wt% [105]. Cl levels below this are assumed to be derived from IM material and are therefore not economically feasible to use. Cl levels below 0.02 wt% are also commonly seen for powders with a PSD less than 45μm. As will be discussed in the next section, powders with particles sizes this small have high oxygen content, which is detrimental to the elongation in the finished part. The histogram for the HDH data set shows that these powders typically have a chlorine content of 0.04 - 0.065 wt% (Figure 40).

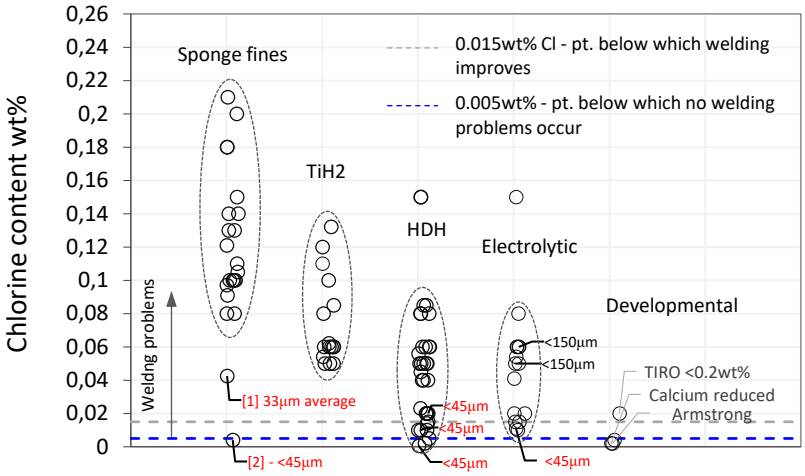

Figure 41: Chlorine content of various titanium powders. Data from literature and quotations - 41 sources. Powder particle sizes labelled in red.

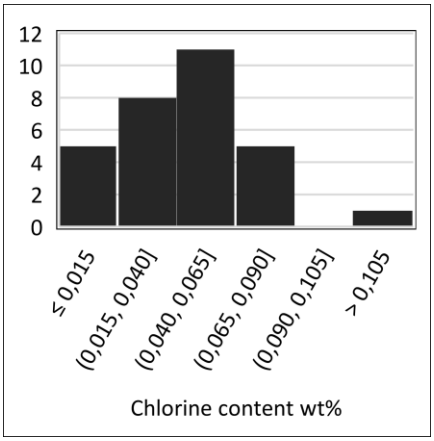

Figure 40: Histogram of chlorine content of HDH powder. Data from literature and quotations - 21 sources.

The electrolytic powders investigated in the 80's show an improvement in chlorine content compared to sponge fines, but levels are above the 0.005 wt% limit identified by Du Pont (dotted blue line), Cl content is again seen to be a function of particle size, and most importantly, these powders are no longer commercially available. Of the developmental powders, calcium hydride powders have relatively low chlorine content (e.g. 0.004 wt%), but were too expensive in the 1980s and did not achieve commercial success [100]. Armstrong powders offer good potential, with chlorine content as low as 0.005 wt% or less [114], but these powders are not widely available, and generally have higher oxygen content due to their high specific surface area (as will be discussed in the next section).

In Summary

The consolidation of data shows that low-cost powders, commercially available today, have chlorine levels that are likely to cause welding problems similar to what Du Pont experienced in their efforts to commercialize the titanium DPR process. HDH, the most commonly used commercial powder, generally has a Cl content greater than 0.02 wt%. Levels lower than this may be possible for powders with a PSD <45µm, as Cl is released during crushing, but exposed surface areas lead to increased oxygen contamination, as discussed in the following section.

3.5 Oxygen Content

A critical problem for titanium powder metallurgy is titanium's affinity for oxygen. Given the high specific surface area of powdered material, the formation of oxide layers on individual particles can lead to unacceptable levels of contamination. This significantly affects the mechanical properties of the final product, particularly tensile ductility [115] [116]. Limiting the exposure to oxygen by carefully controlling storage, handling and processing conditions mitigates this risk, but due to the particulate nature of the starting stock, the final oxygen content is generally higher than levels seen in wrought product.

This section seeks to determine how much higher the oxygen content is, and what powder and processing factors dominantly influence contamination in PM processing. Oxygen content data for product made via DPR and similar powder metallurgy methods was consolidated from literature and compared to:

1. The **maximum allowable** oxygen content as specified by ASTM standards for wrought CP titanium grades 1 to 4 and Ti-6Al-4V (grade 5).
2. The **typical** oxygen content range for the conventional ingot metallurgy (IM) process (many researchers establish only whether the oxygen is within the specification limit, but it is of greater relevance to compare results to the typical properties of wrought product, especially for design and fabrication considerations).

3.5.1 Typical Oxygen Content of Room Temperature PM Methods

Data Collection & Results

The oxygen contents of compacts made via DPR, CIP and die pressing were sourced predominantly from literature. The decision was taken to look at a broader group of powder metallurgy methods to ensure the largest possible sample size. Since CIP and die pressing are similar to DPR (all three involve compaction at room temperature), they offer a good approximation of the typical DPR oxygen content.

The characteristics of the oxygen data set are the following:

- 93 data points were obtained from 25 sources for CP and Ti-6Al-4V compacts. The relative proportion of each of the compaction methods is shown in Figure 42.
- Data is from papers from 2004 to 2016.
- Only data for samples that were at least compacted **and** sintered was selected. The DPR data includes samples that were also cold/hot rolled after sintering which is deemed acceptable as most oxygen uptake occurs before or during sintering before interconnected porosity is closed.
- 90% of the compacts in the data set are derived from HDH powders, and the rest are from sponge fines.
- 92% of the data is for unlubricated compaction. Data that does involve lubrication is for die wall lubrication only. Powders mixed with binders were excluded from the data set as additional oxygen pick-up occurs from a reaction in the debinding atmosphere [117].

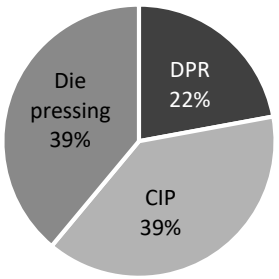

Figure 42: Relative proportion of compaction methods in the PM sample.

Figure 43 below shows the data spread of oxygen content for the three PM methods selected. Due to similar processes and powder feedstock, there is little difference between the data ranges, and the lowest oxygen content achieved for DPR and CIP is identical (0.15 wt%). Figure 44 is a histogram of the same data. Most of the oxygen contents are greater than the ASTM grade 4 maximum (0.4 wt%) and very few samples meet ASTM grade 1 (<0.18 wt%).

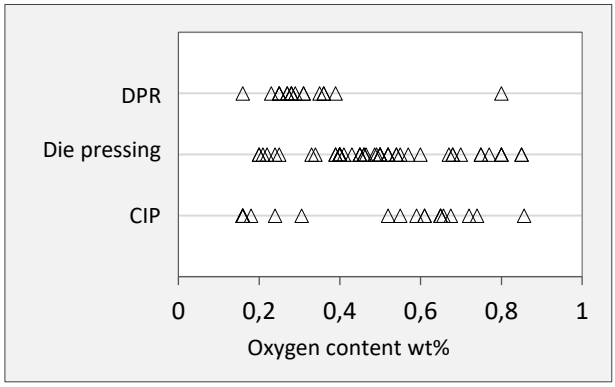

Figure 43: Spread of final oxygen content for compacts made via DPR, die pressing and CIP.

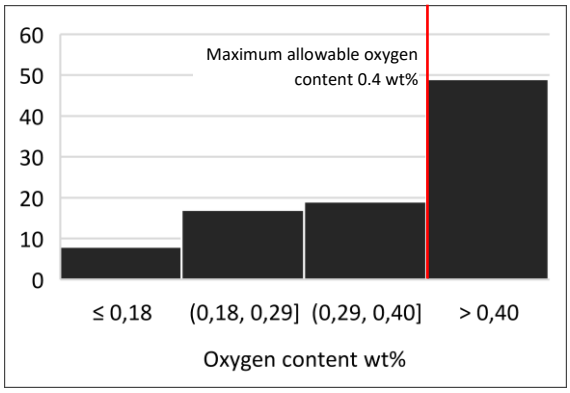

Figure 44: Histogram of final oxygen contents for compacts made via DPR, die pressing and CIP.

3.5.2 Typical Oxygen Content of Conventional Wrought Product

Data Collection & Results

Oxygen content of wrought product was sourced from literature that incidentally reported on the properties of commercial wrought titanium samples used in experimental work (often unrelated to powder metallurgy research). No oxygen data was taken from research that used non-typical or non-commercial titanium samples. In these papers, oxygen values were either tested or reported directly from mill test reports (MTRs). These reports, provided by titanium manufacturers, are quality assurance certificates that confirm the specification and indicate typical properties of the product e.g. tensile properties and chemical composition. Some MTRs were also sourced directly from businesses but these are difficult to obtain without buying the product. The data set for oxygen content of wrought product consists of 92 points from 52 sources. The data is predominantly for coil, sheet and plate and a minority is for ingot and slab.

Figure 45 shows the typical oxygen content data for grades 1 to 5. ASTM specifications are included for comparison. The data is separated into the five commercial grades as specified by the original sources. Grade 2, the largest data set, is the most commonly used of the pure grades, particularly for industrial applications [118]. The ability to produce product within grade 2 specification would strengthen the commercial feasibility of a PM process, hence much of the data analysis will be in relation to this specification.

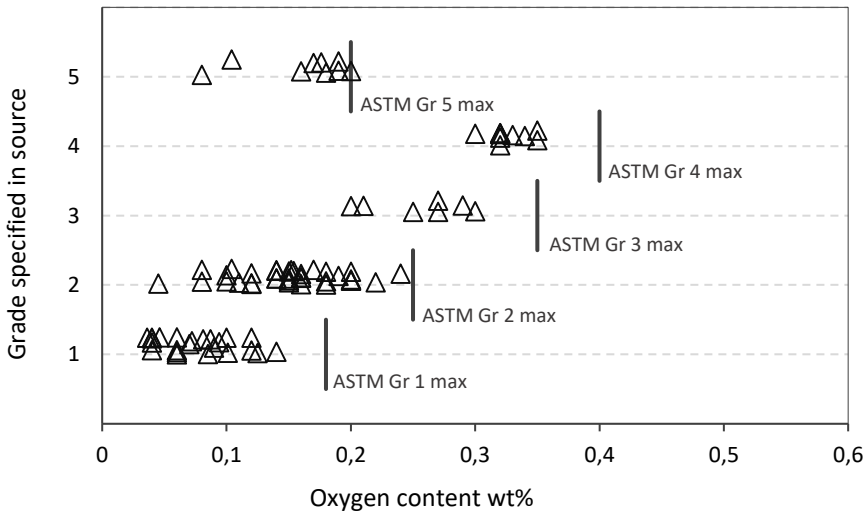

Figure 45: Typical oxygen content for conventional IM product versus ASTM specifications (92 data points from 52 unique sources).

A large range of values exists for each of the ASTM grades and many samples have oxygen contents well below the maximum specifications. A histogram (Figure 46) of the largest data set, grade 2 (specified as <0.25 wt% O), shows a normalised distribution, with 91% of samples having oxygen levels below 0.20 wt%, and 68% below 0.16 wt%. It is interesting to note that some samples, specified as grade 2, have oxygen contents below the grade 1 maximum of 0.18 wt%. These samples are most likely classified as grade 2 based on the content of other chemical components or because of tensile properties that fall within the grade 2 specification.

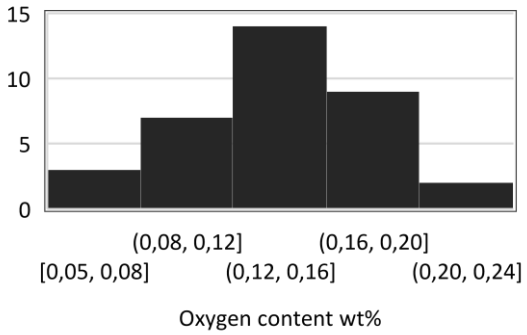

Figure 46: Distribution of typical oxygen content for wrought product that has been specified as grade 2 (ASTM max is 0.25 wt% O). Sample size = 35.

3.5.3 Powder Metallurgy vs. Wrought Product

The typical oxygen values for powder metallurgy compacts and wrought product are compared directly in Figure 47. The oxygen range for wrought product is significantly lower than the lowest oxygen content achieved via PM routes. It is noted that the wider spread in PM data is partly due to experimental testing, while wrought data represents a well-established and finely controlled commercial process. Therefore, in terms of PM performance, the lower range of oxygen values are of more interest as these are likely to have been achieved with optimized parameters.

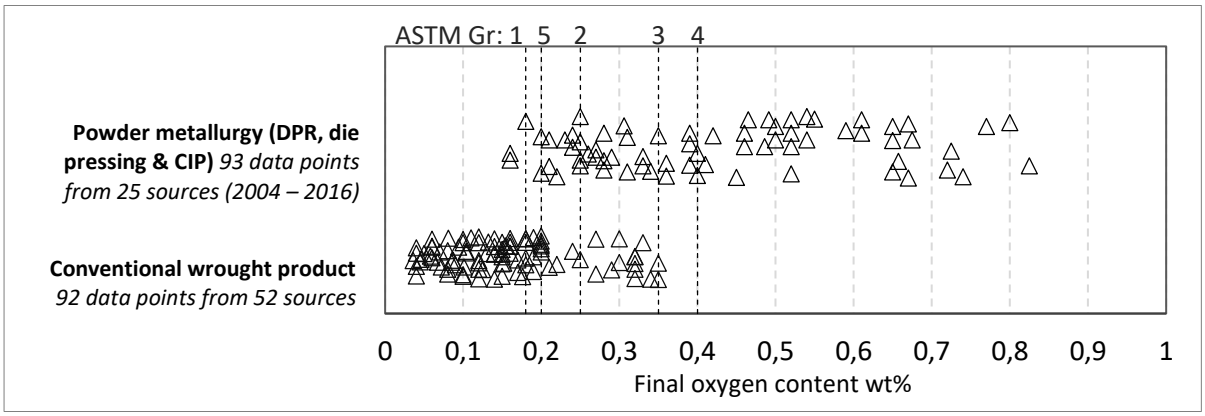

Figure 47: Typical oxygen content for powder metallurgy (PM) versus conventional wrought product.

The consolidation of oxygen data shows that if PM products are to compete with wrought product, achieving only the minimum performance level is not acceptable, as wrought product is often well below the limit. To meet design and fabrication expectations of customers, powder metallurgy routes must achieve properties comparable to the **typical** oxygen values of wrought product.

3.5.4 Factors Affecting Oxygen Content in PM Compacts

The following factors are reported to influence the final oxygen content of PM compacts [117]:

1. The powder manufacturing method, which determines the level of subsurface oxygen in solid solution
2. The powder characteristics: the size and morphology of particles, which determines the specific surface area and possible degree of oxygen pick-up via the forming and dissolving of oxide layers
3. The processing parameters: sintering temperature and time
4. The processing conditions: storage, handling and sintering conditions which impact the risk of exposure

In the oxygen data set, powder size is seen to have a high degree of influence on the final oxygen content of the sintered product. Compacts made from powder with a median particle size of less than 63µm are highlighted in red in Figure 48 below, and most of these points do not meet the maximum specification of commercially pure titanium (grade 4). There is one data point that meets grade 2 (labelled A) from a study by Ivasishin *et al*. [119], who reported the use of low oxygen HDH powder (0.1 wt%) and careful protection from oxidation via storage under argon. Compacts from powder with a median particle size greater than 63µm are highlighted in green. These meet grade 1 (just) and 2 & 3.

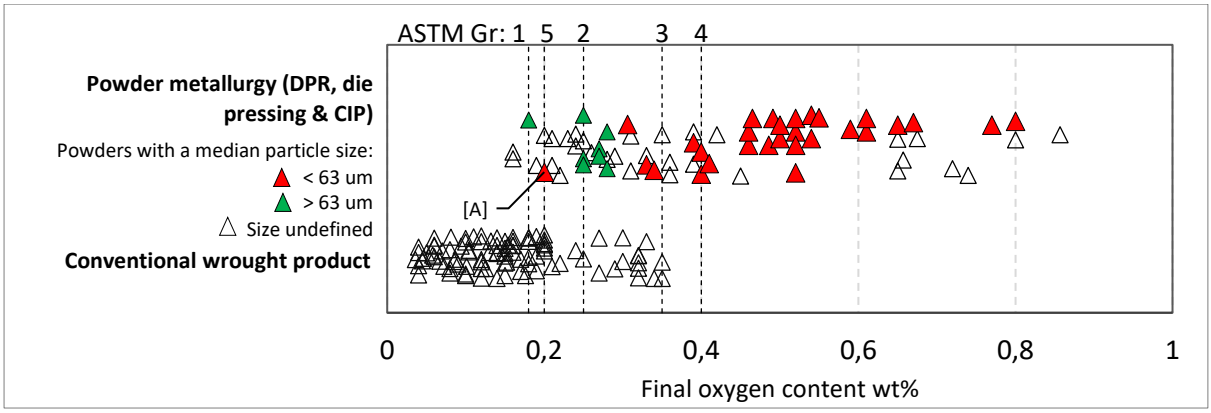

Figure 48: Typical oxygen content for powder metallurgy (PM) versus conventional wrought product. Compacts made from powder with a median particle size <50 µm highlighted in red.

The relationship between mean/median particle size and powder oxygen content is shown in Figure 49. These data points have been sourced from literature (13 sources). Oxygen ranges for particle size ranges reported by Barbis *et al*. [120] support the trendline. The consolidation of this data is helpful in that it assists in the selection of feedstock with a view to minimizing the final oxygen content. In general, powder with a mean or median particle size greater than 50µm is shown to have an oxygen content of less than 0.35 wt% (grade 3). Point [A], discussed above, is highlighted in yellow, and is again positioned as an outlier. The relationship between the **final** oxygen content of sintered compacts and the mean and median particle size of the starting stock is shown in Figure 50. The axes remain the same as those in Figure 49. The general upward shift shows oxygen pick-up during processing.

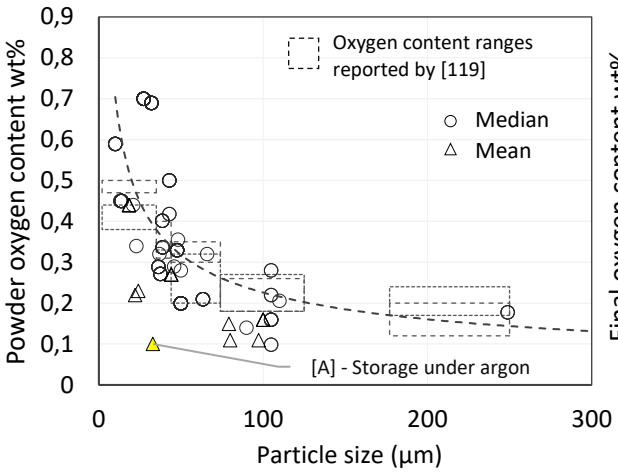

Figure 49: Initial oxygen content of Ti and Ti-6Al-4V powders (sponge fines and HDH) versus particle size. Data points from 13 sources.

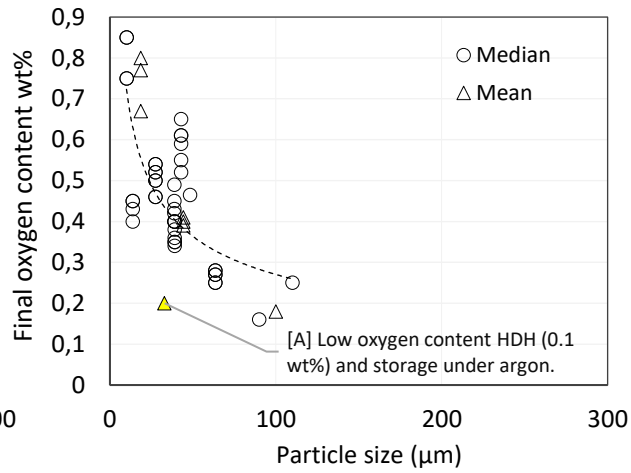

Figure 50: Final oxygen content of Ti and Ti-6Al-4V compacts versus particle size (compacts from sponge fines and HDH powder). Data from 11 sources.

A larger sample size of the typical oxygen values for sponge fines and HDH powder is given in Figure 52. Various other powders are presented, including TiH_2, the intermediate powder in the HDH process. Electrolytic powders, popular in the 80's but decreasingly used in the 90s due to increasing costs [174], have large particle sizes (>180 μm and up to 5000 μm) and as a result, are particularly low in oxygen.

The Armstrong powder manufacturing method has been under development for several years, and of the innovative extraction processes, is the closest to commercialization [18] [25]. However, its oxygen content range is not as low as HDH powder even though the as produced median particle size of Armstrong powder (>100μm) is larger than the typical HDH sizes seen in Figure 49 above. This is because the dendritic "coral-like" morphology of the powder (shown in Figure 51 [121]) results in a higher specific surface area, compared to HDH powder, and hence a greater risk of oxygen pick-up [112]. There are few examples of the final oxygen content of Armstrong derived compacts. Muth *et al*. [112] reported levels of 0.31 to 0.42 wt% for vacuum hot pressed compacts, which is at best, grade 3 and 4, and at worst (>0.4 wt%) not within the specification for commercially pure titanium.

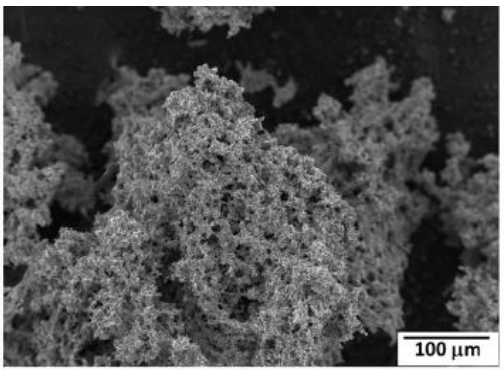

Figure 51: Dendritic "coral-like" morphology of Armstrong titanium powder [121].

The lowest oxygen content for atomised powders (0.01 wt%, labelled B in Figure 52) with its large powder size distribution of >100μm, again emphasizes the impact that powder surface area has on oxygen content. Although the powder production route influences the level of subsurface oxygen in solid solution, the powder particle size is seen to dominantly affect the overall oxygen content. Point [A], again highlighted in yellow, is at the extreme lower end of the HDH oxygen range in Figure 52. This low oxygen content is not typical for such a small particle size. Point [A] is an example of the degree of protection that can be achieved if measures are taken to protect from oxidation. However, the price of such powder and the measures taken to protect from contamination may exclude this powder as a low-cost option, hence it is unclear whether it could be economically feasible in a commercial operation. The histogram of oxygen values in Figure 53 shows that grade 3 is the most common level of contamination for HDH powders.

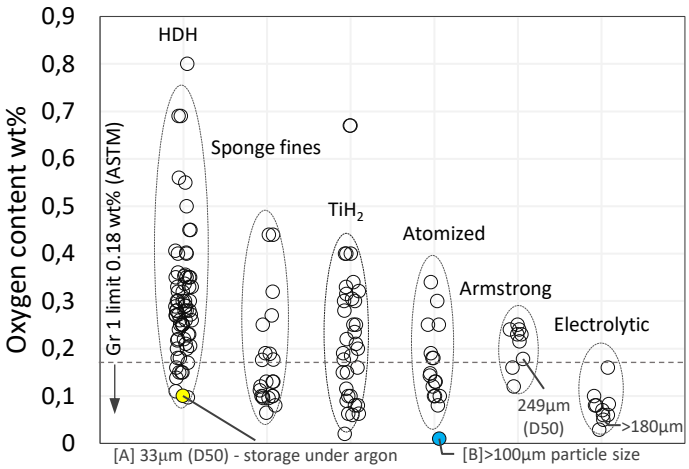

Figure 52: Initial oxygen content of various powders. Data sourced from 86 distinct sources from literature and powder suppliers. A total of 165 data points.

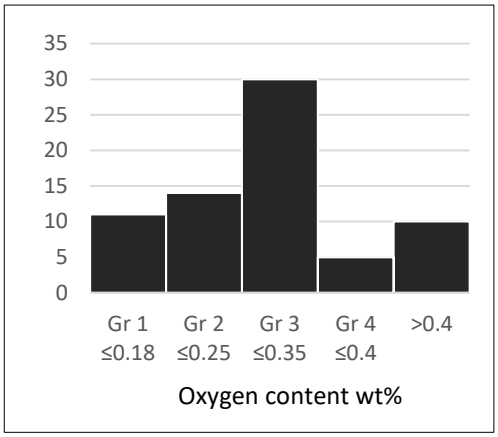

Figure 53: Typical oxygen content of HDH powder (data from 43 sources). Sample size = 68.

The characteristics of the starting powder influence the tendency to pick up oxygen during processing. The higher specific surface area of fine powders increases the risk of surface contamination [117]. Consolidated data from literature in Figure 54 supports this assertion. Compacts made from powders of smaller mean or median particle size are shown to have higher maximum increases in oxygen. Individual studies are identified by different markers. The highest oxygen increases per particle size (circled) are from a range of independent studies, and point to a robust trend. The highest increase for a mean/median particle size greater than 50µm is only 0.07 wt%, whereas for >50µm, the highest increase is 0.1 wt% or more. There are some data points showing a zero increase in oxygen content. However, this does not necessarily indicate that no oxygen pick-up has occurred. The scenario exists where powders are already excessively oxidised when the starting oxygen measurement is taken, and hence there is little further up-take during processing, whereas well protected powders will have a low starting oxygen content, with most pick-up occurring after the initial oxygen measurement. The data points showing a 0% increase all have final oxygen contents of 0.4wt% or greater, hence this argument is supported.

Determining which processing parameters and conditions contribute the most to oxygen pick-up is challenging because there are many variables. Even when isolating for particle size, as in Figure 54, the remaining variables include sintering temperature, time and atmosphere as well as the handling and storage conditions of the powders and green compact. Oxidation of powder inititiates shortly after exposure to air during compaction, and during sintering despite the use of good vacuum conditions (10-3 Pa) [119]. El-Soudani *et al*. [122] tracked oxygen content in the processing of CIP Ti-6Al-4V compacts and reported that the greatest uptake occurred during the grinding of powder to size, the transporting of powder, and compaction. To reduce contamination, the recommendation was to conduct these activies in an inert environment.

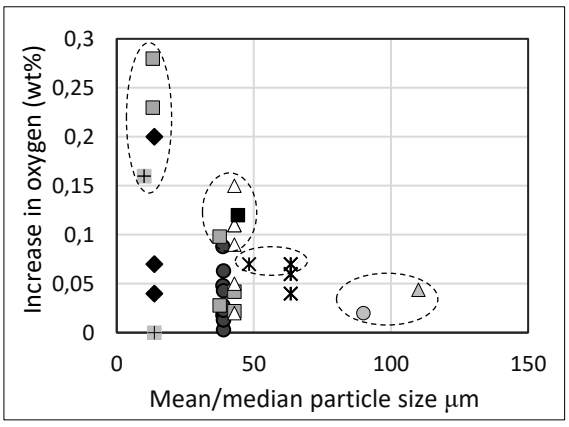

Figure 54: Increase in oxygen content from powder to sintered compact, versus mean/median particles size. (Sponge fines and HDH powder only, DPR, CIP & die pressing). 10 sources.

The following conclusions are drawn regarding the degree of oxygen contamination in powder metallurgy:

- The specific surface area is the most dominant factor affecting 1.) the initial oxygen content in the powders and 2.) the risk of further contamination during processing.
- To produce a compact with grade 3 oxygen (<0.35 wt%) or at best grade 2 (<0.25 wt%), a coarser powder with a mean/median particle size greater than ~50μm is required to limit the starting oxygen content and minimize the risk of further contamination during processing.

3.5.5 Oxygen Content Process Capability for PM

The final oxygen content of PM compacts is compared to typical values for each of the 4 commercially pure grades, as well as the Ti-6Al-4V alloy:

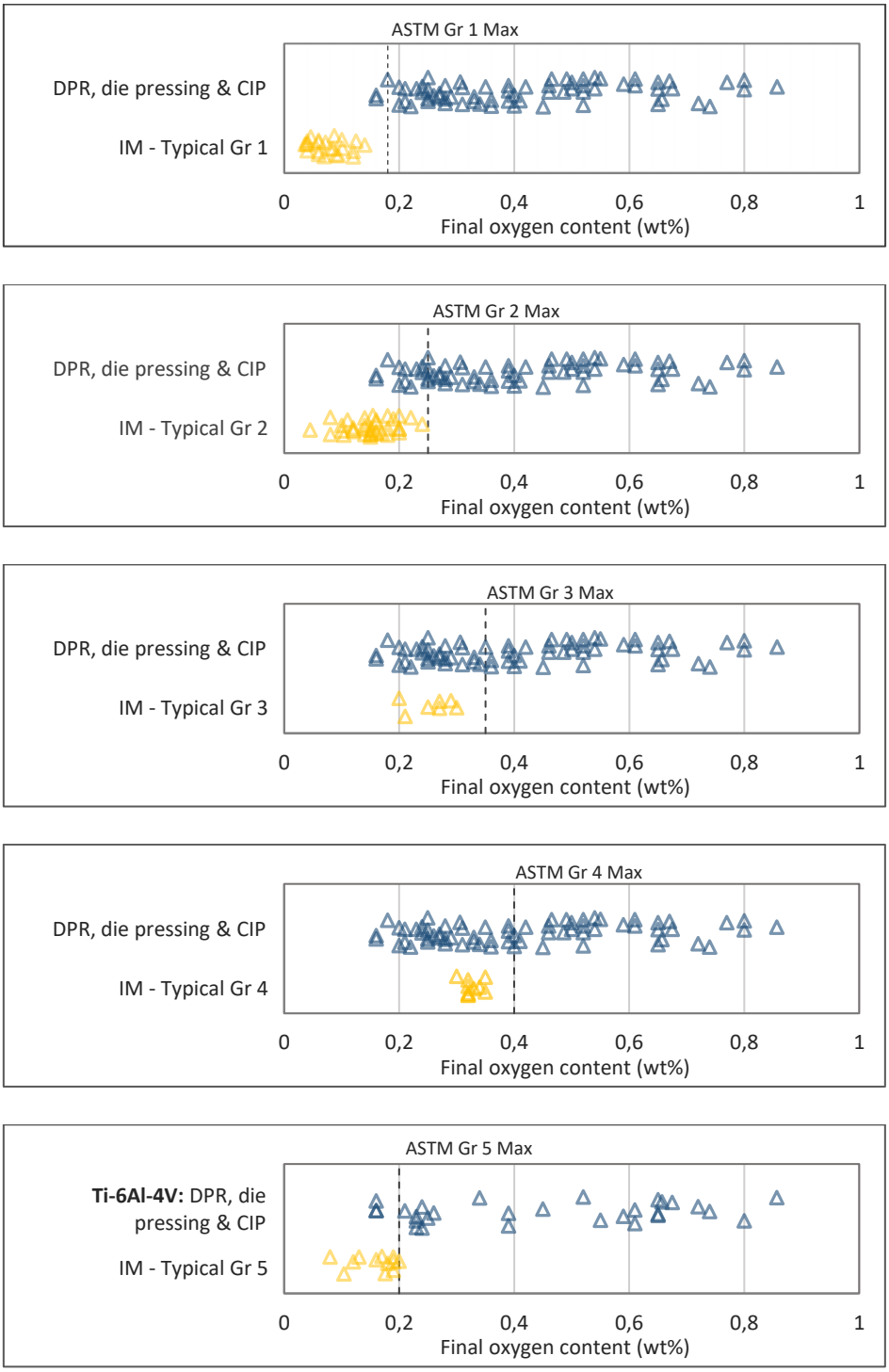

Figure 55: Comparison of final oxygen content for titanium PM compacts and typical oxygen content for wrought product specified to ASTM grades 1 – 5.

The following conclusions are drawn regarding the ability of PM methods to meet each of the ASTM grades:

- **Grade 1:** Some PM compacts are within the grade 1 ASTM limit (dotted line), but most points do not meet the typical oxygen performance of grade 1 wrought product.
- **Grade 2:** The best performing PM compacts demonstrate the ability to match the middle, or more commonly, the tail-end of the typical oxygen content range for grade 2 wrought product.
- **Grade 3 & 4:** PM process capabilities are better suited to meeting the typical performance of grade 3 and 4 wrought products.
- **Ti-6Al-4V:** The oxygen content range for Ti-6Al-4V wrought product is closer to the specification limit than that seen for the pure titanium grades. Even so, only a limited number of PM points are within the typical wrought product range.

4 An Alternative Route to Flat Product

While DPR is the most direct route to producing flat product of near final thickness, the feeding of powder directly into a rolling mill limits the feedstock to only those powders that provide adequate green strip strength. Such powders include sponge fines and HDH powders, which have the morphology (spongy and irregular) as well as sufficient ductility to enable good particle interlocking through deformation, resulting in good green strength. TiH_2 is not suitable for DPR as it is brittle, resulting in poor green strength, but it offers process and cost advantages that make it a contender, albeit via a less direct route. TiH_2 can be cold isostatically pressed into a preform, dehydrogenated via vacuum sintering, and then thermo-mechanically rolled into plate or sheet. The use of hydrogen as a temporary alloying element is said to positively affect sintering and its activation, resulting in higher relative densities and improved mechanical properties [123]. More importantly, the oxygen content of the final product is reportedly lower, as will be discussed below.

The TiH_2 preform route is shown as route 2 in Figure 56. DPR (route 3) and the conventional ingot metallurgy process (route 1) are shown alongside for comparison. The TiH_2 preform route offers a middle way, being more direct than the high temperature, energy intensive ingot route.

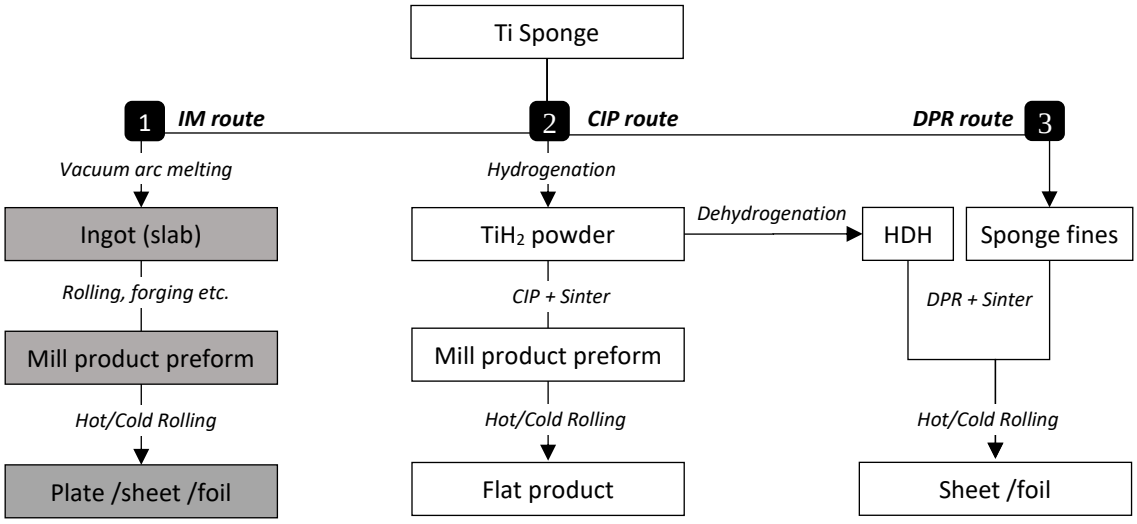

Figure 56: Three feasible routes to manufacturing titanium flat product.

4.1 TiH_2 Sinterability

Much of the interest in titanium hydride powder is due to its enhanced sinterability and, consequently, improved density. The brittleness and low strength of titanium hydride (150–250 MPa [100]) enables additional particle crushing during compaction, resulting in "fine, close-packed fragments with small uniformly distributed pores" [99]. These pores are reportedly easy to heal upon sintering [99], and the freshly exposed fragmented surfaces are believed to be favorable for the sintering process, leading to reduced porosity in the sintered compact [124]. In comparison, compacts made from the ductile, titanium-based powders have been found to exhibit larger pores, the size of which is dependent on the applied pressure during compaction, and these pores survive after sintering [99].

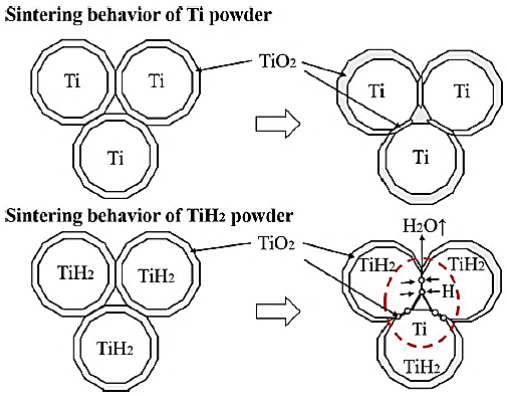

Figure 57: Comparison of Ti and TiH_2 sintering behaviour [124].

During the dehydrogenation of TiH_2, surface oxides are reduced by atomic hydrogen released from the crystal lattice, creating oxide-free areas and activating mass transfer through the interfaces [123]. Figure 57 shows the advantageous sintering behavior of TiH_2 versus Titanium powder. H_20 (g) is released as the thickness of the surface oxide film is reduced, which improves the contact between adjacent particles and accelerates bonding [125]. This mechanism also plays a part in minimizing the oxygen content in the final product, as will be discussed later.

Improving the degree of sintering is a key objective in powder metallurgy research. It has been claimed that if PM alloys are to achieve an acceptable level of mechanical properties in terms of strength, ductility and fatigue strength, they will need to achieve not only 1.) an acceptable impurity content, and 2.) a homogenous chemical composition and microstructure, but also 3.) a relative density of greater than 98% [99]. For high mechanical properties, Ivasishin *et al*. [126] claim that 99% density is required.

While there is evidence that TiH_2 does provide improved results for sintered densities, the ultimate degree of improvement varies from source to source. TiH_2 has enabled the attainment of sintered densities of >98% [99] [115]. Ivasishin *et al*. [126] put this as high as 99%. A range of 98.5-99.5% has also been reported [127]. On the other hand, the consolidation of non-hydride powders (including alloying additions) have been reported to achieve only 90–95% sintered density [127], and simple press and sinter consolidation of non-hydride alloy powders do not normally exceed 95% [99] [126].

Consolidated data from literature in Figure 58, for cold pressed Titanium and Ti-6Al-4V samples from TiH_2 and non-hydride powders, provides a more comprehensive comparison of the sintering capability of the two powders. The sintered density data has been presented in relation to green density due to the dependence on the degree of the preceding compaction. The sintering temperature range has been limited to 1000°C or greater, with 60% of data 1250°C≤ T_6 ≤1375°C. The time at sintering is variable. The assertions reported in literature, regarding upper sintered density bounds for the two powders (hydride and non-hydride), are labelled.

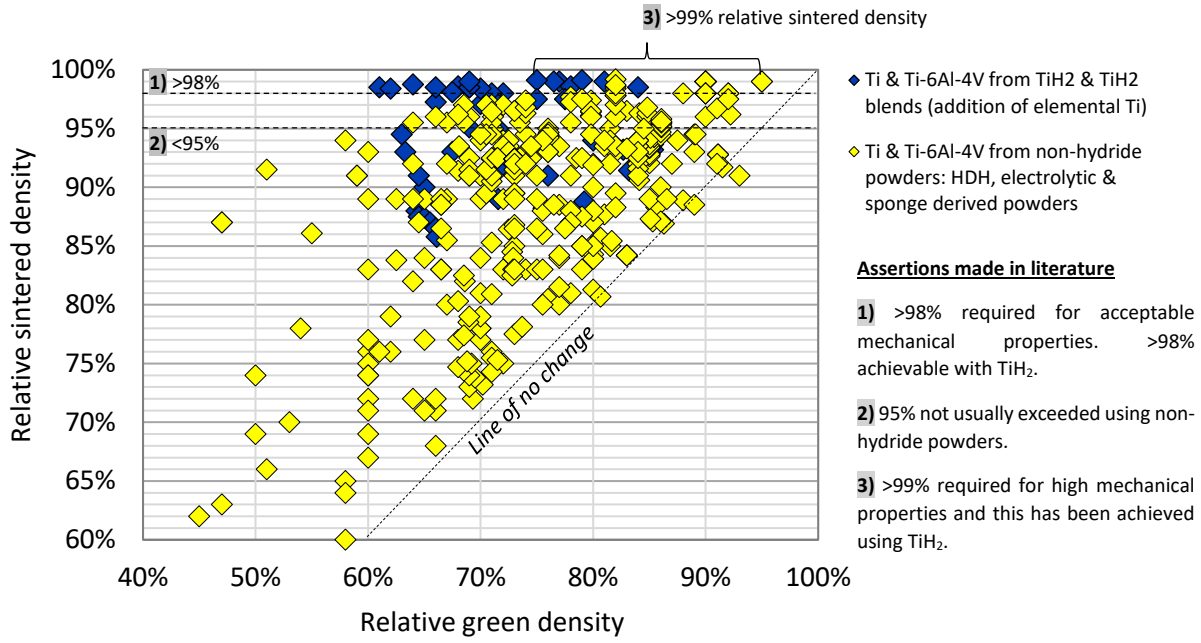

Figure 58: Comparison of green and sintered densities for Titanium and Ti-6Al-4V compacts made from TiH2/TiH2 blends (data from 7 sources) and pure titanium powder (31 sources). Simple cold compaction methods only – CIP, die pressing and DPR. Sintering temperatures ≥1000°C. 360 total data points.

Sintered density data for the TiH_2 route (blue) is positioned predominantly above the 98% line i.e. the target value cited as a requirement for good mechanical properties. TiH_2 also enables sintered densities of 99%, but this is seen to be possible only for compacts that had a green density of greater than 77%. For non-hydride samples (yellow), Figure 58 shows that a minimum green density of 82% is required for the achievement of sintered densities greater than 98%.

For TiH_2 compacts, the lack of dependence of sintered density on green density is evident in comparison to the non-hydride data set. This is seen more clearly when the data are separated as shown in Figure 59 and Figure 60. TiH_2 samples are shown to attain over 98% sintered density regardless of initial green density, which ranges from approximately 60% to 85%. TiH_2 and TiH_2 blends (i.e. addition of elemental titanium powder) have shown to attain over 98% sintered density. The combined data in Figure 60 gives an indication of the upper boundary profile for sintered density, as a function of green density, for non-hydride compacts.

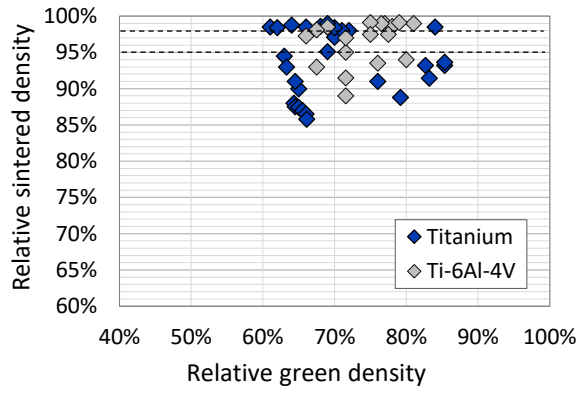

Figure 59: Sintered and green densities for Titanium and Ti-6Al-4V compacts derived from TiH2 and TiH2 blends. Data from 7 sources.

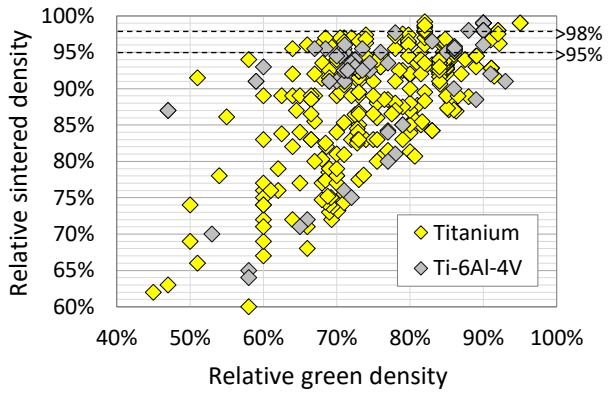

Figure 60: Titanium and Ti-6Al-4V from HDH, electrolytic and sponge derived powders. Data from 31 sources.

While Cui *et al*. [128], Ivasishin *et al*. [126] and Sachdev *et al*. [127] claim that 95% sintered density is not normally attainable for non-hydride compacts, 8% of data in Figure 59 sits above the 98% sintered density line, and as much as 24% sits above 95%. However, the attainment of such high sintered density comes at a cost. Compacts with higher sintered densities are characterized by higher oxygen content, as shown in consolidated data from literature in Figure 61 below. This data is for HDH powder compacts subjected to sintering temperatures >1000°C. The maximum O wt% for the ASTM grade 2 specification is shown alongside, and none of the samples with over 95% density meet this. The correlation between oxygen and sintered density is due to the underlying influence of particle size. As powder size decreases, oxygen content increases, due to the increasing specific surface area on which an oxide layer forms. However, decreasing particle size also leads to shorter diffusion distances and smaller pores, which along with the greater specific surface area, enhances the diffusion process during sintering [129]. This is seen in Figure 63 below, where a decreasing median particle size for HDH powder is accompanied by an increase in sintered density. In this data set, 95% sintered density is attainable only for powders with a median particle size of 53µm or less. However, in Figure 64, HDH powders with a median particle size of 53µm or less have an oxygen content that exceeds the ASTM grade 2 specification. Considering that oxygen content is expected to increase during compaction and sintering, the **final** oxygen content for this powder size will not meet grade 2. On the other hand, TiH_2 data in Figure 62 shows that high sintered densities (>95%) can be achieved while maintaining an oxygen content within the specification of grade 2 (0.25 wt%) and grade 1 (0.18 wt%). The minimization of final oxygen content via the TiH_2 route will be discussed in the following section.

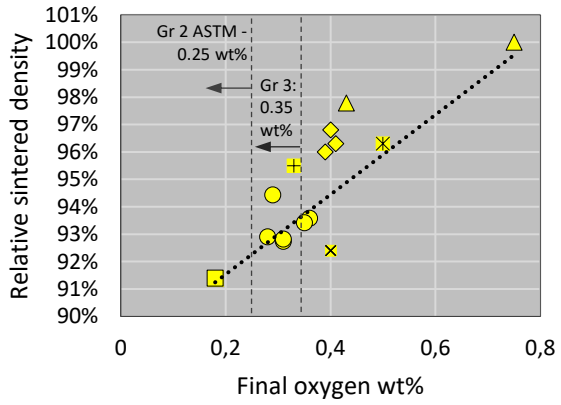

Figure 61: Relative sintered density versus final oxygen content for cold compacted titanium samples from HDH powder. Sintering temperature ≥1000°C. Data from 8 sources.

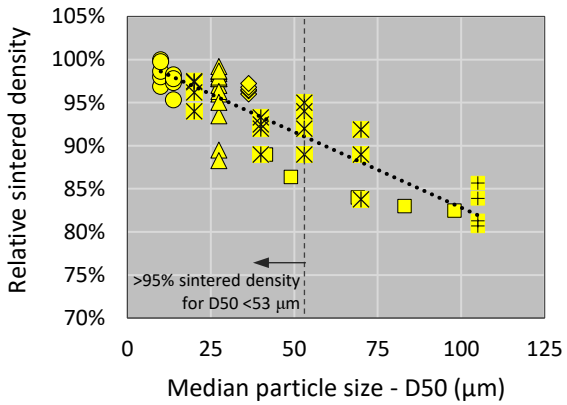

Figure 62: Relative sintered density versus median particle size for cold compacted titanium samples from HDH powder. Sintering temperature ≥1000°C. Compaction pressure ≥200MPa. Data from 6 sources.

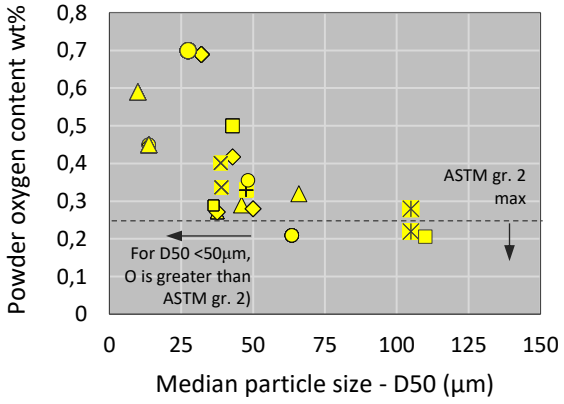

Figure 63: Initial oxygen content versus median particle size for HDH powder. Data from 16 sources.

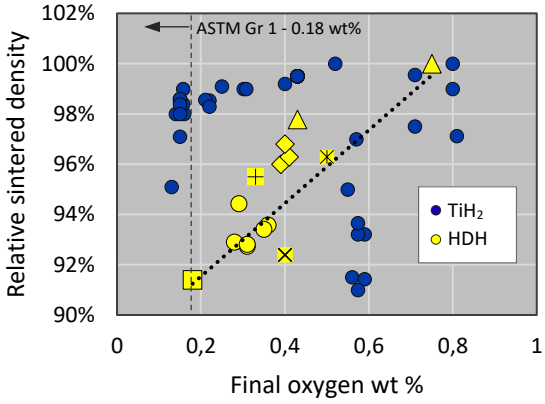

Figure 64: Relative sintered density versus final oxygen content for cold compacted titanium samples from HDH AND TiH_2 powder. Sintering temperature ≥1000°C. TiH2 data from 10 sources.

Even though the data consolidated from literature has been sourced from different studies - comprising various sintering temperatures, atmospheres and sintering times - it is evident that particle size is a dominant parameter. In this investigation, the median has been found to be most effective in characterizing particle size with a single measurement. Therefore, selecting median particle size as a common parameter, Figure 65 shows that the sintered density for compacts made from TiH_2 powder is generally higher than compacts made from non-hydride powder of similar median particle size.

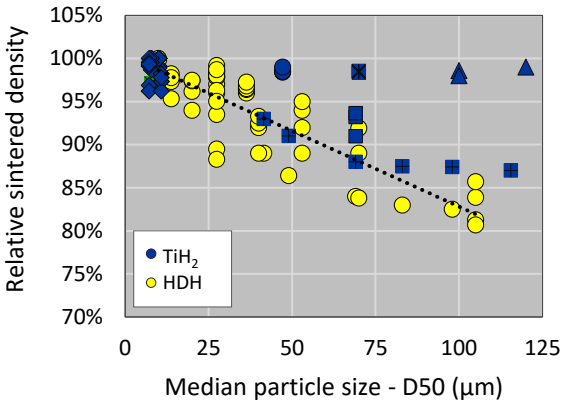

Figure 65: Relative sintered density versus median particle size for cold compacted titanium samples from HDH and TiH_2 powder. Sintering temperature ≥1000°C. Compaction pressure ≥200Mpa. TiH_2 data from 7 sources.

4.2 TiH_2 Refinement

Oxygen Content

Several researchers have observed the advantageous ability of TiH_2 to limit oxygen contamination. In the comparison of TiH_2 and Ti powder derived from the same sponge source and of similar particle size, it was found that TiH_2 derived compacts picked up less oxygen than compacts made from elemental titanium powder [130]. Oh *et al*. [131] and Yang *et al*. [132] reported similar results for Ti-6Al-4V and Ti-C respectively. Ivasishin *et al*. [119] found that the use of TiH_2 powder could limit oxygen content to as low as 0.15 wt%, compared to 0.2 wt% for pure titanium derived compacts. As well as limiting oxygen pick-up, there is also evidence of final oxygen contents being lower than the oxygen of the starting TiH_2 powder. Zheng *et al*. [133] observed a decrease from 0.4 wt% oxygen in the TiH_2 powder to 0.28 wt% in the induction heated and hot extruded compact. Yang *et al*. [132] found that pressed and sintered Ti-C compacts from TiH_2 powder had a lower oxygen content (0.34 wt%) than the starting TiH_2 powder (0.4 wt%).

The limited pick-up or decrease in oxygen during sintering is attributed to the reduction of surface oxides by atomic hydrogen released during dehydrogenation. This has been experimentally validated by Wang *et al*. [125], who used TG-MS (thermogravimetric analysis–mass spectrometry) to confirm that the release of hydrogen is accompanied by the release of H_2O. During the sintering of pure titanium, the surface oxides are instead dissolved, increasing the overall oxygen content of the final product [123]. Using X-ray photoelectron spectroscopy depth profiles of the intermediate TiH_2 powder, and the final HDH powder, Zhang *et al*. [134] suggested that the lower oxygen content in the dehydrided powder was due to a thinner oxide layer. In a similar experiment, Ivasishin *et al*. [119] came to the same conclusion. They found that for both TiH_2 and Ti powder, oxygen was present as TiO_2 scale as well as H_2O adsorbed on the surface due to contact with atmospheric moisture. After dehydrogenation of TiH_2 the thickness of the oxide scale and amount of adsorbed H_2O was lower.

In the TiH_2 route, the removal of oxygen impurities is more effective if water vapor has the chance to escape from the compact before the interconnected porosity is closed [119]. This is the proposed key difference between the use of TiH_2 and HDH powder. Although adsorbed water is also reduced during the dehydrogenation of HDH **powder**, the particles are at risk of reforming oxide layers during subsequent handling and processing, whereas in the TiH_2 route, the **compact** is dehydrogenated and the interconnected porosity closed, preventing contamination of the reduced surfaces.

Data Consolidation

Oxygen data for TiH_2 derived compacts was sourced from literature and consolidated in Figure 66 (colored in blue). This data is compared to the typical oxygen content for non-hydride derived compacts (1) and wrought titanium product (3). In general, the process capability of the TiH_2 route is better, as data is positioned more densely to the left, to the lower end of the oxygen scale, than the non-hydride derived data set.

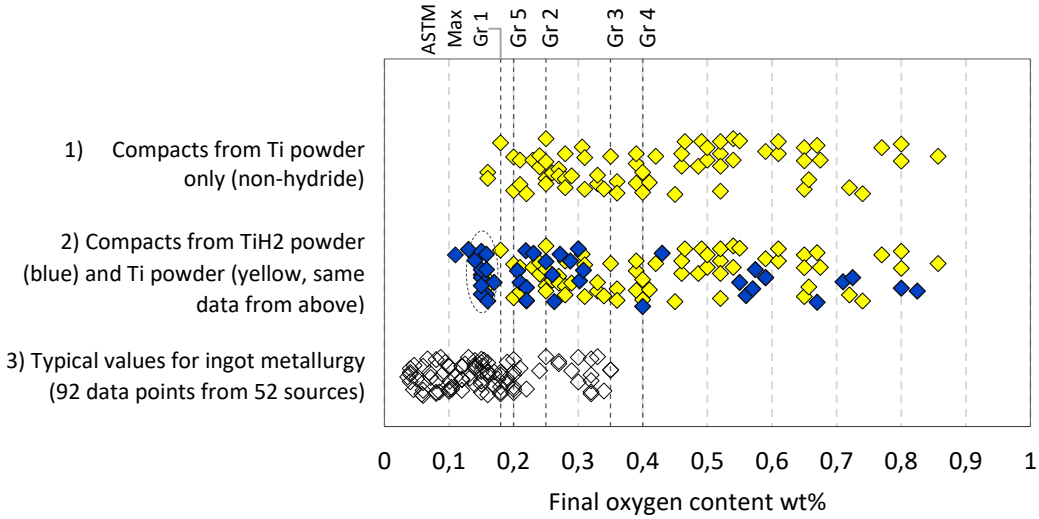

Figure 66: Typical oxygen content for compacts derived from titanium (1) and TiH_2 powder (2). Room temperature consolidation only (DPR, die pressing or CIP). Typical oxygen content for conventional wrought product (3) shown for comparison. TiH_2 data from 14 sources.

Chlorine Refinement

It has also been shown that hydrogen emitted during dehydrogenation can reduce the chlorine content. Evidence of this refinement mechanism is the presence of HCl emitted during the dehydrogenation temperature range, and the lower trace amounts of Cl in the dehydrogenated particulate, the HDH powder, versus the starting stock, TiH_2 [297]. The consolidated chlorine data from literature in Figure 67 supports this. Chlorine levels in the HDH data set are markedly reduced compared to the TiH_2 data set. It has been shown that chloride contamination as high as 0.1 wt% can be reduced to 0.015 wt% when heating TiH_2 in a vacuum [100]. Residual impurities from the Kroll reduction process (Mg and Na) can also reportedly be reduced and removed via this method (e.g. 0.8 wt% Mg has been reduced to 0.0048 wt%) [135].

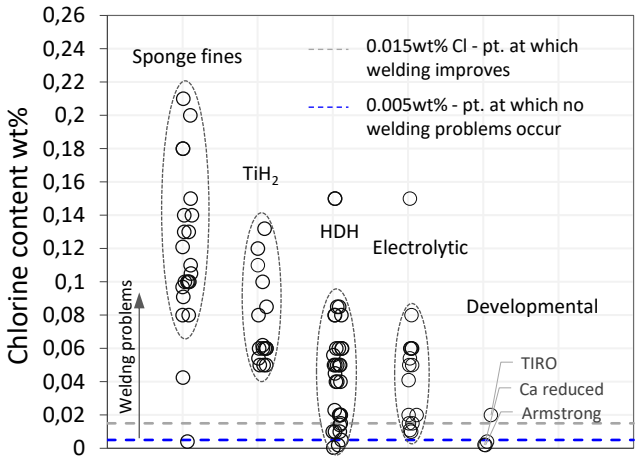

Figure 67: Chlorine content of various titanium powders. Data from literature and quotations - 41 sources.

A key difference between the use of TiH_2 and HDH powder is that during compaction, the more brittle TiH_2 particles are crushed, and residual chlorides are freed from closed pores, decreasing the fraction of sub-surface chlorides and increasing the fraction of chlorides exposed on the surface of the fragments [99]. Since there is still interconnected porosity in the TiH_2 compact during the initial low temperature stage of dehydrogenation, the residual chloride is bound to atomic hydrogen and desorbed as volatile HCl [119]. Hence, the dehydrogenation of the TiH_2 **compact** realizes an additional cleaning advantage over the dehydrogenation of TiH_2 **powder** to produce HDH powder.

Experimental work by ADMA has shown that a starting content of 0.08 wt% chlorine in the TiH_2 powder can be reduced to 0.015 wt% in the final Ti-6Al-4V alloy. A final chlorine content as low as 0.001 wt% has also been reported by ADMA. The implication of chlorine refinement via the TiH_2 route is that the PM product may be weldable, although as discussed earlier, there has been little research on the impact of chlorine on the weldability of PM product, and even less so on TiH_2 derived PM product. ADMA claims that preliminary tests have shown sufficient weldability [136].

5 Performance of PM Product

5.1 Mechanical properties of Titanium PM product

Elongation, UTS and Oxygen

The relative performance of TiH_2 derived titanium compacts was investigated by comparing static mechanical properties of hydride and non-hydride compacts. Data from literature published from 2000-2015 was consolidated, and is presented in Figure 68. The non-hydride data is separated into two process routes:

- **Green markers:** DPR followed by sintering only, or sintering + cold/hot rolling + annealing
- **White markers:** CIP/die pressing followed by sintering only

The Hydride data is separated into two processing routes:

- **Blue markers**: TiH_2 CIP/die pressing + Sintering Only
- **Purple markers:** TiH_2 CIP/die pressing + Sintering + Hot Roll + Anneal

The TiH_2 CIP + Sinter + Hot Roll + Anneal route (purple) is the alternative route (discussed in section 4) to producing flat product (in this case plate) with similarities in processing to the DPR route (green). The comparison of these two routes in Figure 68 shows that the best performing DPR sample, with an elongation of 26% (ORNL), outperforms the best performing TiH_2 CIP sample (ADMA), with 23%. There is a DPR sample with 27% elongation (CSIRO) but this value is only for the rolling direction, and the elongation perpendicular to rolling is only 20%. The ASTM B265 specification for grade 2 sheet and plate titanium is included for comparison. Both the DPR and TiH_2 CIP route (purple) meet the minimum specification, although, overall, the performance of DPR is better. It is noted that the TiH_2 CIP data set is small, and from a single source, ADMA. Even so, it is an important data set due to ADMA's recent commercialisation of this route.

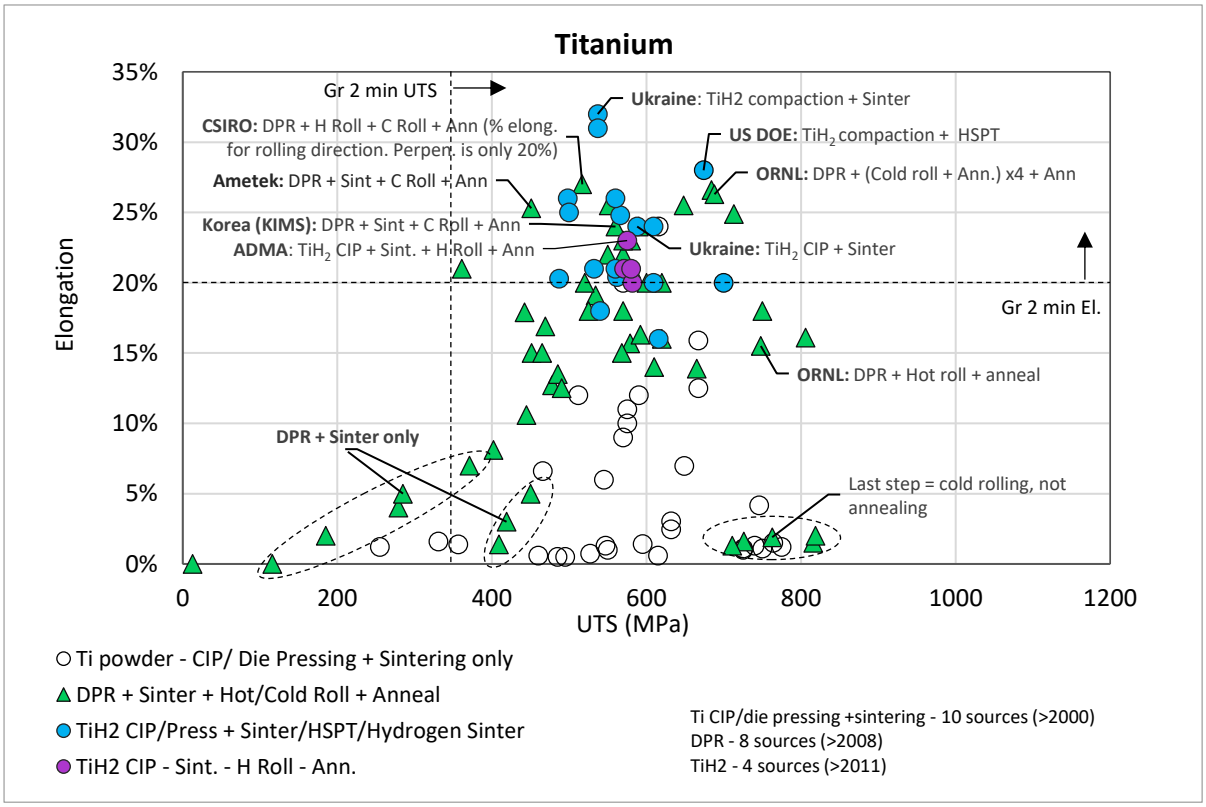

Figure 68: Performance in terms of elongation and ultimate tensile strength of hydride and non-hydride derived compacts from various process routes. Data from research from 2000 – 2015.

Further observations from Figure 68 are the following: firstly, compaction + sintering of hydride powder (blue) outperforms compaction + sintering of non – hydride powder (white). i.e. for a similar processing route, hydride derived compacts exhibit the highest elongation compared to non-hydride compacts. Secondly, compaction + sintering of hydride-derived compacts (blue) outperforms DPR samples (green), even though the DPR strip has been thermo-mechanically worked followed by a final anneal. DPR samples that were only sintered or did not undergo a final anneal exhibit poor ductility (circled in Figure 68). As expected, DPR samples generally exhibit higher elongation than non-hydride CIP/press + sinter only samples due to the additional post-sintering cold and/or hot rolling and annealing which is likely to close remaining porosity. However, a further assessment of the data suggests that lower oxygen content in the DPR data set may also be a contributing factor. Of the data in Figure 68 above, those points with accompanying oxygen data have been presented in Figure 69 below. The CIP/Press + sinter data (white) have higher final oxygen contents, which is likely to also contribute to the low elongation. The TiH_2 data set (blue and purple) is the only set to fall within the limits for both the minimum elongation of 20% and maximum oxygen content of 0.25 wt%. By overlaying gradated density data in Figure 101, it is evident that high oxygen and poor density are the reason for the poor performance of the non-hydride CIP/Press + sinter route (white). Many of the DPR samples do not meet the grade 2 oxygen limit, but do meet the grade 2 elongation requirement, possibly due to high relative densities, as seen in Figure 101. The DPR route, by necessity, involves additional processing, and hence the final product has a relative density of over 99% [10][12][28][29][30] [31][32][34][35].

The titanium hydride derived compacts meet both the grade 2 oxygen and elongation specification, possibly due to a combination of low oxygen content (<0.25 wt%) and high final density (greater than 98%).

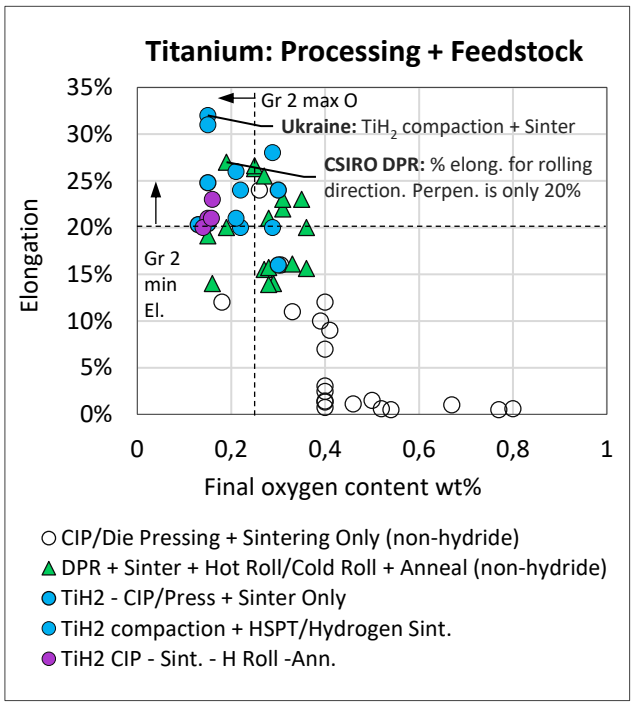

Figure 69: Elongation versus oxygen content for titanium compacts from hydride and non-hydride powder. (12 sources)

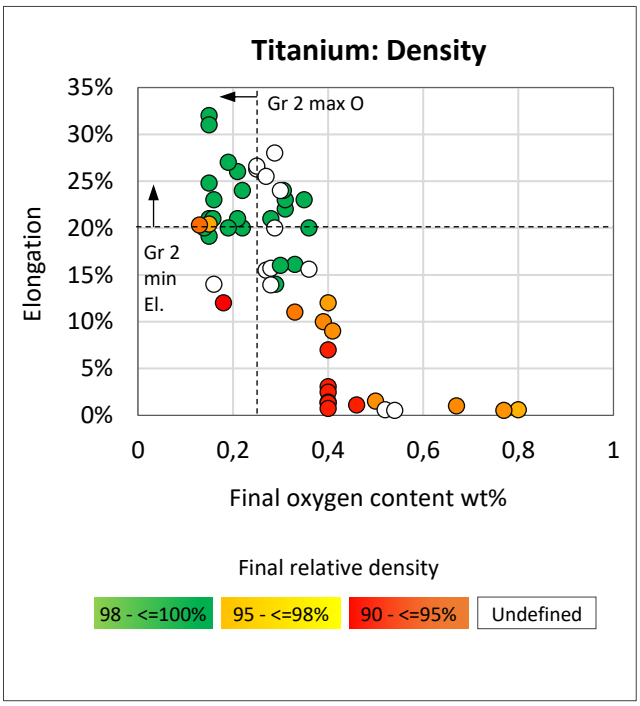

Figure 70: Elongation versus oxygen content for titanium compacts from hydride and non-hydride powder with final relative densities. (12 sources)

Elongation and UTS

The typical properties of wrought product (grades 1 – 4) are shown in comparison to the consolidated PM data, in Figure 71 below. The grade 2 minimum elongation line is given as a reference. It is evident that typical elongation for grade 2 product (orange) is often 5% above this minimum specification. The best performing TiH_2 derived compact matches typical grade 2 properties, although much of the other TiH_2 data meets only grade 3 and 4. The best performing DPR points meets only typical grade 3 and 4 properties (solid circle).

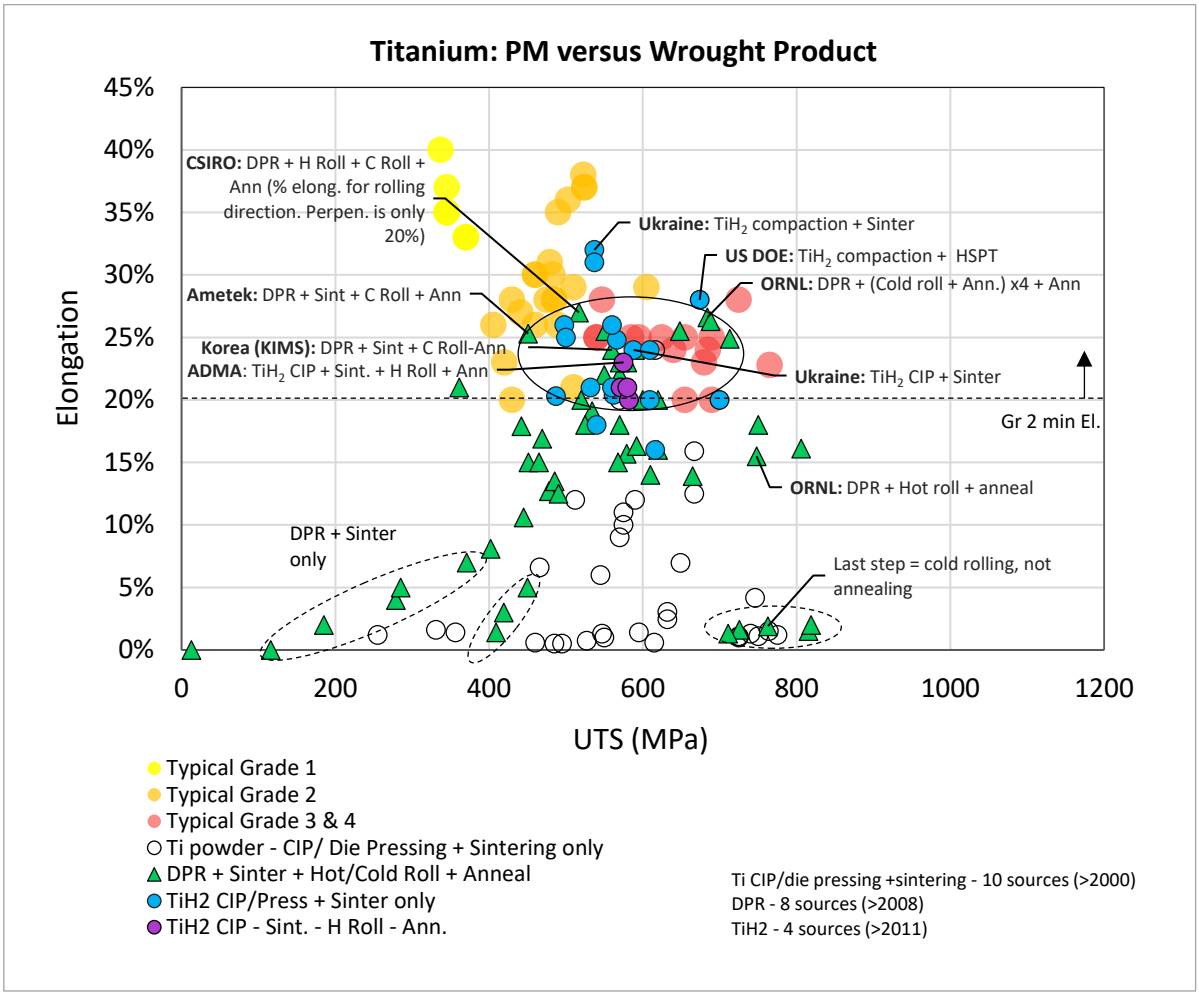

Figure 71: Elongation and ultimate tensile strength performance of wrought product versus PM compacts from various process routes and hydride/non-hydride feedstock.

PM Titanium versus Typical Wrought Performance - Elongation and Oxygen

Reference points for typical oxygen and elongation for grade 1 and 2 wrought product [137] are shown in comparison to the performance of PM, in Figure 72. None of the PM compacts come near the typical grade 1 reference point, and most do not meet the typical grade 2 reference point. The grade 3 and 4 expectation for pure titanium PM product is further confirmed.

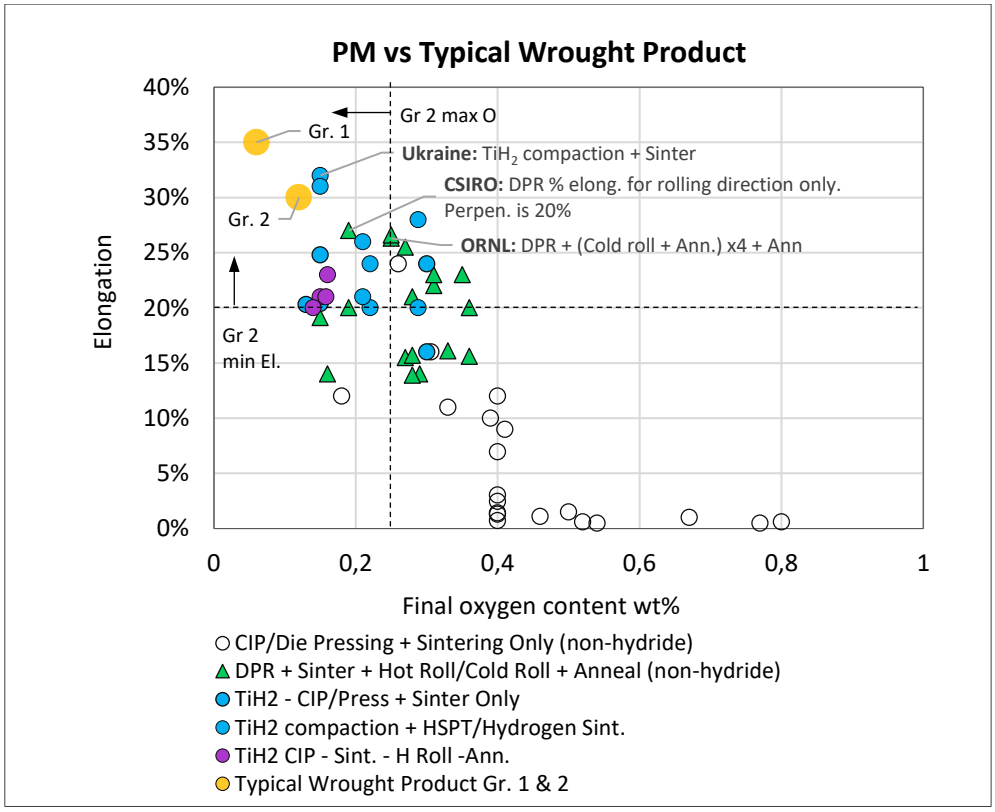

Figure 72: Typical oxygen and elongation content for grade 1 and 2 wrought product versus PM properties.

The consolidation of data suggests that oxygen is the primary factor hindering the tensile performance of pure titanium DPR product. Although additional measures to protect from contamination could reduce the final oxygen content, Figure 73 shows that the lowest DPR oxygen contents are already at the lower end of the PM oxygen range e.g. CSIRO's best performing DPR sample with 27% elongation and 0.19 wt% oxygen in Figure 72 is shown relative to the PM oxygen range in Figure 73.

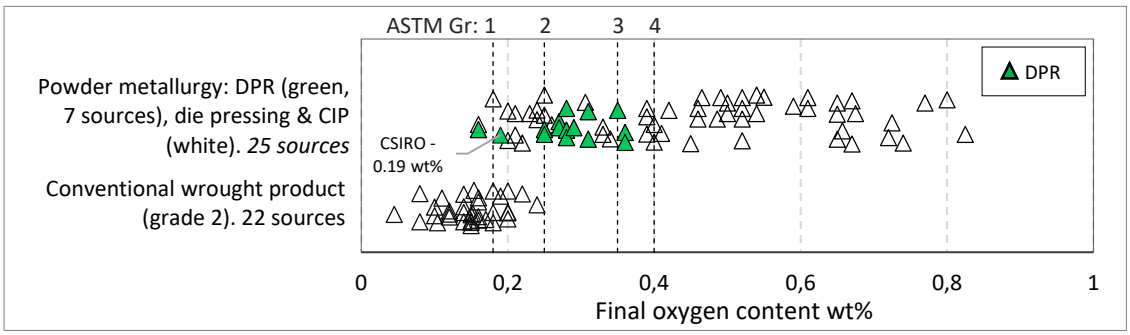

Figure 73: Typical oxygen content for powder metallurgy (PM) versus conventional wrought product.

There is an ASTM specification for powder metallurgy components (B988 – 13), which covers cold isostatic pressing, uniaxial pressing, DPR, hot isostatic pressing, powder forging, pneumatic isostatic forging, sintering and heat treatment. This specification has two tensile requirements for each grade, one of which is the same as

values specified for wrought plate and sheet, the other of which is 90% of these values. This adjustment may indicate acknowledgment of the difficulty in achieving similar properties to wrought product. However, the wider acceptance of PM products ultimately comes down to the customer and their expectation of the properties of that product, around which their processing and fabrication operations are designed.

In Summary

The consolidation of titanium PM data, and the comparison to typical properties of wrought product, has shown the following:

- Titanium DPR strip meets the typical static tensile properties of grade 3 and 4 wrought sheet.
- The best performing TiH_2 derived titanium compacts outperform the non-hydride data set. However, in general, the TiH_2 data set meets the typical static tensile properties of grade 3 and 4 wrought sheet. Hence, TiH_2 has not demonstrated a significant relative advantage over non-hydride derived titanium.
- Fully processed DPR sheet performs better, in terms of elongation, than sheet rolled from TiH_2 preforms (purple points). However, the data set for TiH_2 derived sheet is small, and additional data is required.

5.2 Mechanical properties of Ti-6Al-4V PM product

Elongation, UTS and Oxygen

The mechanical properties of Ti-6Al-4V PM compacts were similarly assessed, as seen in Figure 74. The relative performance of processing routes and starting stock (hydride versus non-hydride) for Ti-6Al-4V compacts were compared. Hydride derived Ti-6Al-4V compacts (blue and purple) exhibit the highest elongation. Most of the DPR Ti-6Al-4V compacts do not meet the minimum elongation of 10% (for annealed sheet [138]). However, the DPR data set is small, and most of the Ti-6Al-4V DPR compacts were not thermo-mechanically worked, and so there is limited data regarding tensile properties of fully processed Ti-6Al-4V DPR strip.

Two sources that did follow through on processing are (green labels in Figure 74):

1. **ADMA**: process route: DPR - C Roll - Ann. - C Roll - Sint. Elongation: 10% (blended elemental powder)
2. **CSIRO**: process route: DPR - H Roll - H Roll - Ann. - Ann. Elongation: 8.8% (blended elemental powder)

The CSIRO reported that poor elongation could possibly be attributed to the relatively coarse microstructure and an oxygen content of 0.23 wt%, which is above the grade 5 max of 0.2 wt%. ADMA just met the minimum required elongation of 10%.

The best performing DPR compact (ADMA, yellow point), with over 12% elongation and no post-sintering processing, was made from a TiH_2 and titanium powder blend. This is the only example of direct rolling of this powder. The green strength of TiH_2 compacts is known to be problematic due to hydrogen embrittling, and use of this feedstock for DPR is unlikely to be operationally feasible. In an email correspondence with ADMA, it was confirmed that their commercial powder rolling operation does not use TiH_2 powder because of these problems.

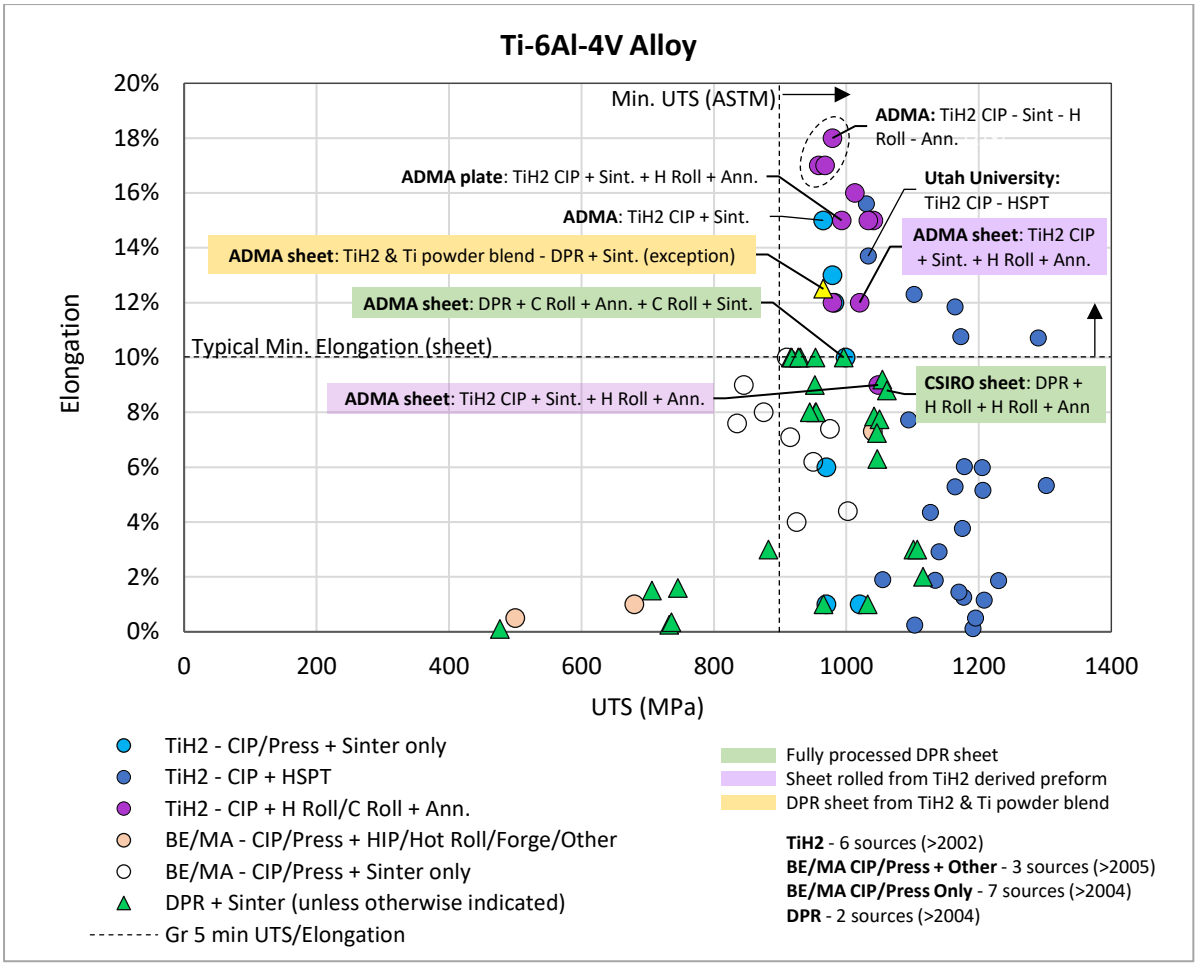

Figure 74: Elongation and ultimate tensile strength performance of hydride and non-hydride derived Ti-6Al-4V compacts from various process routes. Data from papers from 2004 – 2016.

A large proportion of the TiH_2 compacts were processed via hydrogen sintering and phase transformation (HSPT), and exhibit good elongation without post-sintering thermomechanical work. HSPT is a process where TiH_2 compacts are sintered under a partial pressure of hydrogen that is dynamically controlled to refine the microstructure via phase transformations [139]. A further assessment of the data shows that a large proportion of the TiH_2-HSPT derived samples have a high oxygen content (0.4 wt%), as seen circled in Figure 75 below. Additional density information (Figure 76) for the same circled data shows no dependence of elongation on density. All points have a high relative density, indicating that there is another factor at play. The circled data is from a single source, where it was found that the ductility of the sintered compact was dependent on the size of the largest pore, regardless of the high average relative density of samples [115]. The combination of high oxygen content and extreme pore size severely degraded ductility.

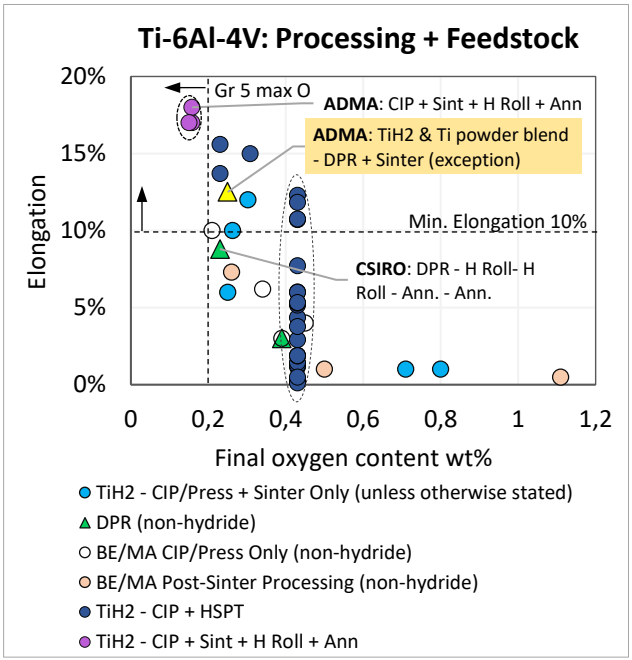

Figure 75: Elongation versus oxygen content for Ti-6Al-4V compacts from hydride and non-hydride powder. (14 sources)

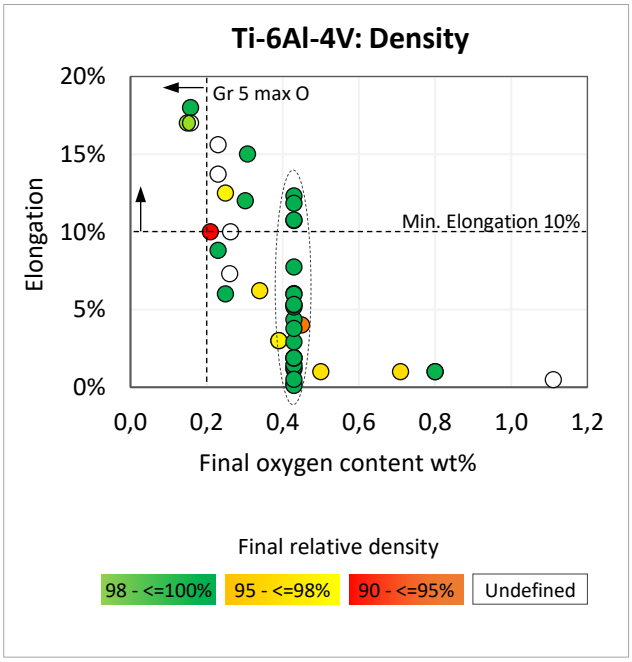

Figure 76: Elongation versus oxygen content for Ti-6Al-4V compacts from hydride and non-hydride powder with final relative densities. (14 sources)

Except for the best performing TiH_2 derived points, most of the compacts in Figure 75 do not meet the minimum oxygen requirement, but several meet the elongation requirement. This may be due to Ti-6Al-4V's tolerance for oxygen. It has been found that the critical oxygen content at which the ductility of Ti-6Al-4V begins to deteriorate severely is greater than the ASTM limit of 0.2 wt%. For injection moulded Ti-6Al-4V compacts, Yan *et al*. [140] and Miura *et al*. [141] reported a critical oxygen level of 0.33 wt% (for 97.1-97.6% density) and 0.35 wt% (for >94.5% density) respectively, at which point ductility deteriorated considerably. Figure 77 (left) shows the data plotted by Miura *et al*. [141]. Ebel *et al*. [142] reported a similar critical value (0.32 wt%) for MIM Ti-6Al-4V, as seen in Figure 77 (right). UTS and YS increase but elongation remains stable until the critical point. The consolidated data in Figure 75 suggests a critical oxygen value of 0.43 wt%, although this is heavily influenced by the large set of HSPT data from [115], in which the high relative density (99.02 to 99.5 %) and fine microstructure, reportedly produced via HSPT, could explain the increased tolerance for oxygen.

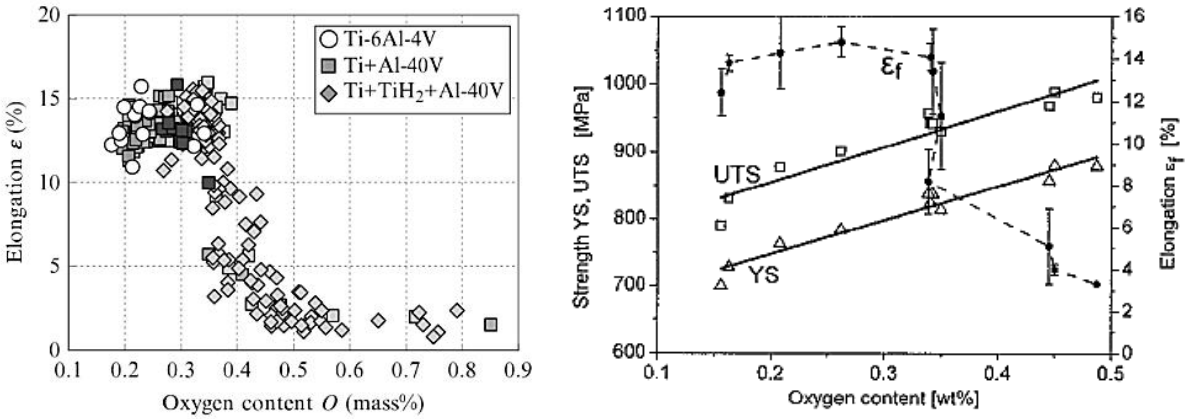

Figure 77: Effect of oxygen content on tensile properties of MIM Ti-6Al-4V. [141] left and [142] right.

In the ASTM specification for PM components (B988 – 13), the chemical compositions for pure titanium (grades 1-4) are the same as that specified for wrought plate and sheet (B265-15). However, for Ti-6Al-4V, the oxygen limit has been adjusted from 0.2 wt% to 0.3 wt%. This decision could have been taken because of Ti-6Al-4V's

tolerance for oxygen, and points to the possibility of relaxing the oxygen limit for PM product if tensile properties comparable to wrought product are still achieved.

Typical Wrought Performance versus PM for Ti-6Al-4V

Typical elongation and UTS values for commercial Ti-6Al-4V plate and sheet are given in Table 4, and shown in Figure 78 (as orange points) in comparison to the performance of PM compacts.

Table 4: Typical mechanical properties of Ti-6Al-4V wrought flat product

Commercial Ti-6Al-4V wrought product	Elongation	UTS (MPa)	Source
0.7 mm thick sheet	14%	1054	[143]
>0.8 mm annealed sheet	14%	990	[144]
1 mm thick sheet	13%	999	[145]
1.5 mm thick sheet	17%	1043	[146]
2 mm thick sheet	10-12%	1045-1120	[147]
4 mm thick sheet	19%	1057	[148]
6 mm thick sheet	17%	987	[149]
Annealed sheet	10%	1160	[138]
Timet Sheet	12%	1035	[150]
AMS (aerospace) annealed sheet & plate	15-20%	951-1068	[151]
Standard grade plate	13%	951	[152]
Standard grade sheet	10%	910	[152]
Timet Annealed plate	16%	940	[144]

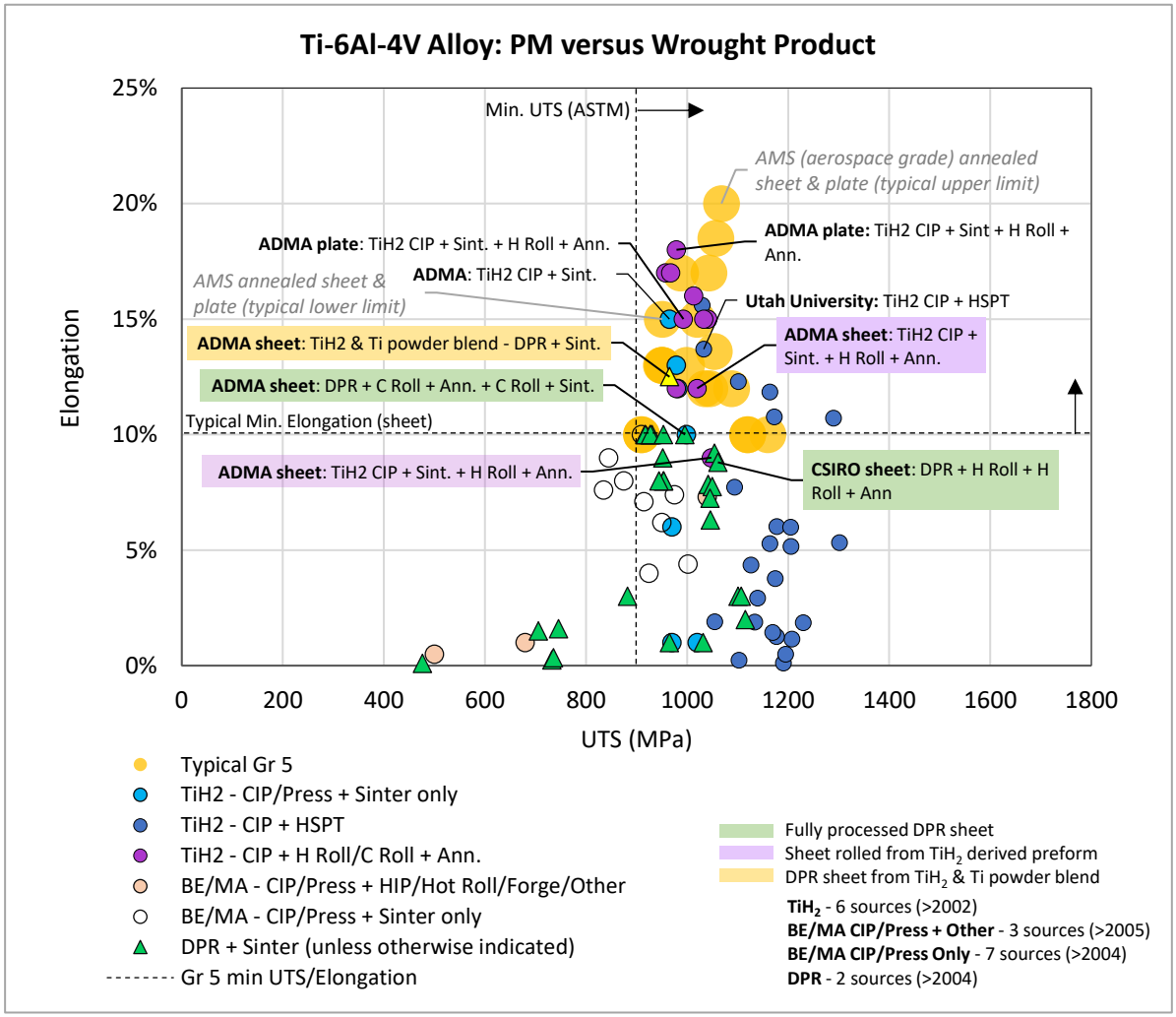

Figure 78: Elongation and ultimate tensile strength performance of wrought Ti-6Al-4V product versus PM compacts from various process routes and hydride/non-hydride feedstock.

TiH_2 derived PM compacts are the only points to fall well within the middle and upper range of the typical properties for Ti-6Al-4V wrought plate and sheet. For a process to be commercially viable, it must be robust, and reliably produce product within specification. However, only a few Ti-6Al-4V DPR compacts meet the minimum elongation of 10%, and only just. It has not yet been demonstrated that DPR can produce Ti-6Al-4V strip reliably within specification. However, the Ti-6Al-4V DPR data is from only two sources. Therefore, no conclusion can be drawn regarding the relative performance in this case. Further research into the optimization of oxygen content, microstructure, homogenization and pore size in Ti-6Al-4V DPR strip may improve elongation, and consequently the process capability.

In Summary

The consolidation of Ti-6Al-4V PM data, and the comparison to typical properties of wrought product, has shown the following:

- The best performing Ti-6Al-4V DPR strip meets the ASTM B265 elongation requirement (10%), but only just.
- Ti-6Al-4V sheet and plate produced via the TiH_2 preform route exceeds the minimum ASTM elongation requirement, and therefore has a relative advantage over fully processed DPR sheet (rolled to full density & annealed).

6 Price and Market Analysis

6.1 Wrought Titanium Market Analysis

6.1.1 Metals Beneficiation and Supply Chain

The metals beneficiation supply chain is divided into four stages of value [153]:

1. Primary stage: mining and production of an ore or concentrate.
2. Refining stage: conversion of ore/concentrate into intermediate product (in this case titanium sponge and ingot) in capital and energy-intensive smelters and refineries.
3. Production of intermediate/semi-fabricated product: plate, sheet, and coil.
4. Transformation into finished product: forming, fabricating, machining of intermediate products into final products.

In addition to these four main, value-adding stages, the industry is also serviced by intermediaries (stockists/wholesalers/distributors) who buy large quantities of mill product to sell on in smaller quantities [154]. They bridge the gap between mills, who produce in bulk to reduce unit costs through economies of scale, and businesses who purchase smaller quantities. These intermediaries hold inventory and are therefore able to supply a full range of products in various shapes, sizes and finishes with shorter delivery times [155]. Many of them have in-house service centres to cut standard mill sizes to customer specifications (e.g. BIBUS METALS [156]). The distributors sell to fabricators or OEMs, who form the sized mill products into final products. Figure 79 depicts the four, main value-adding stages as well as the intermediaries. The revert recovery loop has been included as well.

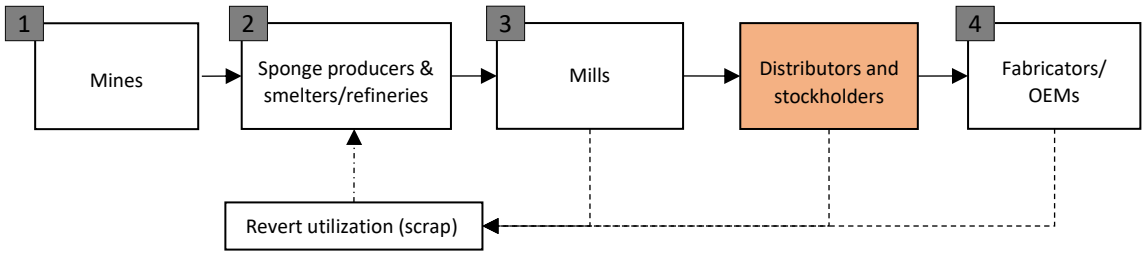

Figure 79: Titanium value chain.

Mill product prices will naturally vary depending on where in the supply chain the metal is bought from as well as the type of operating model the supplier is using. Although buying stock from a distributor is likely to be more expensive than ordering directly from a rolling mill, this is the standard source for mill products for most customers, especially businesses who do not want to carry inventory or wait for long delivery times. Mill products sold and priced by distributors will be the reference point in the price analysis.

6.1.2 The Price of Wrought Titanium

Data collection

For DPR flat product to be commercially feasible, it needs to be competitively priced compared to its wrought counterpart. To identify the primary factors affecting the price of wrought titanium, price data was sourced from import and export records (available online), product lists and excess stock lists from distributors (available online), as well as directly via requests for quotations from distributors. The objective was to determine a reasonable price point estimate for a transaction between a standard distributor and a would-be purchaser.

Price data for grades 1 to 5 plate, sheet, strip and foil were obtained from the sources given in Table 5. 80% of the data is from a US supplier's database of available stock. 278 data points are from an import-export database (for product imported into India from 9 countries). To verify the database and prices quoted on ecommerce websites, quotations for specific product were also requested directly from suppliers. Except for the import-export data which is for October 2015 to October 2016, prices were gathered between October 2016 to February 2017.

Table 5: Sources of price data

Source/Supplier	No. data points	Country	Online/direct quote
Titanium Joe (supplier's database of stock)	2930	USA	Online
Zauba - import & export database (for Oct 2015 to Oct 2016). Data from shipping manifests, bill of lading, bill of entries and shipping bills.	278	9 countries	Online
Ti-shop.com (metal eCommerce company)	138	UK	Online
Online metals (metal eCommerce company). Material Standard(s): ASME SB-265, ASTM B-265	130	USA	Online
Sophia's wholesale titanium, nickel, tantalum	84	China	Online
Ti Grupp	15	Russia	Online
Ticon - ASTM B265 UNS R05400	8	USA	Online
AE Metals	6	AUS	Direct Quote
PTG Performance Titanium Group (Would have requested ASTM B265)	6	USA	Direct Quote
Magellan Metals	5	USA	Direct Quote
Tianjin Oubaige Metal Products	4	China	Direct Quote
Baoji Huaheng Titanium Industry	4	China	Direct Quote
BIBUS METALS	4	UK subsidiary	Direct Quote
Brindley Metals	3	UK	Direct Quote

The following were deemed minor sources of variability compared to the base price of the metal and other more dominant price factors identified in this section:

- **Contracts versus single orders** - it is noted that long-term, contractual agreements are often used to secure more favourable rates. Sourcing contractual price data is not feasible.
- **Order quantity** – as many distributor's product prices are quantity dependent, a range of order quantities is represented in the data set e.g. 3 to 500 kg and even up to 4000 Kg.
- **Surplus/clearance stock or offcuts** – some prices may represent discounted product but the quantity is assumed negligible.
- **Specification -** For direct quotations, ASTM B265 grade product was requested. For the import data, the specification was not always indicated.
- **Large proportion of data set from a single source** – 80% of the data is from the Ti Joe database but as seen in Figure 80 below, this sample (red) is in general agreement with the rest of the data.

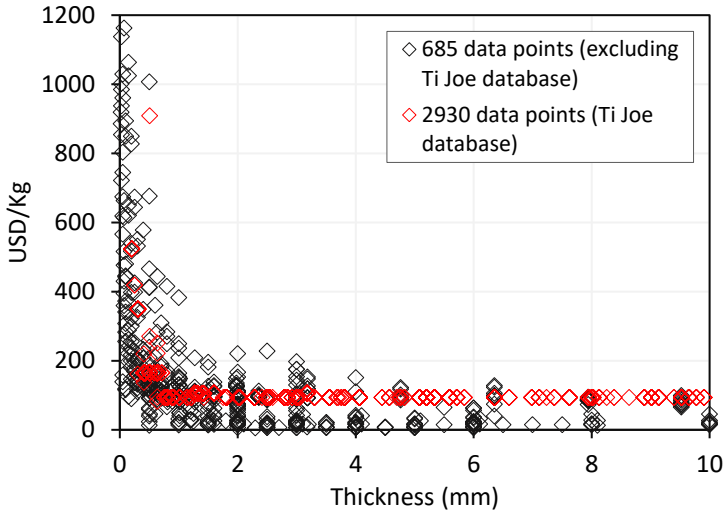

Figure 80: Price per kg of Ti-6Al-4V and CP titanium flat product as a function of thickness. 3615 data points with 80% of data from the Ti Joe database (red).

Country of origin

The countries from which the wrought products originate are given in Figure 81. The price data is for CP titanium plate, sheet and strip (Grade 5 alloy has been excluded). Prices are plotted as a function of thickness. There is little change in the maximum unit price over the thickness range of 10 down to 3mm. At around 3-2 mm, there appears to be a small step increase (to over $200/kg for some data points). This step may represent the change in processing from hot to cold rolling. Hot rolled strip of 3 mm thickness is primarily cold rolled into sheet of thinner gauge [157][158]. Jinshan Titanium from China offers cold rolled product from 4.76 mm or less [159]. Before cold rolling, hot rolled sheet is pickled in a weak acid solution, washed, brushed, dried and then oiled [160]. Cold rolling, as the final processing, allows for better surface finish and dimensional control [161], and the cold workability of CP titanium reportedly allows for up to a 50% reduction before annealing is required. However, to produce thin gauge product such as foil, the number of cold rolling and annealing cycles is considerably large [162]. This cost effect of this is seen in Figure 81, where the unit price increases exponentially due to the additional processing and related costs of rolling product to thin gauge.

The 8 main countries in which global titanium-producing companies reside are reported to be the US, Russia, Japan, China, Britain, France, Germany and Italy (in decreasing order of production) [128]. The sampling of price data is deemed satisfactory as six of these countries are represented in the dataset.

A second graph of the same data (inset) shows where the data points are most densely situated.

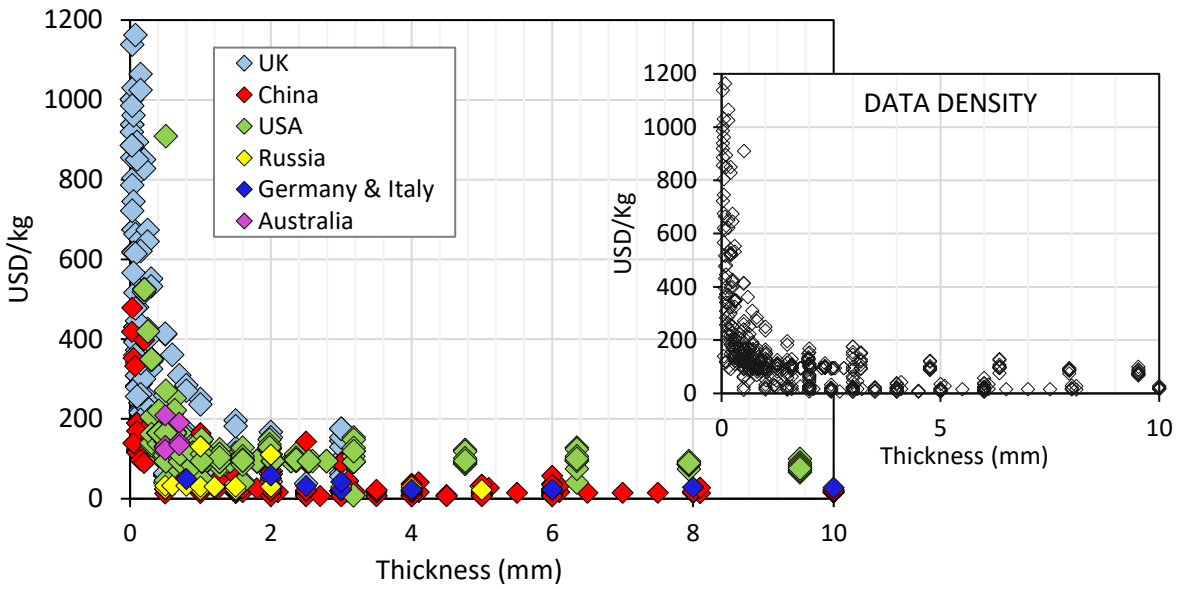

Figure 81: Price per kg versus thickness for CP (grades 1 – 4) titanium flat product (3615 data points). Data segmented by country. Additional graph showing data density is inset for comparison.

Grade

Figure 82 below shows the unit price for the commercially pure grades, 1 to 4, and the grade 5 alloy. Table 6 shows the maximum oxygen content and minimum elongation for each of the grades as per the ASTM B265 specification for sheet and plate. Grade 1 is the purest, and is therefore the most ductile. Grade 4 is the least pure (it has the highest oxygen content) which increases yield and tensile strength but to the detriment of ductility. The grade 3 & 4 price range is positioned lower than the purer grades (1 and 2). Grade 2 is the most commonly used commercially pure grade for industrial applications, having a combination of good strength, formability and corrosion resistance [163]. It is the largest sample in the data set, which confirms its extent of use.

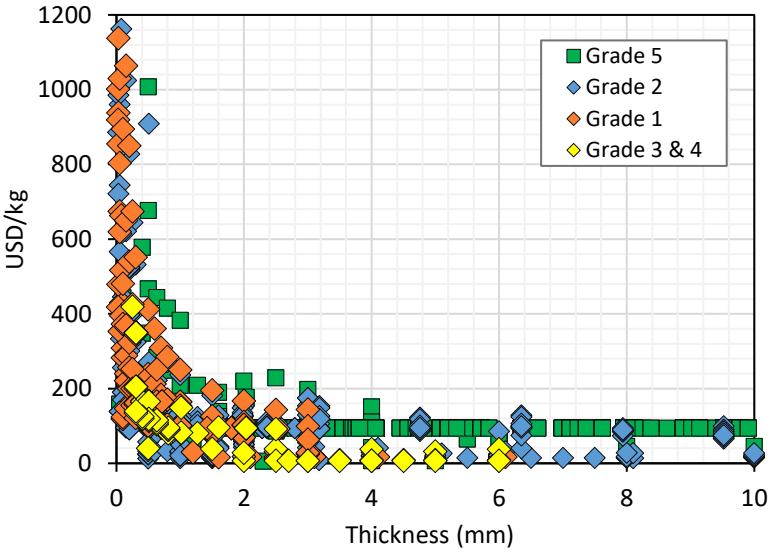

Figure 82: Price per kg of titanium flat product as a function of thickness and grade.

Table 6: ASTM B266 specification

ASTM Grade	Max O wt %	Min % elongation in 50mm
Gr 1	0.18	24
Gr 2	0.25	20
Gr 3	0.35	18
Gr 4	0.40	15
Gr 5	0.20	10

Figure 83 below shows the data separated into the three main countries of origin - the UK, USA and China. Much of the UK data is for thinner gauge product (<3mm), while data from the US and China has a wider spread. Prices for the Ti-6Al-4V alloy (grade 5), are highlighted in green, and are priced higher compared to pure titanium, particularly in the Chinese and UK sample set. This is expected as the Ti-6Al-4V alloy (grade 5) is the more expensive of than the four pure titanium grades due to the addition of vanadium, which is an expensive alloying addition [164].

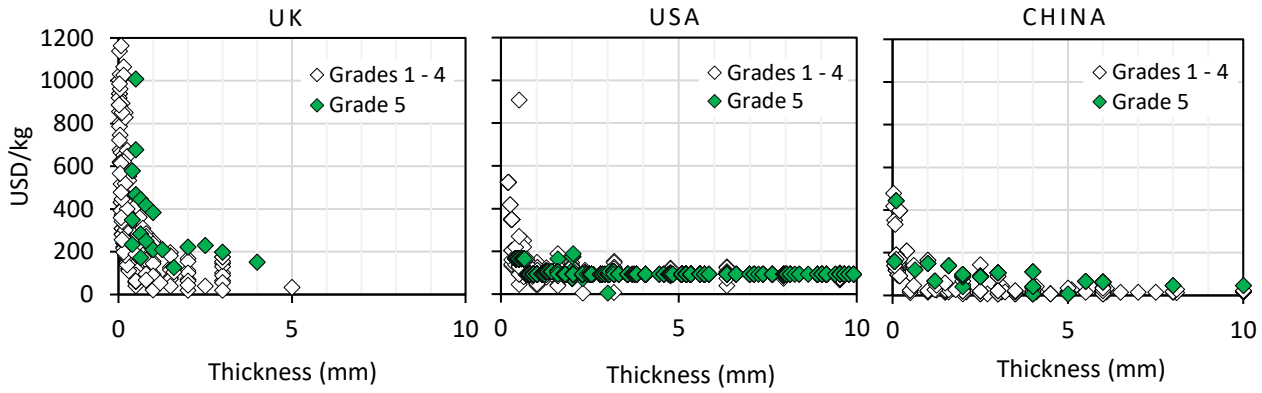

Figure 83: Price data for grades 1 – 4 and grade 5 (Ti-6Al-4V) from the three largest sources of data - the UK, USA and China.

Figure 84 below shows that there is little difference in price range for grades 1 and 2, even though grade 1 is purer. While some suppliers did quote a higher price for grade 1 product, others made no distinction in unit price between 1 and 2.

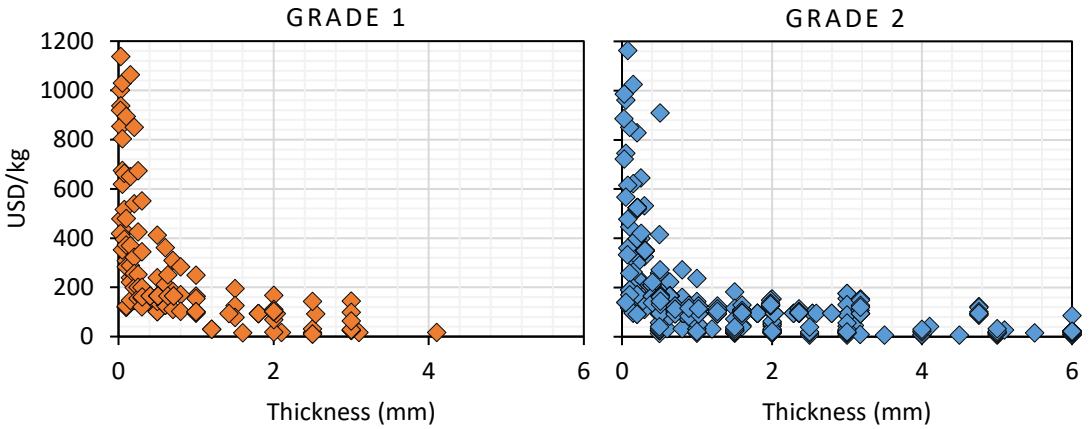

Figure 84: Price data for CP grades 1 (left) and 2 (right).

Product

Flat product is specified as strip, sheet and plate as per ASTM B265 (shown in Table 7). Strip and sheet are of the same thickness (<4.75mm), the only distinction is width.

Table 7: Dimensional specification for sheet and plate (ASTM B265 standard)

Flat product	Thickness (mm)	Width (mm)
Strip	<4.75	<610
Sheet	<4.75	>610
Plate	>4.75	>610

Standard flat mill product comes in the form of sheet or coil (Figure 85 [165]). This process flow, for a large Chinese titanium manufacturing company, shows two separate process lines for coil and sheet. Sheet is processed on four-high reversible hot rolling mills to thicknesses of 0.6 – 0.8 mm (width <600 mm) and > 0.8 mm thickness with width > 1000 mm. Coil of 0.3-4.7 mm thickness and width of <=1350 mm is processed on a 20-high cold rolling mill. This coiled product, shown in Figure 86, is cut on slitting lines into thinner strips which are welded into tubes.

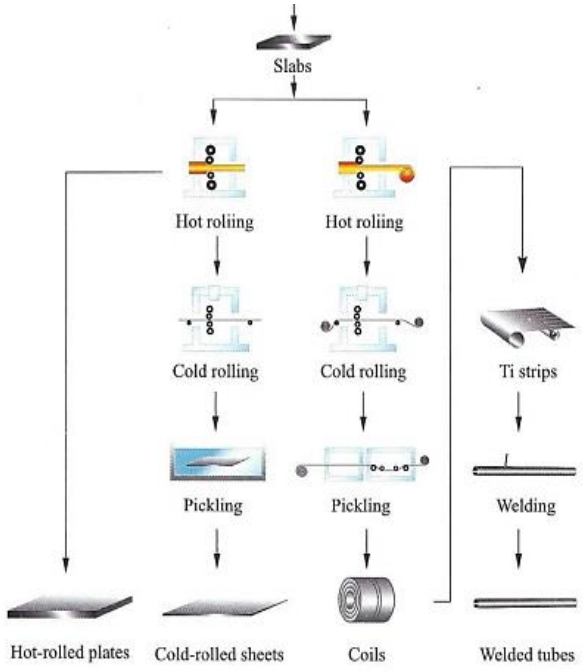

Figure 85: Process flow of the manufacturing of titanium plate, sheet, coil and welded tubes [165].

Figure 86: Coiled titanium manufactured in China.

Naturally, there is great variety in the dimensions produced, as standard, by mills, as well as the dimensions stocked by suppliers. Figure 87 below shows width and thickness ranges available from various suppliers. Product with a thickness of 0.4 mm or less is available mainly as strip with a width of 600 mm or less. Widths of 2000 mm or more are available for product with a thickness greater than 0.5mm.

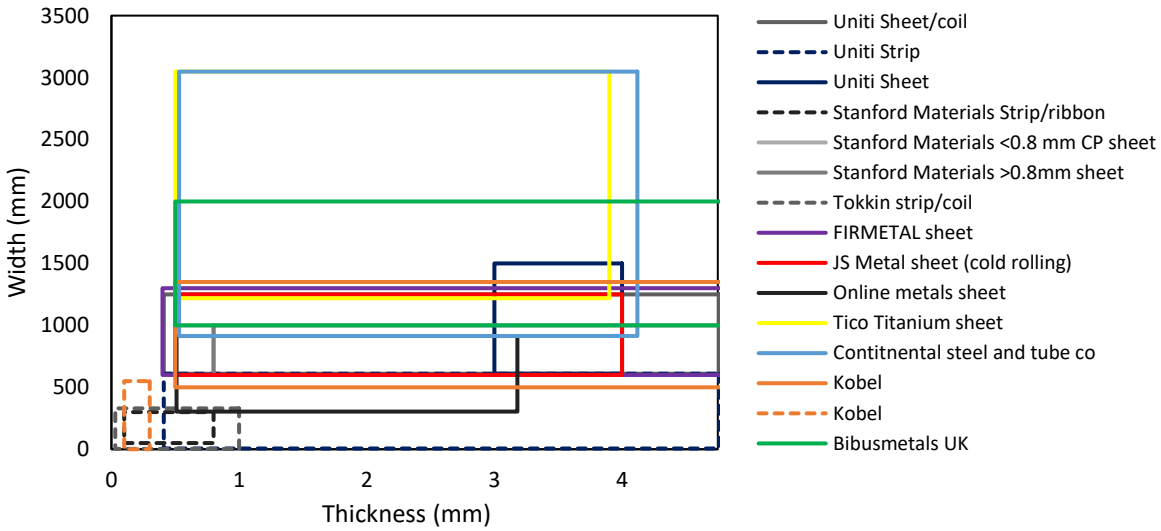

Figure 87: Common maximum width and thickness ranges for titanium flat products (grades 1-5)

In addition to the base cost of the metal, width and length are itemized as cost extras due to the additional processing of cutting standard mill sizes down to smaller dimensions. Figure 88 shows width x length (m^2) as graded colour for strip, sheet and thin plate (excluding grade 5 alloy). The left graph, which presents data for all width and length sizes, shows that products with smaller width and length dimensions (dark orange and red) are sold at a premium. This is a similar result to the foil analysis and confirms the influence of product dimensions on price. In comparison, the graph on the right, which is limited to only width x length values greater than 7.5 m^2, shows reduced variability in price.

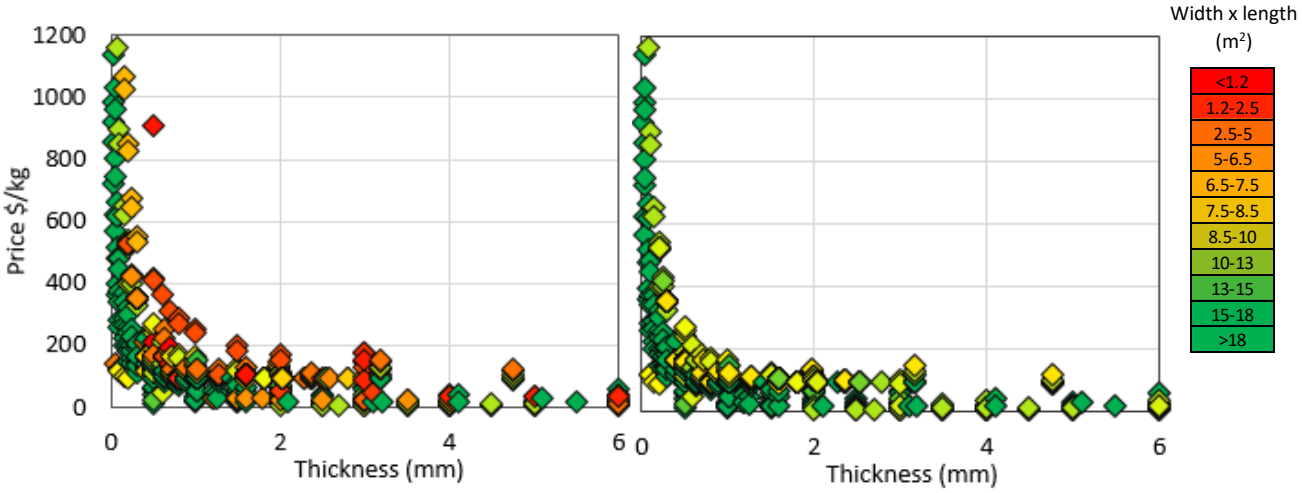

Figure 88: Price per kg for grades 1 – 4 titanium flat product as a function of thickness. Colour gradation scale represents width x length (m^2). Right graph - limited to only width x length values greater than 7.5 m^2.

To date, ADMA, whose commercialisation is the most advanced, has the widest rolling mill, with a width of 660 mm (26”). Since this is marginally larger than the maximum width specification for strip (610mm), DPR product is likely to be in the form of strip.

The data set comprises mainly strip of 150 – 300 mm in width (6 to 12 inches) (Figure 89). Strip unit prices are given in Figure 90. Grade 5 product has been removed, only grades 1 – 4 are presented. Strip sold as coil (highlighted in yellow) is cheaper than strip cut to pieces of similar thickness. Cutting coiled strip to length is additonal processing and therefore an additonal cost.

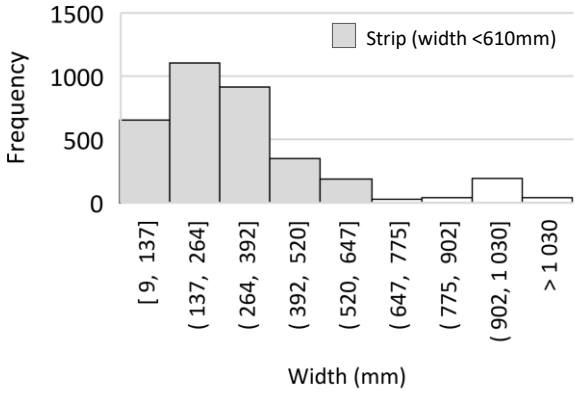

Figure 89: Histogram of product width for price data set.

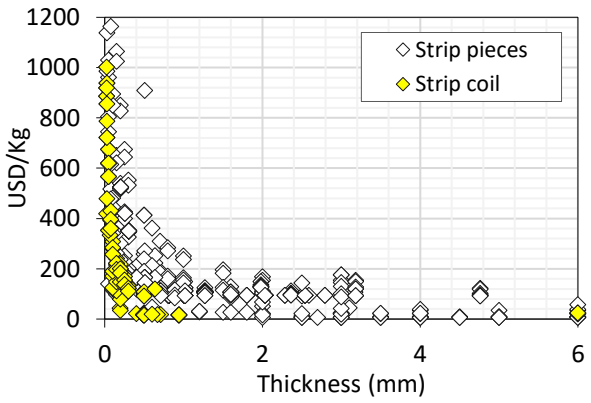

Figure 90: Price data for grades 1 – 4 strip pieces and coiled strip.

Figure 91 separates out strip thicknesses of less than 0.5 mm, which are typically designated as foil. The smaller graph inset shows the influence of width and length on the price of foil. In general, product with a greater surface area e.g. coil of standard mill width, is much cheaper than foil that has been cut down to customized size (e.g. shortened in length or processed on slitting lines).

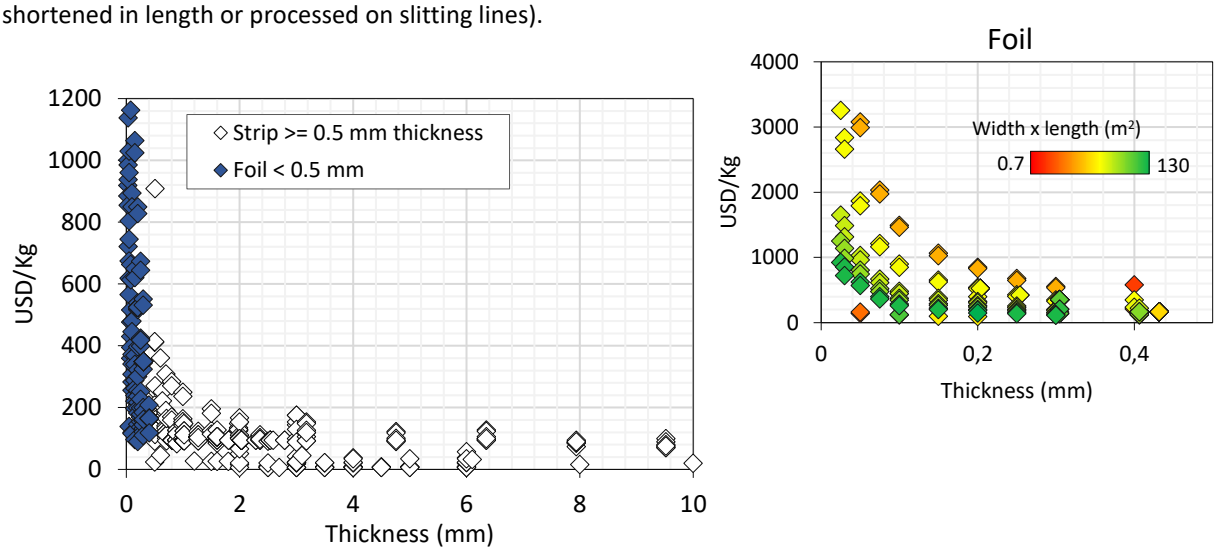

Figure 91: Price per kg of CP titanium strip and strip foil as a function of thickness. Graph on the right shows cost influence of width x length for foil only. The maximum unit price of foil is too large to include in the data set on the left.

6.1.3 Price range estimation

The price data set was filtered to include only products with dimensions similar to product that is likely to be produced via DPR:

- A width of 660 mm (26") or less. As mentioned before, 660 mm is the widest mill used for DPR to date, and this is estimated to be the maximum width for DPR product.
- A width of 120 mm (5") or more. This excludes very thin product such as ribbon. Ribbon is produced on a slitting line by cutting narrow coils from main coils. For this analysis, the objective is to establish a price range for wrought product that has a width range comparable to the standard width rolled via DPR. It is assumed that ribbon will be cut from a standard DPR width.
- A length of 500 mm (20") or more. This somewhat limits price variability from customized product (sold at a premium) or offcuts (sold at a discount).
- Grades 1-4 only. Grade 5 has been excluded to simplify the comparison.

Figure 92 below is the result of the above filtering strategy. The graph on the left shows that filtering for standard strip sizes has removed the smallest width x length values (dark orange to red) as well as product with large surface area (except for coiled strip). The graph on the right shows country of origin for the remaining data. It is evident that mill product from China is consistently lower in price across the thickness range in question.

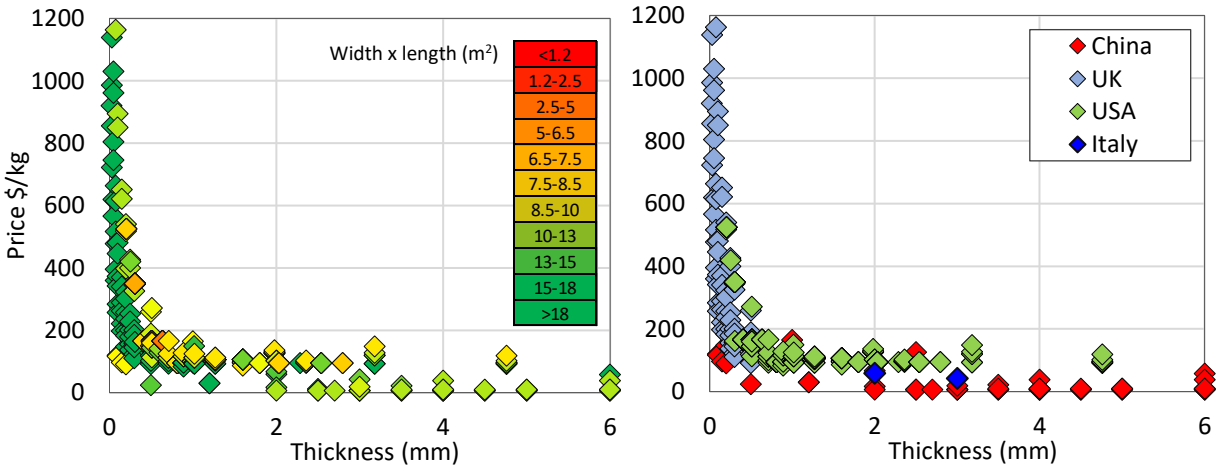

Figure 92: Price data for grades 1 – 4 titanium strip with width >120 mm and <660 mm, and length > 500 mm. Left graph shows width x length colour gradations. Right graph shows country of origin.

6.1.4 Market Analysis

The question is why there is such a large price difference between mill product from China and mill product from the US and the EU? Several sales managers from China, who provided quotations, were questioned as to why titanium mill product from China is so much cheaper than titanium sold in the US or Europe. Chinese suppliers emphasized that their product is not inferior to US and EU product, that they meet ASTM B265 standards and that a growing amount of their product is being sold outside of China. They gave the following reasons for the lower prices:

1. Lower labour and processing costs
2. Extensive stock supplies
3. The selling of Chinese product to Europe (e.g. to Germany, France and Spain) that is then sold on at a mark-up.
4. Concentrated raw material and integrated processing in the "titanium valley"

China has the world's largest ilmenite reserves, with 28.5% in 2016 (Ilmenite accounts for 89% of the world's consumption of titanium minerals) [1]. Rapid development in the Chinese economy and a resultant increase in Chinese sponge production capacity has seen a relative decrease in the share of global capacity for other major titanium sponge producers, such as the CIS (Commonwealth of Independent States[4]), whose share of global capacity has dropped from 40% to less than 30% in the last decade [166]. Today China is the largest sponge producer, accounting for 38% of global capacity. The Commonwealth of Independent States (CIS) and Japan rank second and third (Figure 93) [1].

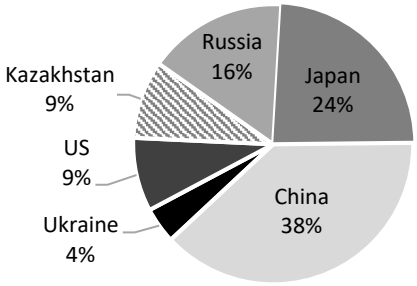

Figure 93: Global sponge capacity [1].

China's aggressive expansion of sponge production facilities has far exceeded demand growth, resulting in overcapacity [167]. Evidence of this is also seen in the unbalanced scrap market. Scrap is usually added to sponge melt to dilute the quality and bring the unit price of ingot down. With the availability of extensive sponge supplies in China, mills are buying less scrap, leading to a slump in scrap prices (Vasily Semeniuta, President of Grandis Titanium Co. [168]).

Excess sponge capacity and oversupply has led to a slump in market prices, as shown in Figure 94, [169]. This price data is for aerospace grade sponge for the years 2012 – 2015, and prices have changed little since, averaging between 6.8 and 7.9 $/kg for June 2016 [170]. In 2014, most of the global sponge surplus was industrial-grade material in China [171]. Consequently, a downturn in the Chinese market occurred, with a 20 – 25% drop in prices in 2012 and 2013, from 12.34 $/kg in Dec 2011 to 7.41 $/kg in Dec 2013 [172]. In addition to the oversupply of sponge, the slump in Chinese market price has also been attributed to a decrease in development of desalination plants and nuclear power plants, as well as fewer shipbuilding projects [173].

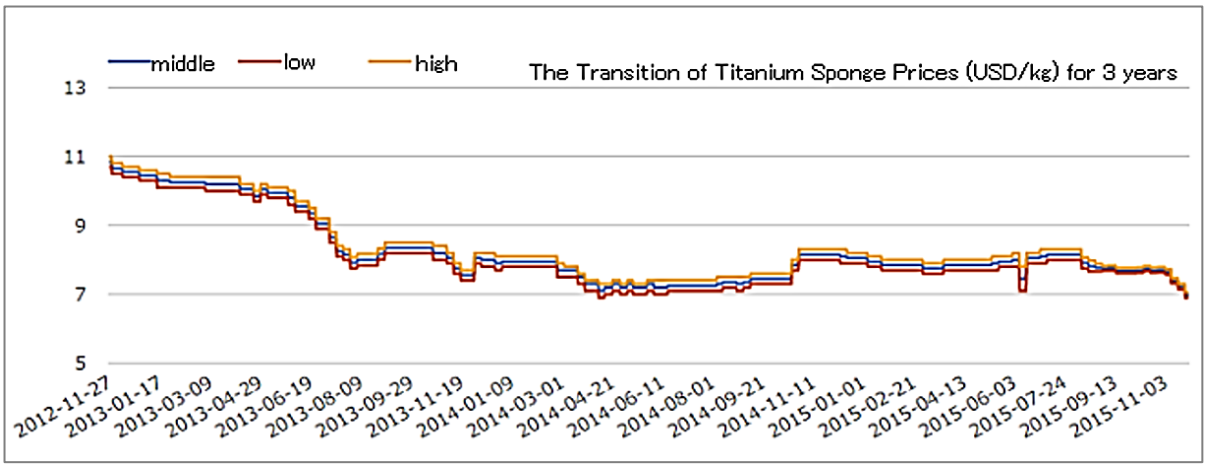

Figure 94: Price of titanium sponge (aerospace grade) for years 2012 – 2015 [169].

Titanium manufacturers have struggled with the current market downturn. Liu *et al*. [173] report that almost all Chinese sponge producers are not profitable and that many enterprises have subsequently closed down. Under Beijing's 12th five-year plan (2011 – 2015) the Chinese sponge industry was pushed to reduce costs by consolidating and phasing out smaller, inefficient plants with a capacity of less than 5000 t/year [174]. Titanium Metals Corporation (TIMET) has filed antidumping and countervailing duty petitions over the dumping of cheap sponge on the US market by Kazakhstan (with an alleged dumping margin of 33%) and Japan (allegedly 31 – 69%) [175] [176]. In 2016, a titanium sponge plant in Utah announced that it would temporarily halt production due to global overcapacity. Their inability to compete was put down to the availability of aerospace and standard grade sponge that could be secured, under long-term supply agreements, at prices lower than their production costs [1].

[4] CIS countries producing sponge are Russia, Ukraine and Kazakhstan.

6.1.5 Reasons for price dissimilarities

Interestingly, although China is the largest sponge producer, it exports only a small amount to the US (the US imports most of its sponge from Japan - 65% in 2014) [167]. Most of China's sponge is for domestic use. In 2014, only 6000 of the 68 0000 tonnes produced were exported, going mainly to South Korea (36%), followed by the US (28%) [167]. China and the US have the largest titanium melting capacity, followed by Russia and Japan [176]. Like the sponge market, there is excess capacity of melted titanium product (i.e. ingot/slab) and this is attributed to China's expansion in vacuum arc melting (VAR) facilities [176]. In China, an increasing amount of mill product is being exported, to Taiwan, Russia, South Korea and the USA, but the unit value is low, signifying industrial or consumer grade products [177]. Liu *et al*. [173] report that most of the sponge produced in China is for industrial applications, with only 10% meeting aerospace specifications for stationary parts. Aerospace grade ingot and slab is typically manufactured via double or triple melting (VAR) [178], whereas industrial grade material is often manufactured via melting in a cold hearth (electron beam or plasma arc) furnace which is more cost effective due to the ability to include a higher percentage of scrap [179].

While the market for mill product in China is mainly for industrial applications, the aerospace industry accounted for 63% of the global consumption of mill product in 2016 [180], and 77% of US domestic consumption in 2015 [181]. The production of sponge and mill products outside of China is "largely oriented towards this market" with aerospace grade sponge produced in the US, Japan, Russia, and Kazakhstan [182]. Hence, 80% of the US titanium ingot capacity in 2005 was produced by VAR, whereas only 20% was produced by cold hearth melting [183].

In China, the dominant sector is the chemical industry (as seen in Figure 95), accounting for 47% of mill product consumption in 2014 [166], while only 11% serves the aerospace industry. Prior to 2009, all of China's aerospace grade sponge was imported [172].

The use of titanium mill product in China for industrial applications far exceeds industrial consumption in other parts of the world, as shown in Figure 96 [184]. The second largest consumer of titanium for industrial applications in 2012 was South Korea. The market for industrial applications is different to the aerospace market, where strict specifications have driven prices up. In the industrial market, less rigorous specifications and increased competition from other metals has made industrial titanium more price sensitive (i.e. more importance is placed on price than on quality) [171]. The titanium market is characteristically volatile, with demand in the aerospace industry traditionally having a strong influence on market price. This volatility arises because the market is small compared to other metal markets, and it is an oligopoly, with a small number of suppliers, making it more susceptible to supply and demand variations [185].

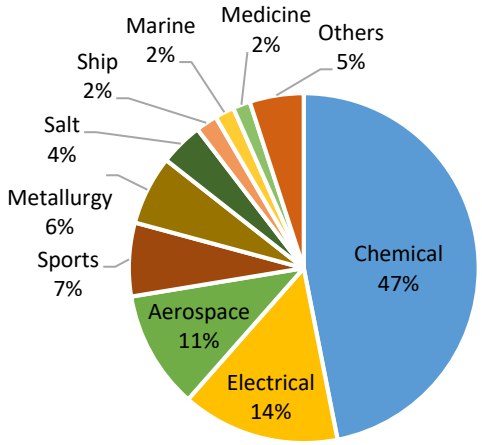

Figure 95: Percentage consumption, by industry, of titanium mill products in China at the end of 2014 [166].

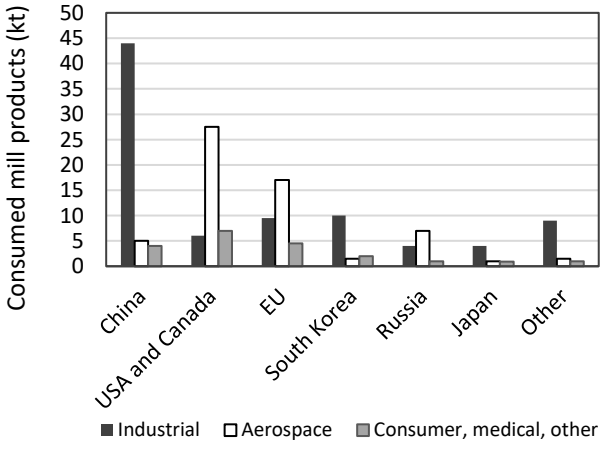

Figure 96: Quantity of mill product consumed in 2012 by country and industry [184].

The production and consumption of titanium mill product in China has grown rapidly, as shown in Figure 97 (right) [166]. China has seen a transition from a reliance on the importation of titanium products to a state of self-sufficiency, allowing them to serve their large and growing domestic demand. Strategic goals identified by the Chinese Non-Ferrous Metal Association in 2010 included the need to broaden titanium product lines and improve the quality of sponge and semi-finished products for use in higher end applications [186]. Tax incentives have been put in place to encourage investment in "High and New Technology Enterprises (HNTEs)", with a preferential corporate income tax rate of 15% applicable to the titanium industry, versus a statutory rate of 25% [187][188].

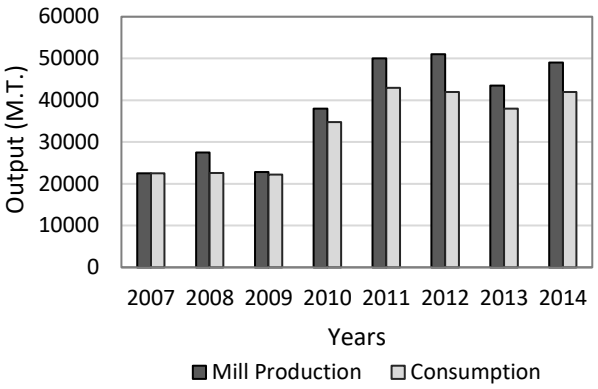

Figure 97: Output and consumption of Chinese titanium mill products in the last 8 years [166].

Until recently, China relied on the importation of titanium strip coil due to an inability to produce locally, and this product was earmarked as an important area of investment [189]. A pickling, grinding, cutting, slitting and annealing line was commissioned [189] and in 2012, the first strip coil production line, with a 20 high cold rolling mill, was trialled by the largest titanium company in China, Baoji Titanium Industry Co., Ltd [190]. Their strip and coil system produces grades 1 – 4 flat products for use in heat exchangers, welded tubes and other applications.

Stakeholders in the Chinese titanium industry have recognised that the quality of their sponge and mill product inhibits exporting for higher-end applications such as aerospace and nuclear power stations [186]. Chinese sponge plants do not currently have the technology required to produce high-grade titanium sponge [173], so the largest Chinese producer of aerospace products, Baoji Titanium Industry Co., imports aerospace quality grade. The Ukrainian sponge producer, ZTMC, has recently been awarded the right to supply sponge to Baoji [191]. Baoji claim that their Ti-6Al-4V sheet and plate has been approved by Boeing, Airbus, Bombardier, Goodrich and Rolls Royce. A RAND Aerospace report corroborates part of this claim and lists Baoji as a supplier of ingot, plate and sheet for Boeing [192]. It has also been recently announced that Airbus and China have signed an MoU to "strengthen and deepen mutually beneficial collaboration"[193].

In summary

In summary, the price dissimilarity between product from China and the US and Europe exist because of the following:

1. There is overcapacity and oversupply of sponge and mill product globally, but particularly so in China, which has seen a slowdown in demand after rapid expansion in line with its economic development plan and tax incentives.
2. Although China is the largest producer of sponge, most of it is consumed domestically, while the US imports predominantly from non-Chinese producers. Of the mill product and sponge that is exported by China, it is predominantly for industrial applications, whereas the US or global sponge and mill markets are driven predominantly by aerospace applications. Although quotations for ASTM B265 were requested from US suppliers (not aerospace certified material), these products are likely to be of higher grade because their markets are oriented towards higher end applications.
3. Industrial mill product does not need to adhere to stringent aerospace specifications. This lowers the price. In addition, the industrial titanium market experiences price pressure from other metals competing for industrial applications.

6.1.6 Two markets

Based on the market analysis, two distinct markets have been identified:

1. Higher grade product from the US and Europe.
2. Industrial product from China.

As seen in Figure 98 below, excluding the Chinese price data greatly reduces the range in price. The graph on the right shows the data density, and the estimated price for wrought strip from this market. This estimate is the first market in which DPR cost estimates will be evaluated.

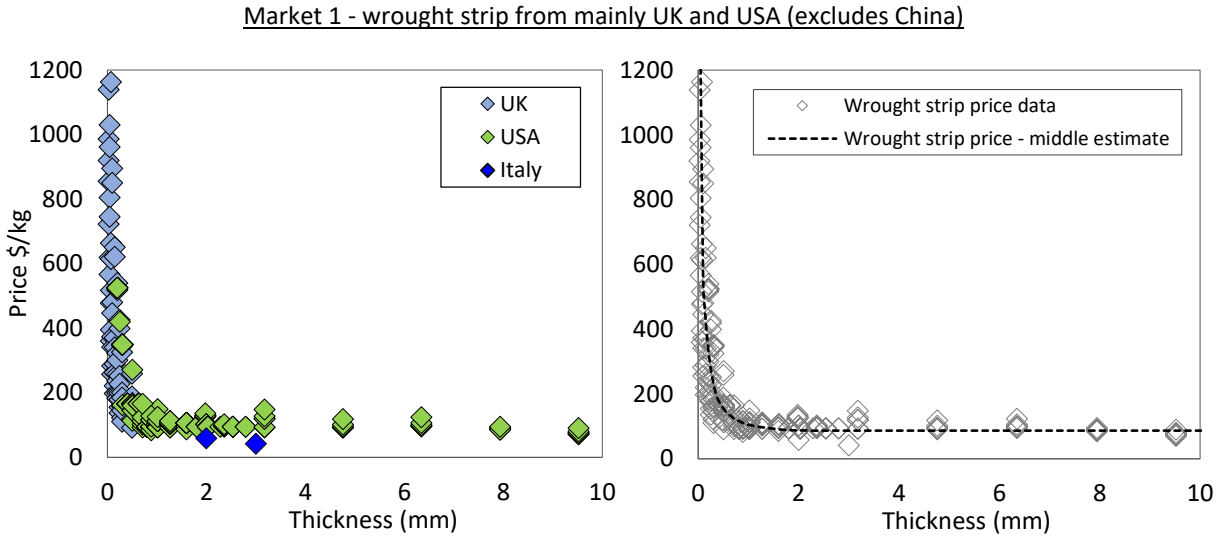

Figure 98: Price data for grades 1 – 4 titanium strip with width >120 mm and <660 mm, and length > 500 mm. Left graph shows that product is only from the UK, USA and Italy (product from China excluded). Right graph shows data density ad median price estimation.

Product from China is the second market in which DPR cost estimates will be evaluated. Additional price points and ranges were sourced directly from Chinese suppliers for further confirmation of prices. While most Chinese price points are well below UK and US prices, some are in line, as shown in the graph on the left in Figure 99 below. In the graph on the right, variability has been reduced in the Chinese data set by removing CIF prices (i.e. prices that include cost of insurance and freight) or "free shipping" deals (it is likely that the freight cost has been included in the price). These measures were unnecessary for the UK and US data set because prices were quoted as FOB/EXW[5].

[5] EXW (ex-works): the value of the goods loaded on leaving the factory.
FOB (free on board): plus, the value of services performed to deliver goods to the border of the exporting country.
CIF (cost, insurance and freight): includes the total cost of the main transport (by air, sea or land) to the border of the importing country.

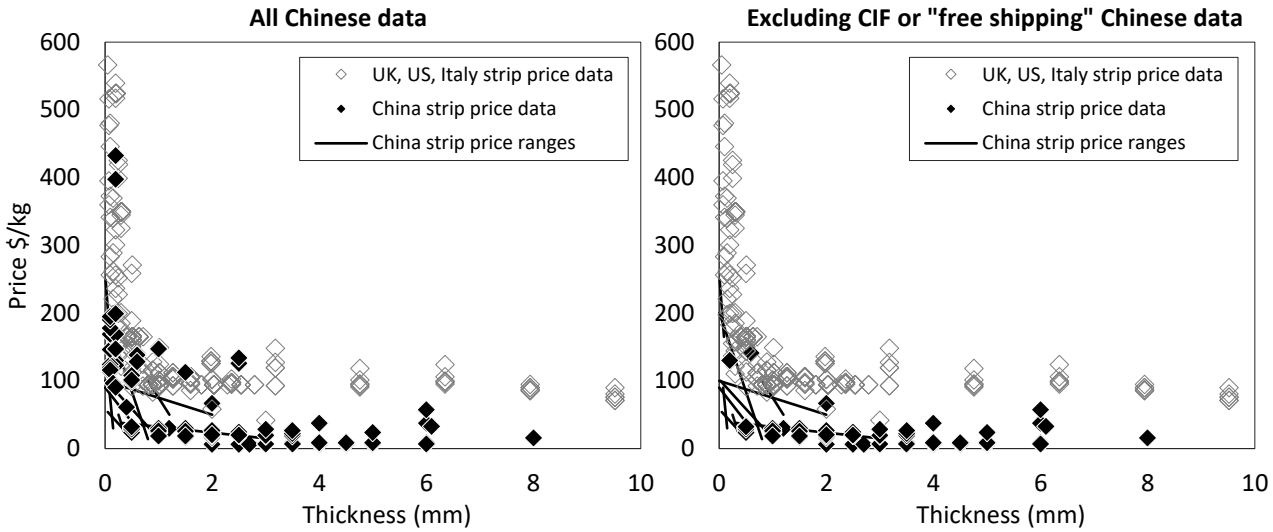

Figure 99: Grades 1 – 4 titanium strip price data for the UK, US and Italy versus China (only strip widths of >120 mm and <660 mm and lengths of 500 mm or more).

Most Chinese prices were sourced from businesses operating within Baoji City, also known as titanium valley, which is China's largest titanium development cluster, with over 400 titanium enterprises [194].

Based on the consolidated data, price lines can be drawn for each of the two markets. The price estimate for Chinese product is shown in red. The UK, US and Italy is in blue.

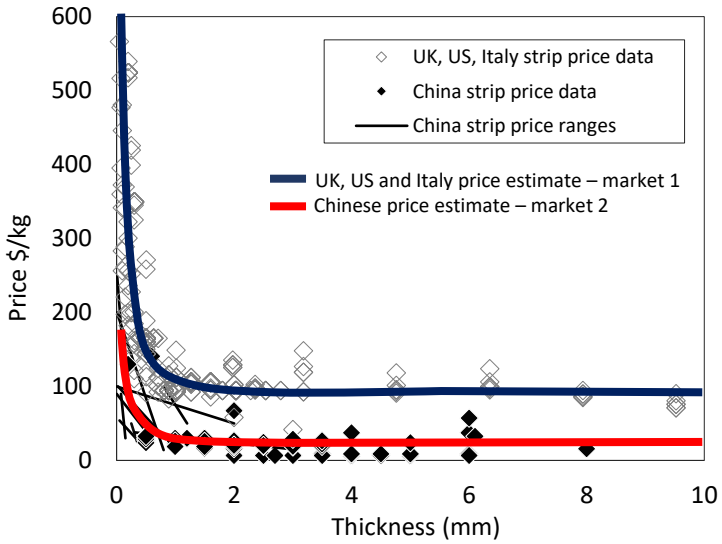

Figure 100: Middle price estimates for grades 1 – 4 titanium strip for the UK, US and Italy versus China. Data is for only strip widths of >120 mm and <660 mm and lengths of 500 mm or more.

6.2 The Powder Market

6.2.1 Market Size

One of the greatest barriers to the commercialisation of titanium powder metallurgy is the lack of high volume powder of reasonable quality and price [195]. The market for titanium powder is significantly smaller than the market for wrought titanium, and there is limited data available. Common commercially available powders are all sponge derived, as shown in **Error! Reference source not found.**. High value, pure Ti or prealloyed spherical powders, manufactured by melting or spheroidizing ingot derived product, are predominantly used for metal injection moulding or additive manufacturing applications (e.g. selective laser printing, selective laser melting and electron beam melting). The production of HDH, TiH_2 and sponge fines do not involve the melting of sponge feedstock and are therefore termed "low-cost" powders.

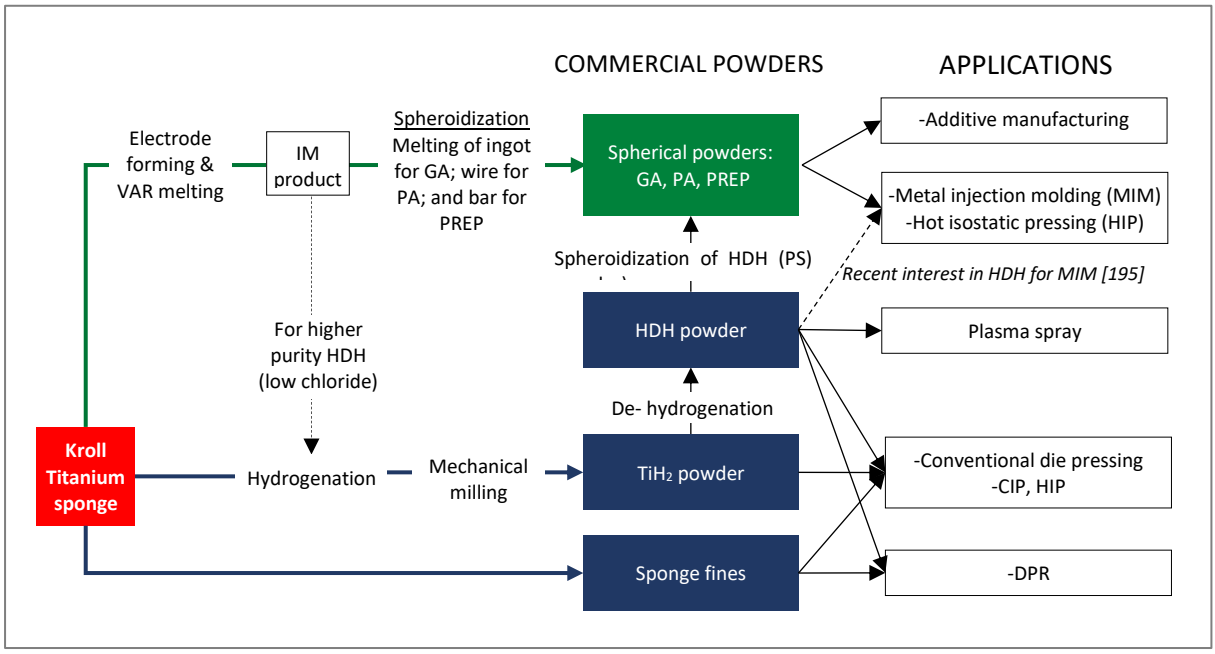

Figure 102: Processing routes and typical applications of commercial powders derived from sponge.

Estimated global production quantities for titanium powders for 2008 are given in Figure 103 below, and are just over 6000 tonnes in total [196] (a very small market compared to the 213 000 tonnes of global titanium sponge capacity for the same year [197]). The largest production quantities are for sponge fines, followed by HDH powder. A second and similar estimate of market size for 2008 is 7500 tonnes [92]. Global HDH shipments for 2012 (1000 - 2500 tonnes [198] in Figure 104) were greater than production quantities in 2008 (625 tonnes in Figure 103), indicating some market growth. High value spherical powders, which are used in advanced powder metallurgy methods such as additive manufacturing, accounted for only about 300 of the 6000 tonne production estimate for 2008. For 2016, Roskill analysts estimated that 500 to 1000 tonnes of high-value spherical or near-spherical titanium powder were produced [178], indicating moderate to 3-fold

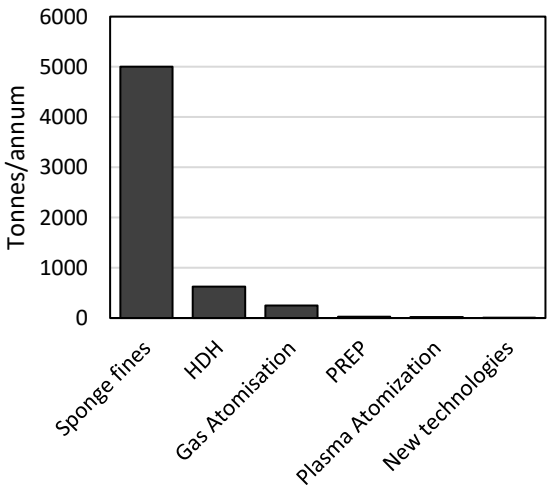

Figure 103: Estimated global production of titanium powder in 2008 [196].

growth depending on the estimate range. This can possibly be attributed to growing interest in additive manufacturing applications (as discussed later in this section). Although high-value powders have seen some growth, the most recent powder capacity estimate (2016) for all titanium powders is 4000 tonnes [178], which is a decrease compared to the 2008 global production estimates of 6000 [196] and 7500 tonnes [92]. However, given that the titanium powder market comprises many small suppliers, the difficulty in consolidating reported quantities to accurately determine the size of the market is noted. Furthermore, the relative proportion of powder demand for PM applications is difficult to determine as most titanium powder is reportedly used for non-PM consolidation methods e.g. alloying additives, pyrotechnics and reagents for chemical processing [196].

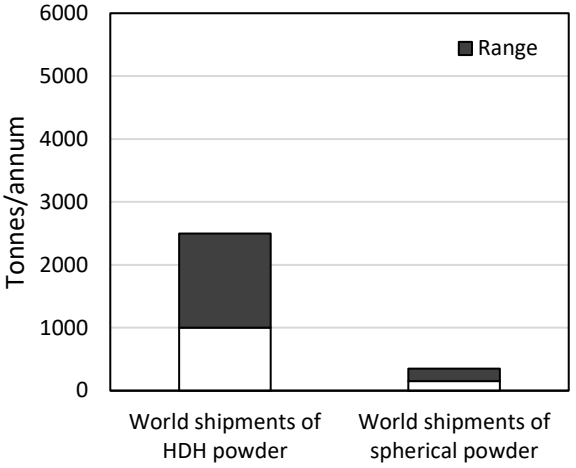

Figure 104: Estimated annual global shipments of HDH and spherical powder for 2012 [198].

A large stable powder production base and the associated production efficiencies, increased price competition and economies of scale could bring the price down. Naturally, increasing interest in a technology spurs development of surrounding infrastructure to support a primary process. The PM process that is currently gaining considerable interest is additive manufacturing (AM) (which uses spherical, instead of angular powders as feedstock) [103][199]. Spherical powders are preferentially used in AM due to better flowability [87]. The powder metallurgy panel in the *Titanium Europe 2016* conference comprised speakers from industry and research institutions who presented exclusively on additive manufacturing and metal injection moulding [200]. The overriding expectation was that the aerospace industry would be the main driver of growth (which is not unexpected given that the US and European titanium markets are geared towards this industry). In the 2016 and 2017 *Powder Metallurgy Review*, much of the titanium research and industry development news concerned additive manufacturing. As part of a joint venture with TLS Technik, GKN Hoeganaes has begun production of titanium powders in North America for AM applications. They believe that "AM offers the highest growth potential for the supply of metals in North America and Europe", but also cite increased demand for AM in the industrial and automotive industries [201]. Arcast has formed a new company, Arcast Materials, to produce titanium powder for AM and near net shape components [201]. Alcoa has opened an additive manufacturing powder plant in Pennsylvania USA to supply feedstock for aerospace parts, and Norsk is planning to commission an additive manufacturing plant in Plattsburgh by the end of 2017 for aerospace structural components [1]. In 2016, OSAKA Titanium technologies Co. in Japan reported on the ramping up of their existing spherical powder production facilities [202]. US company Praxair, who has more than 50 years of experience producing gas atomized powders for thermal spray coating, has begun marketing spherical powder for additive manufacturing [203]. Praxair purchased Iowa Powder Atomization Technologies, who owned a recently developed technology (a "hot shot" pour tube) reported to be more efficient than traditional spherical powder manufacturing methods [204]. The low yield of fine powder produced by the current methods is reported to be the main technical reason for the high cost of spherical powder [205]. Roskill analysts forecast substantial growth in the AM industry [178], and Mellor *et al*. [86] further confirm that at present, spherical powders are attracting the most interest, with special focus on additive manufacturing.

As it stands, HDH powder production and shipment volumes are still greater than spherical powders (Figure 103 and Figure 104), but it is evident that interest in AM is spurring development and expansion of spherical powder manufacturing processes. Although HDH powder is not suitable for direct use in AM, the Plasma Spheroidization (PS) method converts non spherical powders (HDH, TiH_2 or Armstrong) to spherical shape [205], and recent efforts to use HDH in MIM have shown promise [195]. The use of HDH as a feedstock in the AM and MIM supply chain could drive HDH production volumes up, improving production efficiencies and potentially lowering powder costs, which would in turn benefit other powder metallurgy processes such as press and sinter and DPR.

However, the oxygen levels and current costs of these powders are reported to limit their use as a feedstock in the production of spherical powders [195].

As discussed previously, there are a number of developmental extraction processes, some of which are looking to produce titanium metal in powder form. The Armstrong process and the FFC Cambridge process are the two most well-known. FFC is an electrochemical process that converts TiO_2 to titanium metal in molten salt. In the Armstrong process, $TiCl_4$ vapour is reduced with liquid sodium. Both these processes are reported to be lower in cost [206] but pricing is not publicly available. The patents for the FFC Cambridge process are owned by Metalysis, who is currently producing only spherical powders for Electron Beam (EB) and Selective Laser Melting (SLM), again an indication of the interest in AM powder production. Cristal Metals is the exclusive producer of the Armstrong process. They sell Armstrong powder converted to spherical shape for AM as well as the as-produced powder for near net shape and cold spray. There has been extensive research on the compaction and sintering capabilities of Armstrong powders [207][208][209][210][211], but little investigation of the final properties, especially the final impurity content. Although Armstrong powders are low in chlorine, the high specific surface area of the "coral like" morphology increases the risk of oxygen pick-up. Since the starting oxygen content is commonly over 0.25 wt% (as seen in Figure 52 in section 4.5.4), the final product is unlikely to meet grade 2.

6.2.2 Powder price

This section seeks to characterize the cost of titanium powder by consolidating prices sourced from suppliers. The objective is to compare these price point estimates to wrought product prices to estimate how tight profit margins will be.

DPR relevant powders – HDH and sponge fines

To determine the current price of commercial titanium powders applicable to DPR, quotations were sourced from manufacturers and distributors in China, the UK, USA, Russia and the Ukraine. Most of the data is for HDH powder. A minority is for sponge fines. The suppliers contacted are shown in Table 8.

Table 8: Sources of price data for HDH and sponge fines

Source/Supplier	No. data points	Country	Online/direct quote
Chengdu Huarui Industrial	2	China	Direct Quote
Whole Win Materials	4	China	Direct Quote
Shaanxi North Steel	2	China	Direct Quote
TC titanium	1	China	Direct Quote
Wellmet International	2	China	Direct Quote
Changsha Vday Metallurgical	2	China	Direct Quote
Chengdu Huarui Industrial Materials	1	China	Direct Quote
Brightever Titanium	2	China	Direct Quote
TC Titanium	2	China	Direct Quote
Arosa-Sintez	3	Russia	Direct Quote
Titan Lab	2	Ukraine	Direct Quote
William Rowland	1	UK	Direct Quote
Zauba - import & export database (for Oct 2015 to Oct 2016)	1	UK & US	Online database
Stanford Advanced Materials	2	US	Direct Quote
Phelly Materials	1	US	Direct Quote

The price data, in Figure 105, is given as a function of powder size ("<μm" indicates that the particle size distribution (PSD) is below this value). The country of origin is indicated by colour. Powder from China is the largest sample and is generally cheaper (<$50/kg) than powder sourced from US, UK and Russian suppliers. In 2012, Qian *et al*. [212] reported on China's growing HDH powder industry, possibly off the back of the expanding sponge industry, with HDH powder priced at ~$15/kg to ~$40/kg at the time, which is similar in range to the current prices for Chinese product seen below.

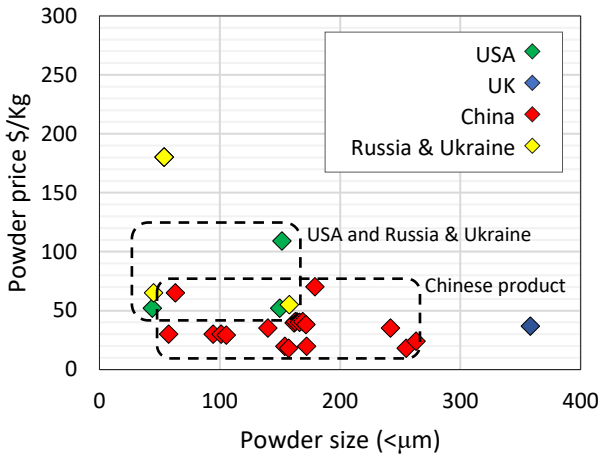

Figure 105: Price per kg of titanium powder (HDH and sponge fines) and powder size (-μm). Country of origin indicated by colour.

Figure 106 and Figure 107 below present the same data but with oxygen and chlorine content indicated by colour. Points with no colour indicate that this information was not available. In Figure 106, none of the powders have an oxygen content of grade 1 (<0.18 wt%) and most are specified as grade 2 (<0.25 wt%, in yellow). Finer powders with a particle size distribution beneath 100μm exhibit the highest oxygen content (greater than 0.35 wt% as shown in red). Although finer particles are more desirable due to enhanced sintering and better packing densities [213], these powders are characteristically higher in oxygen, as discussed in section 4.5.4, due to the increased surface area. Producing fine powders with a low oxygen content can therefore demand very high prices. Sponge fines are cheap, but have a coarse particle size, and cannot be easily milled to finer powder due to the ductility of the metal. HDH powders are often more expensive than sponge fines due to the additional processing that enables milling of the brittle TiH_2 intermediate [214]. Low cost HDH powder is produced from both sponge and scrap, but because the scrap is contaminated with grease, lubricating oil or oxide film, these cheaper powders can have greater contamination [213]. Therefore, it is assumed that the lowest priced powders in the dataset (~$20/kg) have the highest levels of contamination.

Chlorine is problematic for most of the powders for which prices were sourced. As seen in Figure 107, except for four price points (green), it is not guaranteed that that the chlorine content is less than 0.015 wt%, the value below which welding is reported to improve. The powder with the lowest chlorine content (0.003 wt%) is the most expensive, at 180 $/kg. This is in line with German [215], who reported in 2013 that powders with low interstitial levels are priced in the range of $110/kg to $220/kg. There are only two low-chlorine data points priced below 50$/kg, one of which has an unacceptable maximum oxygen content of 0.4 wt%. As discussed in section 3.4, the high chlorine content in low-cost powders such as HDH and sponge fines is a function of their processing and the circumvention of melting.

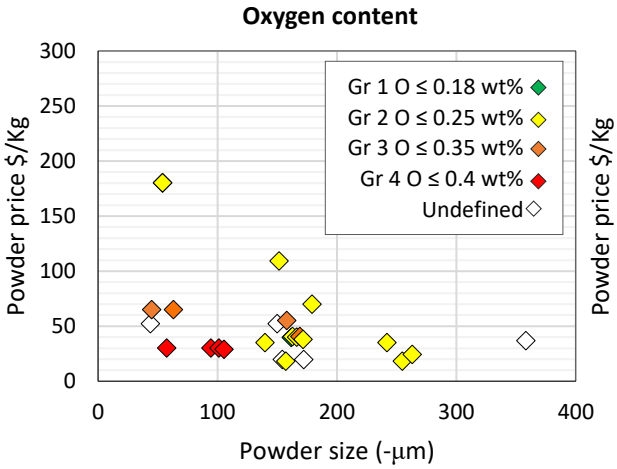

Figure 106: Price per kg of titanium powder (HDH and sponge fines) versus powder size (<μm). Oxygen content indicated by colour.

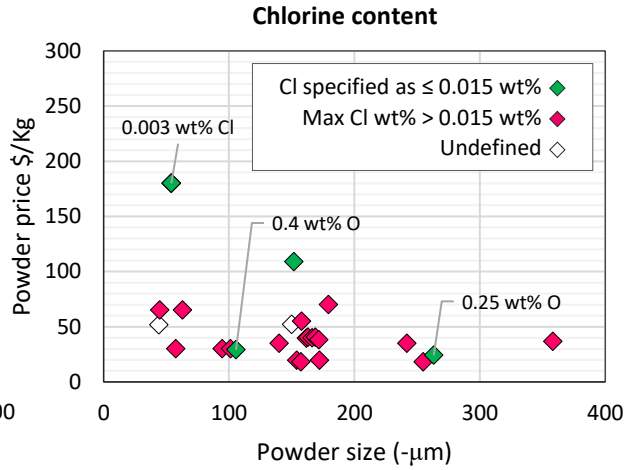

Figure 107: Price per kg of titanium powder (HDH and sponge fines) versus powder size (<μm). Chlorine content indicated by colour.

TiH_2 and Atomised powders

Quotations for TiH_2 and atomised powders were sourced from manufacturers and distributors in China, the USA, and Germany. The suppliers contacted are shown in Table 9.

Table 9: Sources of price data for HDH and sponge fines

Powder	Source/Supplier	Country	Online/direct quote
TiH_2	Luoyang Tongrun Info Technology	China	Direct Quote
	Tritrust Industrial	China	Direct Quote
	AG Materials	China	Direct Quote
	Tunique	China	Direct Quote
	American Elements	USA	Direct Quote
	Noah tech	USA	Online
Atomised	Sophia's wholesale	China	Online
	Beijing GaoYe Technology	China	Direct Quote
	Goodfellows	USA	Online
	Phelly	USA	Direct Quote
	SMB Powders	USA	Direct Quote
	TLS Technik GmbH & Co Spezialpulver	Germany	Online

Figure 108 compares prices for TiH_2, atomised and DPR applicable powders. Atomised powder prices are included as a reference, showing the relative increase in cost for high purity melt powders. As expected, the atomised powders are considerably costlier than the sponge derived powders. TiH_2 and HDH powders are similarly priced, even though TiH_2 is an intermediate in the HDH process. This may be due to the small size of the TiH_2 market and resultant price inefficiencies, in comparison to the well-established HDH market.

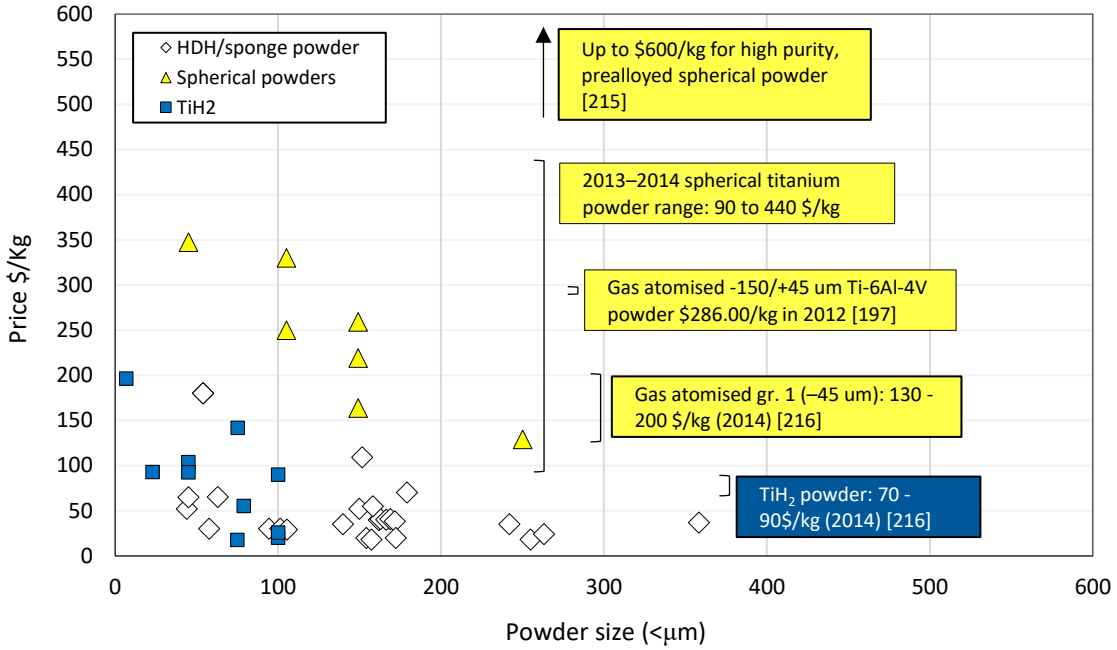

Figure 108: Comparison of HDH/sponge, spherical and TiH_2 powder prices.

7 DPR Strip versus Wrought Strip

The price of wrought strip is compared to the current price of powder in Figure 109. Wrought strip is divided into the two distinct markets identified in section 6.1 (China, and the US and EU). The strip is also divided into two groups of thickness, <1 mm and >1 mm. The price of sponge, slab and ingot is provided for reference. Based on the current powder price range (blue), DPR product would not be able to compete with most of the wrought strip from China (red) as the upper powder price estimate exceeds the market price of most Chinese product, and the lower powder price estimate leaves little margin for processing and overhead costs.

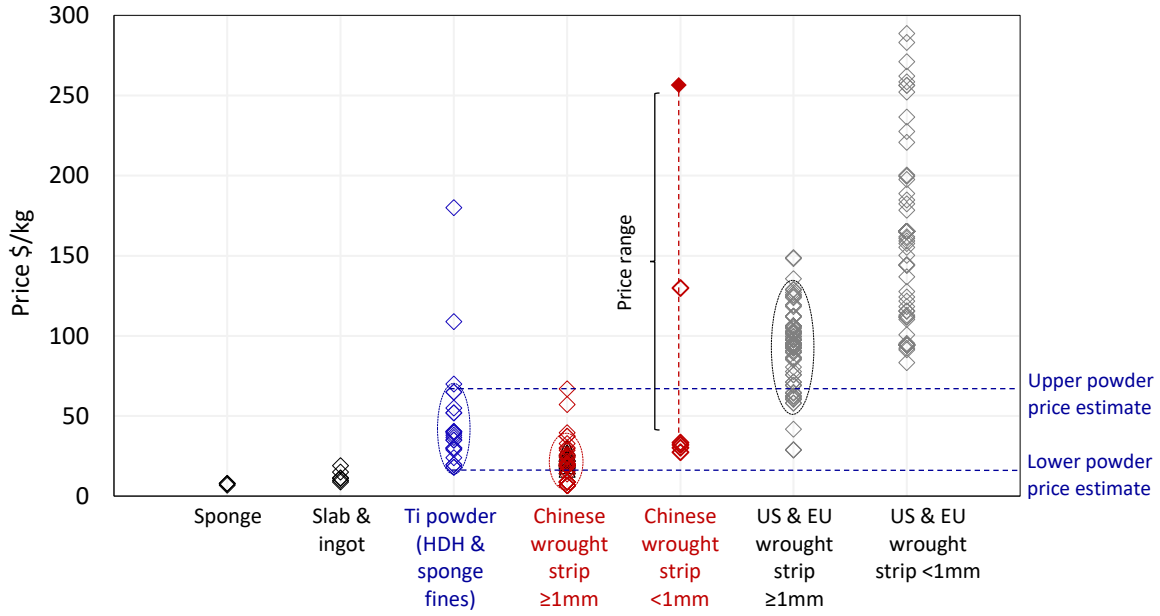

Figure 109: Price comparison of wrought titanium products versus the current price of titanium powder.

There are only a few discrete price points in the data set for Chinese strip that is less than 1 mm thick. Therefore, price ranges, seen in Figure 109 (as red lines), are used as an estimate. Since the price of <1 mm thick Chinese strip is high (>$100/kg), there is the potential for DPR to compete with this very thin gauge product.

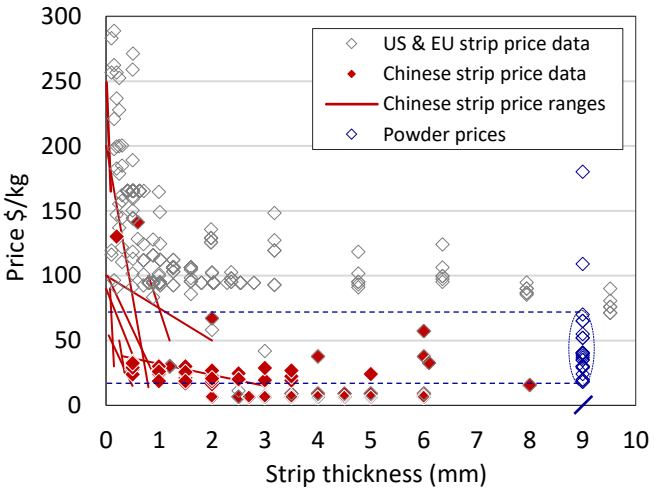

Figure 110: Price of wrought strip from China and the US and EU versus the price of titanium powder.

For US and EU product (grey in Figure 109 and Figure 109) the market is geared towards the aerospace industry, where high quality aerospace grade sponge (as well as tight tolerances, and stringent production and testing controls [217]) account for the higher price. Although lower cost powders (those under $50/kg) are priced well below US and EU strip prices (allowing for commercially feasible margins), the quality of this powder is unlikely to yield a product with properties equivalent to the US and EU product. As seen in Figure 111 below, almost all the powder priced under $50/kg is from China, which, as established in section 7.1.4, is derived from industrial grade sponge, and caters predominantly to the industrial market.

The impurity levels and country of origin for the powder price data are shown in Figure 111 (1 - chlorine & 2 - country). For most powders priced below the US and EU price estimate for wrought strip (dotted line), it is not guaranteed that the chlorine content will be less than 0.015 wt%, (the point at which welding is reported to improve), and as established in section 3.4, it is unlikely to be lower than 0.005 wt% (the critical point identified by Du Pont for acceptable weld quality).

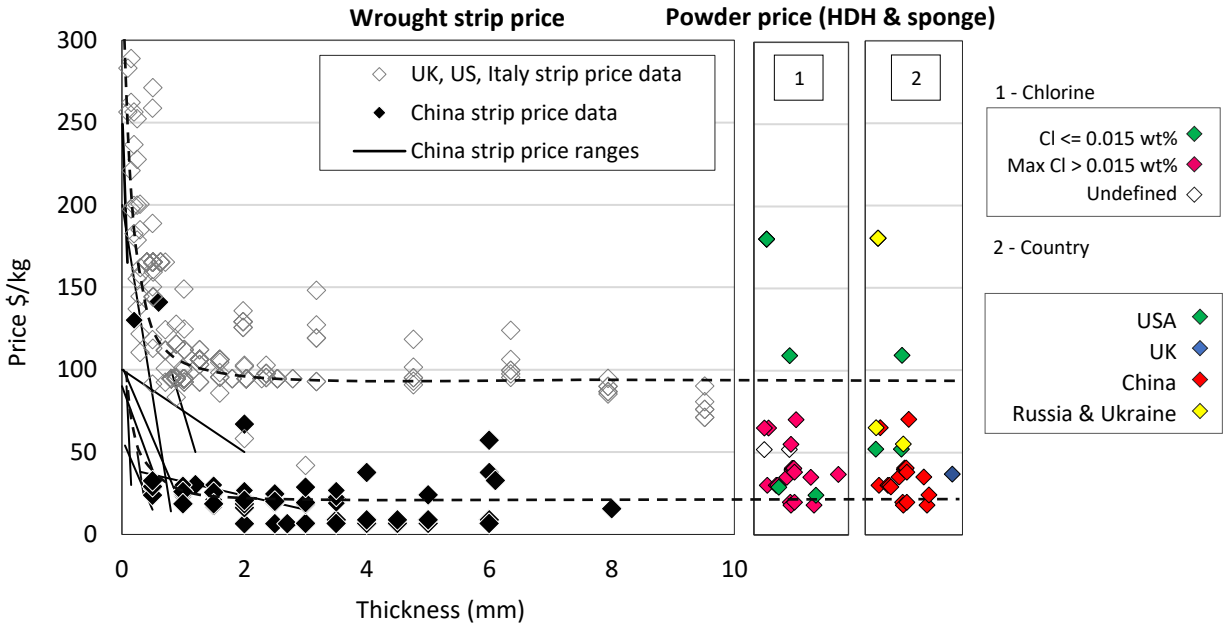

Figure 111: Unit price of wrought strip versus unit price of commercially available sponge derived titanium powder

In Summary

- The price of powder in the Chinese market, in relation to the price of wrought product in the US and EU market, allows for a margin of profit. However, the markets are not comparable, as the US and EU wrought market is geared towards the aerospace sector, and the Chinese titanium market is geared towards the industrial sector. Hence the quality of powder from China is unlikely to produce a product equivalent to US and EU wrought standards.
- Comparing Chinese powder prices to Chinese wrought product prices shows that the potential for commercial viability exists for thin gauge strip of less than 1 mm thickness.
- There is limited powder price data for the US and EU market, hence further price points would need to be gathered. It is assumed that like the Chinese market, the greatest commercial potential exists for thin gauge strip of less than 1 mm thickness.

8 Potential Product Applications

As discussed in section 7.1.4, the aerospace industry accounts for most of the global consumption of titanium mill product [180], of which Ti-6Al-4V (grade 5) is most widely used. Alpha and beta stabilizers (Al and V respectively) make grade 5 heat treatable, enabling significant increases in strength. Its combination of high strength at low to moderate temperatures, light weight and corrosion resistance offers all-round performance, making it particularly suitable for strength-to-weight critical aerospace applications [218].

The pure titanium grades (1-4) are used predominantly in chemical, marine, power generation and refining industries where excellent corrosion resistance is a critical requirement. Major applications include heat transfer (condensers, shell and tube heat exchangers and plate and frame heat exchangers) and welded tubing [219]. Oxygen content determines strength and cold formability. Grades 1 is the purest form, exhibiting the best room temperature ductility and formability, but the lowest strength. It is used where maximum formability is required. Grade 2 titanium is considered the “workhorse” for industrial applications. Its combination of strength and formability make it the most popular choice of the unalloyed grades. It is used where formability and corrosion resistance are important, and strength requirements moderate. Grade 3 is a higher strength grade, and is moderately cold formable. Grade 4 has the highest strength and hardness, and the lowest ductility and formability. The influence of the interstitial content decreases with increasing temperature, hence warm forming of the moderately cold formable grades 3 and 4 is common if the required forming strains are not large [220]. Most forming of grades 3 and 4 is reportedly performed at room temperature [221]. All four of the commercially pure grades can be satisfactorily welded and machined [221].

Typical product applications for grade 1 – 5 titanium were soured from literature, catalogues, standards and reference manuals. These applications are listed in Table 10. Applications using flat mill product (foil, sheet and plate) are in the left-hand column. Applications using non-flat mill product (tube, bar etc.) as well as forged or machined parts are listed in the right-hand column.

The higher strength grades, particularly 3, 4 and 5 (Ti-6Al-4V), have fewer applications derived from flat product, especially thin gauge sheet. Most of the applications for the higher strength grades are for larger, strength-to-weight critical parts e.g. Ti-6Al-4V for moving parts or exposure to environments of elevated temperature (aerospace engines and power generation systems) and structurally critical parts (aircraft and automotive frames). The more ductile, lower strength grades are “economically available” in thin strip and tube form, while the higher strength grades require hot forming into seamless pipes or forgings [222]. Titanium alloys, including Ti-6Al-4V, are not easily cold worked as they have a low elastic modulus’s and high yield strengths, which causes springback (it tends to resume its prior shape) [223]. Forming problems are “formidable” as forces and tooling loads are high, and sheet constructions made from titanium alloys are rarely found [224].

Grade 3 is used almost exclusively in pressure vessels as the higher strength allows for reduced wall thicknesses [225]. Although grade 3 is still moderately cold-formable [225], and available in all product forms, it is the least used of the commercially pure grades [226] [227], and is consequently not stocked by all titanium distributors (for example Continental Steel and Tube Company, Permascand and POSCO). The same is true for grade 4, which is used used interchangeably with grade 3 [221]. Grade 4 has recently found a niche in the bio-medical field (surgical hardware) [228].

Most of the applications for flat product are fabricated from the purer, more ductile, grades 1 and 2. The formability of these grades is a likely factor, given that forming, bending and stamping are common methods of fabricating flat product into shapes. Excellent corrosion resistance and ease of formability make grade 1 and 2 the main grades of choice [229], especially in the chemical processing industry, where material selection is driven less by strength and more by the ability to resist corrosion, or to transfer heat, such as in heat exchangers.

Grade 2 titanium and Ti-6Al-4V see dominant use as they satisfy most performance requirements, and the extent of their usage contributes significantly to efficiencies in production and cost-effectiveness (for example, welding consumables are easily available) [149].

Table 10: Product applications for grades 1 – 5 titanium

ASTM grade	Flat product applications (foil, sheet and plate)	Non-flat product (other mill shapes, customized product forms - forgings, castings, parts machined from thicker product)
1	• High purity foils and sheet for coating and thin film chemical vapor deposition [230] • Airframe structural items e.g. panels [231] • Architecture - exterior cladding (0.4 to 1 mm thick) [225] • Laptop casing (Apple PowerBook G4). Thin foil outer skin wrapped [225] • Sheet metal for explosive claddings. Cladding for steel reactors [225] • Honeycomb (used in aero structures) [232] • Welded tubes and pipes for heat exchangers [233] • Plate & shell heat exchangers (welding required) [234] • More complex shaped plates in plate and frame heat exchangers [235] • Surface protective layer in explosively clad (bonded) plate or parts [235]. Steel substrate (for structural strength) clad with Ti (for corrosion resistance) [229] • Platinized anodes [236] • Mountaineering products - Bottles, cups, other food ware [237] • Tubes in desalination and water treatment systems [238]	• Slip joint connectors fabricated from tube (automotive exhaust systems) [239] • Extruded seamless tubes [240] • Exhaust pipe systems in race cars and motorcycles [238]
2	• Stacks and chimney linings in flue gas desulphurization plants [225] • Straight lengths of condenser tubes used in nuclear turbines [241] • Tubes in desalination and water treatment systems [238] and condensers [242], and seawater lift pipes (offshore oil and gas) [243] • Boilers and pressure vessels [244]. Reaction vessels [221]. Reactors, crystallisers, columns [245] • Cryogenic vessels – used only for tubing/small scale cryogenic applications that involve low stresses [229] • Plates and welded tubes and pipes in heat exchangers for condensers and evaporators [233] [235]. Thin wall condenser tubing (0.5mm) [246] • Sheet for airframe skins & non-structural components [247]. Fire wall panels [231] • Anodes for chlorine production cells, electro dialysis plants, electroplating equipment, cathodic protection of condensers [221] • Offshore oil and gas – ballast water systems, penetration sleeves, seawater pipework, drilling riser, booster lines, anchor system pipework, penetrations and manholes [243] • Ductwork (by-pass ducts and hot-air ducts in aircraft) [221] • Firewater systems (offshore oil and gas) [243] • Formed brackets [221] Gaskets [248] • Cathodes/starter sheet blanks in electrochemical metal-refining operations [221] • Plate cladding material [249]	• Automotive - exhaust system, outlet valves [252] • Valves [253] chlor-alkali industry, soda industry, pharmaceutical industry, fertilizer industry and nitric acid industry • Flanges (to transition from Al or stainless to Ti intake and charge piping) [239] • Extruded seamless tubes [240] (extrusion of hollow billets)

	• Containment and tank construction – full wall structures, loose linings, and plated construction styles (to 15 mm thickness) [250] • Orthodontic brackets [251]. • Forged cases for watches (Garmin Watch) • Mountaineering products - Bottles, cups, other food ware [237]	
3	• Heat exchangers [221] [254]. Used for matrix-plates in shell and tube heat exchangers [255] [256]. Main use in plate and shell heat exchangers [257]. • Non-structural aircraft parts [247] Airframe skin [221] • Watch cases (Unity Watches) • Welded tubes and pipes for heat exchangers [233]. Thin-walled welded tubes in the drain line system of a civil aircraft [258] • Cryogenic vessels [221] • Nearly exclusively used for pressure vessel applications. [482] [259]. Boilers [244].	• Flanged and gasketed piping systems [260] • Valves [253] chlor-alkali industry, soda industry, pharmaceutical industry, fertilizer industry and nitric acid industry • Seamless tubes [261]
4	• Plate fin heat exchangers. Fin and plate stock. [262] • Orthodontic brackets [251]. Most widely used titanium alloy in medical implants but not common in dental implants [228]. Rigid Mesh for neuro implants (0.4 mm thickness) (Synthes CMF) • Tube sheet in heat exchangers [263] (labelled in figure 112 below) • Fin sheet in heat exchangers [263] [262]	• Automotive frame structures (body) [252] • Brake pad carrier plates [482] • Commonly used in orthopaedics/surgical implants [264] • High speed fans [236] • Gas compressors [236] • Preferentially used for mountings and fittings due to high strength [225] • Extruded seamless tubes [240] • Used in hydraulic and instrumentation tubing [265]
5 (Ti-6Al-4V)	• 0.3 mm thick foil for composite material in aerospace applications [266]. Not widely used in the chemical process industries [257] • Foil - forming into pacemaker shields [267] • Watch cases (Planet Ocean 600m Omega Co-Axial Master Chronometer) • Sheet in aerospace – stringer structures, frames, fire-walls, stiffeners, gussets and ducts [236] • Orthodontic brackets [251] • Pressure vessels [236] Pressure bottles [236] • Plates used in military/defense armor applications [268] • Ti 6Al 4V ELI (extra low interstitials) sheet has found application in medical implants owing to its excellent biocompatibility, high strength, and MRI compatibility. Maximum oxygen content is 0.13 wt%. [269] • Ti 6Al 4V ELI usually preferred for cryogenic vessels – storage and handling of liquefied gases, storage pressure vessels [229] • Ti3Al2.5V - better formability than Ti6Al4V with lower strength. Seamless tubes. Honeycomb core (laser welded) [Benecor Inc.]	• Gas turbine engines for static and rotating components [252] • Aircraft - fuselage, nacelles, landing gear, wing, and empennage, floor support structure, including galleys and lavatories. [252] • Automotive frame structures – body, suspension springs; Engines – outlet & intake valves, connecting rods [252] • Aircraft frames, jet & engine rocket components, pressure vessels, fasteners, prosthetic implants, geothermal-well casings, automotive components, sports equipment [270] • Steam turbine blades, blades and discs for aircraft turbines and compressors, Landing gear wheels and structures [236] • Fasteners, brackets and fittings [236]. • Valves (chlor-alkali industry, soda industry, pharmaceutical industry, fertilizer industry and nitric acid industry) [253] • Commonly used in orthopaedics/surgical implants [264] • Airframe applications - cockpit window frame, Wing box, Fastener, bolts, seat rails [271]

Heat exchangers (HE's) are a major industrial application for pure titanium sheets [219] [272]. Although the thermal conductivity is lower than other commonly used HE materials, titanium's excellent corrosion resistance allows for the use of thinner gauge product [243]. Grade 1 is the grade commonly used for plate heat exchangers (PHEs) [273] (shown in figure 112). Thin sheet (e.g. 0.5 to 1 mm thickness (HISAKA), or 0.4-0.6 mm (HYDAC International)) is press formed into complex corrugated patterns which increases the effective heat exchange area. Plates are packed between a fixed and a movable steel frame and tightened together with bolts. The edge of each plate is sealed with a synthetic rubber gasket, so no welding is required (alternatively they are brazed together). PHE plate patterns are usually cold stamped from any metal that can be cold worked [273] [274]. Grade 1 and 2 meet the fabrication requirements of reasonably complex patterns in PHEs [220].

Grade 2 is the most widely used material in heat exchangers [165] [257]. Its combination of strength, weldability, formability and corrosion resistance make it the "explicitly preferred" grade [224]. It is typically used as welded and seamless tubing in shell and tube heat exchangers [273] (figure 113). Welded tubing offers commercial potential for DPR because the wall thickness requirements (0.4 mm ≤ WT ≤ 2.77 mm [275]) are within the range producible via DPR, and secondly, the tube is fabricated from coiled strip. In a highly automated process, coiled strip is fed into a series of dies which roll bend it into the tube shape, followed by welding in an inert environment using a non-consumable tungsten electrode, or laser technology [275]. The construction of the shell and tube heat exchanger is more complex than PHEs. The welded pipes are bent into U-tubes and bundled together (figure 113) and the open ends of the tubes are fixed to a tube sheet (labelled in figure 113). There are various tube expansion methods to ensure a tight joint between the tubes in the tube bundle and the tube sheet. These methods include direct hydraulic expansion (where fluid pressure expands the tube diameter), explosive expansion, and mechanical rolling (figure 114 and 115) where a tapered rotary mandrel expands the tube diameter [276]. Consequently, material requirements for these tubes include - a uniform response to the applied bending and expansion methods, and good weldability [220]. The product must pass the flaring test set out in the standard specification for seamless and welded Ti and Ti alloy tubes for condensers and heat exchangers (ASTM B338 – 17). Grades 1, 2 and 3 are included in this specification. Grade 3 has also been used for the tube sheet [263]. There is little evidence of the use of grade 4 in heat exchangers. The few existing applications are lightweight plate-fin HEs in aircraft cabin control systems that cool bleed air, which can reach temperatures of 316°C-538°C [262].

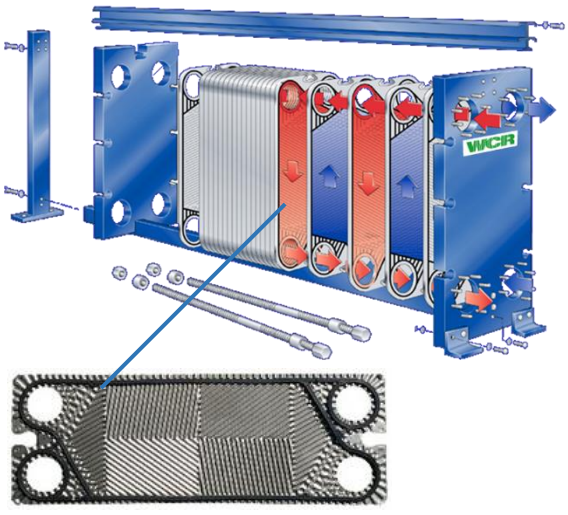

Figure 112: Plate heat exchanger (WCR Inc) and example of plate pattern.

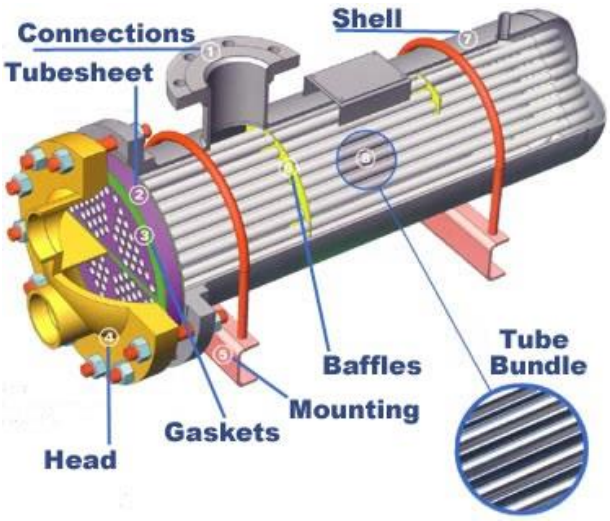

Figure 113: Shell and tube heat exchanger (South West Thermal Technologies Inc.).

Figure 114: U-tubes in a tube bundle [277].

Figure 115: Tube expander fixing tube to tube sheet [278].

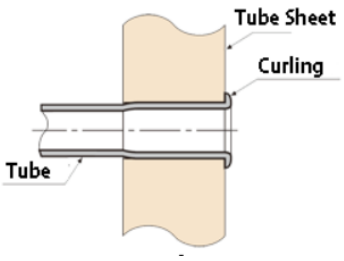

Figure 116: Tight joint between tube and the tube sheet [279].

Another widely used titanium product is welded piping which is used in power generation; chemical processing industries; and oil, gas and petroleum processing [96]. Titanium is immune to crevice corrosion in ambient temperature seawater, and is consequently used extensively in piping in marine and offshore oil and gas operations [243]. The standard specification for Ti and Ti alloy welded pipe (B862-14) is applicable to grades 1,2,3 and 5, and wall thicknesses of 1.24 mm up to 30 mm depending on the outside diameter of the pipe.

Most Promising DPR Product Applications

Ti-6Al-4V is used predominantly in high performance aerospace applications, as its cost is justified by its high strength-to-weight ratio. Such applications necessitate careful, and often costly, control of mill processing to meet the stringent standards [96]. Titanium is also used for non-structurally critical parts in aerospace applications (the nacelle, parts of the pylon and bleed air tubes) but here it is preferentially selected for its resistance to temperature effects and its corrosion resistance. As a result, the pure titanium grades are more functionally suitable, and selected over Ti-6Al-4V [271]. Hence, the stringent specifications and regulatory barriers for applications in which Ti-6Al-4V is most commonly used, as well as the small range and number of applications for thin gauge Ti-6Al-4V strip, greatly reduces the commercial potential of Ti-6Al-4V DPR strip. Furthermore, the minimum oxygen content for grade 5 (0.2 wt%) is not within the typical PM process capabilities, with HDH powders commonly having >0.18 wt% oxygen (figure 53, section 5.5.4) and with final product typically above 0.2 wt% (figure 55, section 5.5.5). Furthermore, it has not yet been demonstrated that Ti-6Al-4V DPR strip can match elongation values for **typical** wrought product (as seen in figure 78 in section 5.2).

Pure titanium for plate or shell and tube heat exchangers, as well as titanium piping, would be particularly suitable for production via DPR for the following three reasons:

1. Unlike aerospace, medical and pressure vessel applications, the quality standards and expectations for product used in industrial heat exchangers and piping are less stringent, offering a natural market entry point.
2. The dimensional requirements are within the process capabilities of DPR (width <610 mm and thickness <3mm).
3. Heat exchangers and piping are the most common applications for pure titanium and flat mill product (welded CP titanium tubing is deemed an important intermediate product [220]). The market is therefore large enough to warrant commercial potential.

However, the use of DPR product in heat exchangers and piping is problematic due to requirements for good formability and/or weldability. Plate heat exchangers sealed using gaskets do not require welding, but excellent formability is key, warranting the use of high purity grade 1. For tube heat exchangers, commonly made from grade 2, the sheet stock must be weldable and must have sufficient biaxial formability to meet flaring requirements.

DPR Strip Fabricability - Formability

ORNL [12] investigated the applicability of DPR sheet for use in heat exchangers. They tested elongation, bend radius and dome height, and stamped herringbone and dimple patterns. The elongation performance of the DPR sheet tested by ORNL is shown in Figure 117 (in blue) in relation to other fully processed DPR samples in the data set (green), as well as the typical properties of grade 1-4 wrought product. Pairs of longitudinal and transverse elongation are circled. ORNL samples with both longitudinal and transverse elongation within the grade 2 limit are some of the best performing in the DPR data set, and are technically grade 2 as they meet the minimum elongation requirement. However, the sheet performed poorly in the dome height test, and the low biaxial formability was attributed to the presence of voids. Consequently, the sheet could not be stamped successfully at room temperature (improved formability was found at 300°C and excellent formability at 600°C). Duz *et al* [13] concluded that the sub-standard formability of the DPR product made it unsuitable for die pressed plate heat exchangers. A recommendation for flat-plate heat exchangers was made, with reference to Campbell Applied Physics, who required very thin flat sheet (0.2mm) for a proprietary heat exchanger.

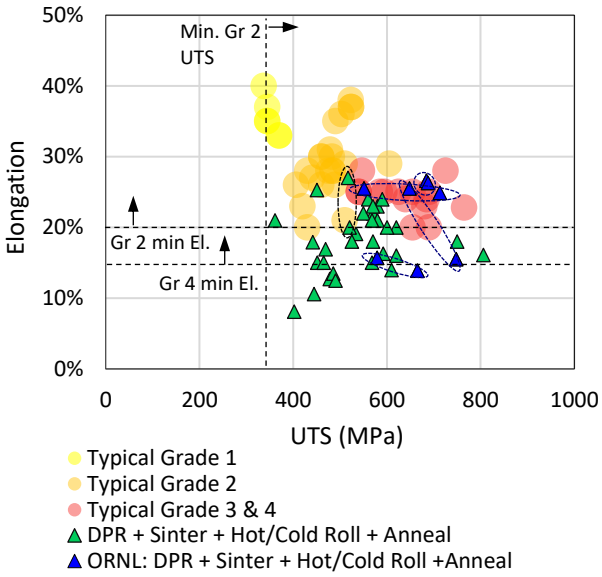

Figure 117: Elongation and UTS of fully processed DPR strip versus typical properties of grade 1-4 titanium. DPR - 8 sources (>2008).

Kapranos *et al*. [280] claim that because ductility is critical for the fabrication of plate heat exchangers (and for expansion of tube sheet in shell and tube HEs), the upper range of performance of grade 2 product is preferred. In Figure 117 it is evident that DPR product is not of typical grade 2 quality (25-30% elongation), and is certainly not upper grade 2 quality. Lunde *et al*. [281] claim that oxygen content is even more important than ductility, and that no more than 0.16 wt% should be present in grade 2 material to avoid micro-cracks during cold forming. In Figure 118 is evident that an oxygen content less than 0.16 wt% has not been achieved for PM product (that is non-hydride derived), whereas most of the grade 2 wrought product sample is well below this (Figure 119).

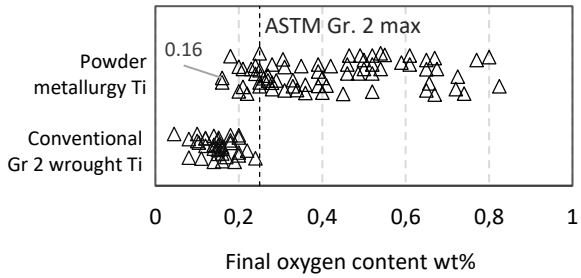

Figure 118: Final oxygen content of PM product versus conventional wrought Ti.

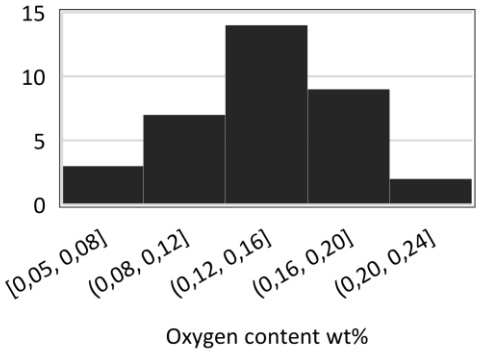

Figure 119: Distribution of typical oxygen content for grade 2 wrought product (ASTM max is 0.25 wt% O). Sample size = 35

The difficulty in commercializing a powder metallurgy route is that it must compete with the existing, well-established and streamlined wrought processing route that has evolved through years of incremental optimization. Peter *et al*. [10] claim that such improvements are not reflected in titanium specifications, as minimum requirements are well below the actual performance of wrought product currently on the market.

DPR Strip Fabricability - Weldability

Welding problems due to remnant chloride impurities from the Kroll reduction process were discussed in section 3.4, and it was established that the low-cost, non-melt, Kroll sponge derived powders available today are still above the chlorine content (0.005 wt%) identified by Du Pont, above which welding problems occur. Further problems, not related to chlorine impurities, have also been observed in the welding of powder metallurgy components. Muth *et al*. [112] recently investigated the ability to fusion weld various **low chlorine** containing Ti and Ti-6Al-4V plates made from the following powders:

- Armstrong powder (the low Cl, developmental powder discussed in section 4.2)
- HDH powder made from revert scrap (ingot derived and therefore low in Cl)
- TiH_2 (Ti-6Al-4V plate purchased from ADMA with low Cl due to "cleaning" effect of TiH_2).

Although all plates had a chlorine content less than 0.001 wt%, and were consolidated to full density, the weld quality was unacceptable. Weld porosity was attributed to hydrogen gas from water adsorbed on the surface of powder particles, as well as gas-forming sodium or magnesium species, remnant from the reduction of sponge (which is usually removed during triple VAR melting of sponge). Muth *et al*. ultimately concluded that the PM product could not be reliably fusion welded. Greenfield *et al*. [282] reported similar porosity problems in the welding of fully-dense Ti-6Al-4V HIPed compacts made from low chlorine pre-alloyed HDH powder (i.e. ingot derived). Although the welding of compacts made from spherical prealloyed Ti-6Al-4V powder was not problematic, linear porosity (an array of porosity positioned in a line) in the weld zone of the HDH compact was attributed to adsorbed gases, other than hydrogen, on the higher specific surface area of the HDH powder (a six-fold difference in surface area was determined). The as-welded tensile properties of the fully dense HIPed HDH compacts were not "appreciably affected" by the linear porosity, but Greenfield *et al*. concluded that HDH derived compacts would not be acceptable for fatigue related applications. Compacts that were not fully dense (99.9% - which is still very high) were found to be unweldable due to outgassing in the fusion zone, which destabilized the arc.

The low chloride containing specimens used by Greenfield *et al*. [282] and Muth *et al*. [112] were made from powders that are not suitable for a commercial DPR operation, as they are either too expensive (HDH derived from wrought product), developmental and not readily available (Armstrong), or not compatible with the process (brittle TiH_2). Low-cost commercially available powders that are suitable for DPR (e.g. sponge derived HDH) contain higher chlorine levels (as established in section 3.4), and hence welding problems are likely to be more severe that those observed by Greenfield *et al*. and Muth *et al* for low chlorine compacts. Given the critical requirement for weldability in many sheet applications and the welding problems so detrimental to Du Pont's DPR endeavors in the 1960's, it is surprising that there is so little research on the welding of PM flat product.

Potential Product Applications

The profile of DPR product has been narrowed down to the following: unweldable strip, of up to 2-3.2 mm thickness, matching the typical tensile performance and oxygen content of grade 3 and 4 wrought product. The maximum thickness of 2-3.2 mm is what has been identified as technically feasible. A thickness of 1 mm or less is likely to be economically feasible based on the powder price and market analysis in section 8.1. Applications for thin gauge grade 3 and 4 product are limited, as seen in Table 11 below. It is evident that grade 3 and 4 is typically selected for thicker product where greater strength is a requirement e.g. matrix plates in shell and tube heat exchangers and pressure vessels.

The range of applications for the DPR product could be expanded if customers are willing to adapt their fabrication operations, for example, forming the less-formable grades 3 and 4 at higher temperatures for applications in which grade 2 is typically selected for its room temperature formability. This could be justified if the DPR process demonstrates a considerable cost advantage relative to conventional wrought processing.

Table 11: Grade 3 and 4 wrought flat product applications

ASTM grade	Flat product applications (foil, sheet and plate)
3	• Heat exchangers [221] [254]. Used for matrix-plates in shell and tube heat exchangers [255] [256]. Main use in plate and shell heat exchangers [257]. • Non-structural aircraft parts [247] Airframe skin [221] • Watch cases (Unity Watches) • Welded tubes and pipes for heat exchangers [233]. Thin-walled welded tubes in the drain line system of a civil aircraft [258] • Cryogenic vessels [221] • Nearly exclusively used for pressure vessel applications. [482] [259]. Boilers [244].
4	• Plate fin heat exchangers. Fin and plate stock. [262] • Orthodontic brackets [251]. Most widely used titanium alloy in medical implants but not common in dental implants [228]. Rigid Mesh for neuro implants (0.4 mm thickness) (Synthes CMF) • Tube sheet in heat exchangers [263] • Fin sheet in heat exchangers [263] [262]

In Summary

- The inability of DPR product to meet the upper range of typical grade 2 elongation (>25%) and the lower range of oxygen (0.16 wt%) excludes the largest proportion of potential product applications for pure titanium – heat exchangers and tubing.
- Strip produced via DPR has not demonstrated the ability to meet the fabricability requirements, mainly formability and weldability, for applications in which pure titanium is most commonly used – heat exchangers and piping.
- The performance profile of DPR strip, in terms of elongation and oxygen content, is equivalent to typical grade 3 and 4. At best, it is the lower end of the range of typical grade 2 in performance. The process capability of a representative and continuous DPR process would need to be assessed to determine if the upper limit of DPR performance could be reliably produced in a large-scale, commercial process.
- The range of potential product applications for thin gauge grade 3 and 4 strip is limited.
- Due to the preferential use of Ti-6Al-4V in high performance, stringently regulated, aerospace applications, as well as the preferential use of pure titanium in applications requiring better formability, the range of applications for thin gauge Ti-6Al-4V strip is small.

9 DPR Strip versus TiH_2 derived flat product

The TiH_2 preform route is currently the only other alternative route to producing flat product. This section discusses the potential for this route to compete directly with DPR product.

TiH_2 has shown enhanced sinterability, but achieving full or near full sintered density without additional thermomechanical work is, primarily, critical for near-net shapes, while a sintered density of 95% or less is not critically disadvantageous for DPR given that there is further deformation after sintering. Therefore, the relative advantage of the sinterability of TiH_2 is marginable.

The advantage of the TiH_2 preform route is that a greater range of thicknesses can be produced. As established in section 3.3, DPR strip is limited to 3.2 mm or less following a reduction of 50% or more, which limits the range of product applications. In the TiH_2 route, the thickness of the preform is not as limiting a factor. TiH_2 billets as large as 215 mm in thickness, 304 mm in width and 1320 mm in length have been produced via CIP + sintering [136]. The disadvantage of the CIP route is that it involves additional processing to reduce a thick preform to final gauge, and is less economical the thicker the starting preform and the thinner the final sheet.

ADMA has reduced 10cm thick "low cost" sintered Ti-6Al-4V preforms by 50% to 5cm, 2.5cm and 12.7 mm plate (shown in Figure 120). Their objective is to manufacture preforms of near-net size with subsequent rolling involving *"just enough thermomechanical processing to meet the material specification requirements, thus reducing the overall cost of the required processing steps"* [99]. There is little research on the minimum degree of thermomechanical work required to resolve remaining porosity, but for aerospace applications, ADMA claims that a reduction of at least ~66% is required for full densification and microstructure refinement [99].

Figure 120: 12.7 mm (0.5 inch) Ti-6Al-4V thick plate rolled from a TiH_2 derived preform. ADMA Products Inc.

The range of product thicknesses for the ADMA CIP preform route as well as the DPR route are compared in Figure 121 below to show the overlap of the two processing routes. The thinnest TiH2 derived sheet (1.7 mm from a 19 mm preform) is within the thickness range in which DPR operates.

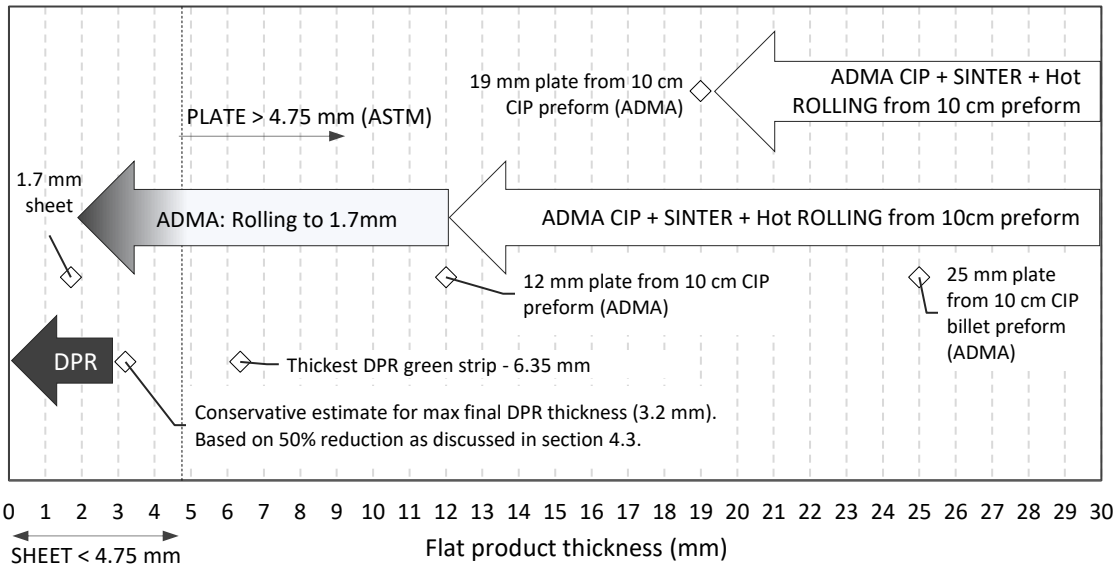

Figure 121: Thickness ranges for flat product produced via the CIP preform and DPR route.

The relative advantages and disadvantages of flat product derived via TiH_2 preforms are the following. Although it is a less direct route than DPR, there are still cost advantages relative to the conventional wrought route. The VAR melting step is bypassed (15% of the cost of a ~25 mm plate), and if starting with preforms close to the intended thickness, the route bypasses part of the processing of ingot to plate (which is as much as 47% of the total cost of a ~25 mm plate) [9].

In terms of feedstock cost, TiH2 is an intermediate in the manufacturing of HDH powder and is therefore likely to be cheaper if the market expands, although the current cost of TiH2 is on par with HDH, as discussed in section 6.2.2, affording little relative cost advantage now. ADMA's modified Kroll process, with 50% energy savings and 20% cost reduction expected at full commercialization [136], could offer potential for further cost savings (although HDH powder costs would benefit from this too). TiH2 derived product is not technically limited to thin gauge product, and wider product is possible too, i.e. sheet (>610mm). In terms of performance, ADMA's TiH2 derived Ti-6Al-4V plate has exhibited acceptable properties (both static tensile and fatigue and fracture properties [136]) using low-cost blended elemental feedstock (ADMA) (as opposed to better quality but costly prealloyed powder). Ti-6Al-4V sheet derived from TiH2 meets minimum and typical grade 5 elongation properties, and therefore outperforms DPR product, which only just meets the minimum specification (as seen in Figure 122: TiH2 derived Ti-6Al-4V flat product versus DPR. below). Pure titanium sheets derived from TiH2 preforms perform no better than DPR product, as seen in Figure 123 below, so no relative advantage has been demonstrated in this case.

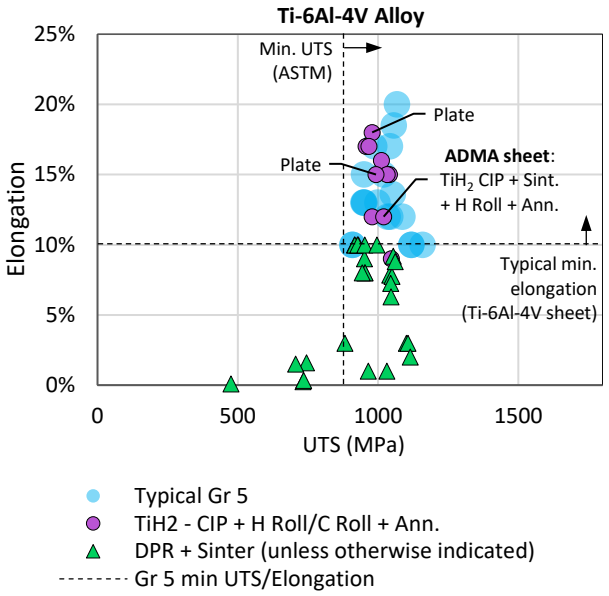

Figure 122: TiH_2 derived Ti-6Al-4V flat product versus DPR.

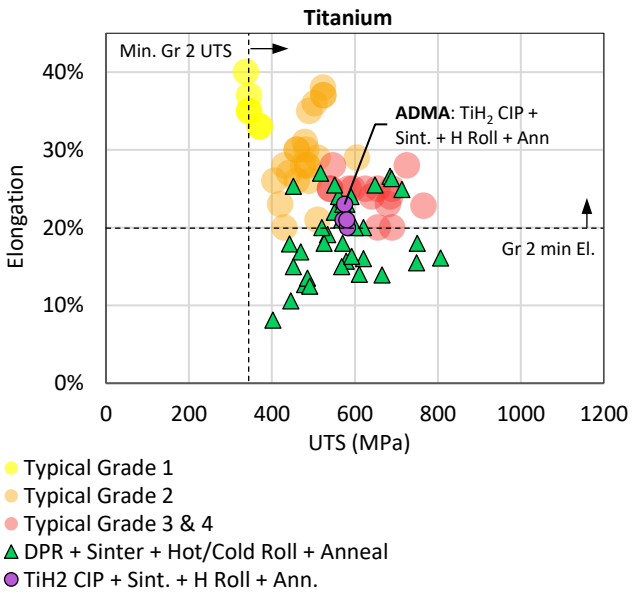

Figure 123: TiH_2 derived titanium flat product versus DPR.

In terms of product fabricability, the main advantage of the TiH2 preform route is the potential to remove, and therefore limit the adsorption, of interstitials (as discussed in section 4.2). This is particularly important given the degradation of ductility due to oxygen, as well as the detrimental effect that chloride impurities and adsorbed water have on weldability. However, there is little research demonstrating the weldability of TiH2 derived plate. ADMA claims to be able to produce weldable titanium and Ti-6Al-4V plate containing less than 0.16 wt% oxygen and 0.0015 wt% chlorine [135], but as discussed in the previous section, Muth *et al*. [112] observed weld porosity in welded TiH2 derived Ti-6Al-4V plate from ADMA. The weld porosity is shown in Figure 124 and Figure 125 below.

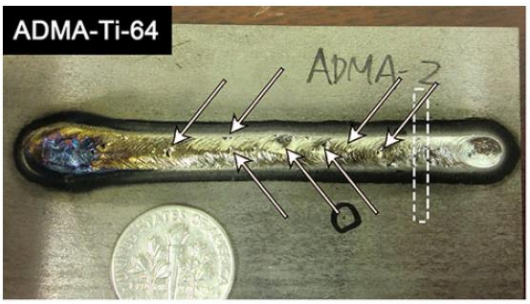

Figure 124: GTA weld of ADMA Ti-6Al-4V plate. Plate and weld porosity shown. Dotted white rectangle shows position cross-section. [111]

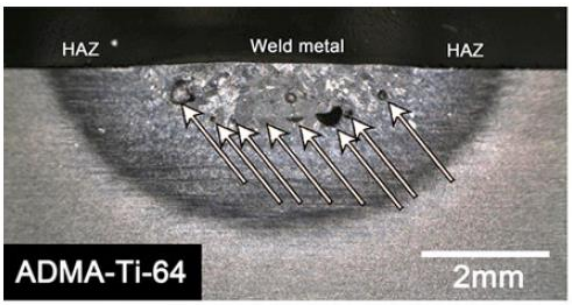

Figure 125: Cross-section of GTA weld of ADMA Ti-6Al-4V plate. [110]

In the as-received condition, the ADMA plate contained residual porosity, and consequently required a 20% hot rolling reduction to attain full density. The plate had minimal chlorine content, but an oxygen content of 0.248 wt%, which is above the grade 5 minimum of 0.2 wt%, and well above the 0.16 wt% reportedly attainable in their patent (US 20150328684). Although not confirmed, Muth *et al*. attributed the porosity in the ADMA plate to residual sodium and magnesium, which was present at detectable levels.

It is noted that Muth *et al*. [112] published their research in 2013, whereas ADMA's claims of weldability were made in a patent published later (2015). As shown in Table 12, it is possible that subsequent to the investigation by Muth *et al*. [112], improvements in ADMA's product (particularly Na content) via process optimization or better feedstock selection have improved the weldability of the product.

Table 12: Comparison of trace elements in ADMA plate tested in 2013 and values reported in a 2015 patent

Contaminant	Wt% in plate tested by Muth *et al*. [112] in 2013	Wt% in example 3 in ADMA Patent [135] published in 2015
Cl	<0.001	<0.001
Na	**0.072**	<0.001
Mg	0.001	<0.004
O_2	**0.248**	<0.15
H_2	0.0048	<0.0055

If TiH_2 derived product proves to be weldable, and non-hydride derived product i.e. DPR, does not, then it may be the only viable alternative for applications where welding is a requirement, even though the cost reduction for thin gauge sheet via the TiH_2 route may be only marginal compared to the wrought metallurgy route. Due to evidence of the reduction of gas forming impurities, as well as ADMA's assertion that the product is weldable, the TiH_2 route is better positioned to demonstrate weldability. However further welding research for both DPR and TiH_2 derived product is required.

The overall degree of cost reduction via DPR, relative to the TiH2 preform route, is unclear, but for thin gauge strip, the DPR route is likely to be cheaper because it is the most direct route. The TiH2 preform route is therefore unlikely to compete directly or threaten the commercial viability of the DPR route (unless DPR proves to be unweldable and TiH2 derived product does not). ADMA has demonstrated the ability to produce sheet via the TiH2 preform route, but much of the product development is directed towards Ti-6Al-4V in bulkier forms (e.g. plate, extruded near net shapes, hot rolled bars, and flow formed tubes) for critical applications, and armour plates in the aerospace and defence market [136]. Ti-6Al-4V, the most widely used titanium grade, is often in thicker product form where it is functionally appropriate for high strength-to-weight applications. This, and the fact that the TiH2 derived Ti-6Al-4V product compares well to the typical wrought product (as seen in Figure 122) may explain ADMA's current commercial focus. Therefore, a likely scenario is the establishment of the TiH_2 preform route as a complementary process, producing plate or thicker sheet, although the product is likely to be plate (>4.75mm) as this would be more cost-effective due to less thermomechanical work from preform to final product.

10 Commercial Viability Assessment

The aim of this research was to determine the commercial viability of direct powder rolled titanium. The three analyses around which the research was structured are highlighted in (the framework discussed previously in section 3). The key conclusions drawn from each of the analyses are identified below.

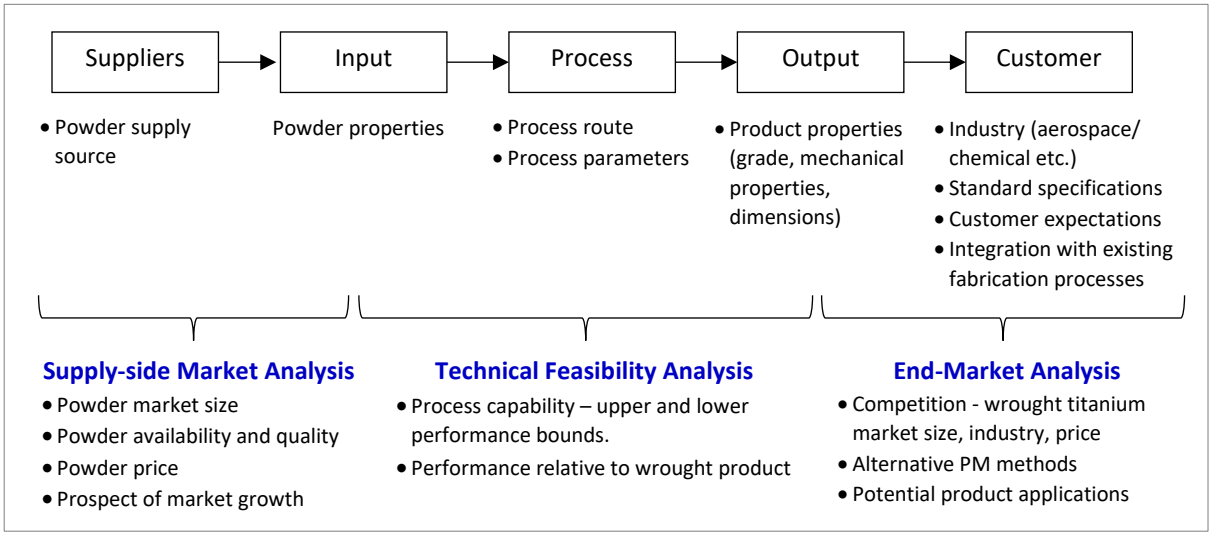

Figure 126: Commercial viability framework

The supply-side market

The lack of availability of low cost titanium powders produced in high volume and suitable for roll compaction, continues to be a commercialization barrier. The current powder market is small, and the potential for market growth is presently more promising for the AM industry, in which HDH powder is not a common feedstock. Continued research into alternative extraction and powder manufacturing processes indicates that the current cost and/or quality of commercially available powders is not yet optimal. Some of these "developmental" processes are already on the market, but they are either processed into spherical powders for the growing AM market (e.g. FFC Cambridge), or have not demonstrated improved properties or performance (e.g. Armstrong powders have a starting oxygen content that is typically greater than 0.25 wt%).

Of the long-established and widely used commercially available powders, these are either high purity and expensive, having been manufactured from wrought product, or are low cost and high in residual impurities from the Kroll reduction process. The level of chlorine has decreased following the introduction of the HDH process, however sponge derived HDH powders still typically have a chlorine content of 0.02wt% or more. Hence, chlorine is still above 0.005 wt%, the point below which Du Pont reported improvement in weldability.

Technical feasibility of process

A comparison to the typical properties of wrought product has been crucial to the analysis of the commercial viability of DPR product. As seen in the consolidation of wrought data, typical properties are commonly far better than the ASTM specifications, possibly due to the continued optimization of sponge-to-ingot processing over the years. Since the typical properties of wrought product are representative of the design and fabrication expectations of customers, producing a product that meets these expectations is a critical factor for market acceptance. The consolidation of data from literature has provided an estimate of the upper and lower bounds of the process capability of DPR. Based on the current quality of powders available, as well as the process boundaries identified, the profile of DPR product is: unweldable strip, of up to 2-3.2 mm thickness, matching the typical performance of grade 3 or 4 wrought product.

In terms of impurities, oxygen content remains the single greatest problem in powder metallurgy. Limiting the exposure to oxygen by carefully controlling storage, handling and processing conditions mitigates the risk of

contamination, but due to the particulate nature of the starting stock, some degree of oxidation is inevitable. The review of existing PM research has shown that a final oxygen content less than 0.2 wt% is not commonly achieved. The lowest oxygen content, via non-hydride derived PM, is 0.16 wt%. However, further research is required to determine whether 0.16 wt% could feasibly be achieved in a full scale operational environment, given the difficulty in operating consistently at the extreme limits of a process's capability. Ultimately, a robust process is preferred, with reasonable measures to minimize oxygen contamination. Hence, the DPR process capability is better suited to meeting the typical performance of grade 3 and 4 wrought product. This has been confirmed in terms of both the oxygen and elongation performance of product made via DPR and similar PM methods (die pressing and CIP).

The review of the literature has shown that in addition to chlorine, adsorbed water on powder particles (due to exposure during processing) is detrimental to the weldability of PM product. Adequate weldability has not yet been reliably demonstrated for PM product.

In terms of competing PM processes, the TiH_2 preform route, with its potential to lower oxygen content to less than that achieved via non-hydride methods (0.16 wt%), is a viable alternative to the production of flat product. However, it is most likely to be in plate form, and hence does not threaten the commercial viability of the thin gauge product produced via DPR.

The end-market

For DPR flat product to be commercially viable, it must have a competitive advantage over wrought product, e.g. a lower cost or enhanced performance. Since it has been established that the performance of DPR product is unlikely to exceed that of wrought product, the cost of the product will ultimately determine commercial viability. For flat product manufactured via the conventional route, the additional processing and related costs of rolling plate is seen in the exponentially increasing unit price as the sheet gets thinner. The comparison of powder prices to wrought product prices (on a market for market basis i.e. Chinese powder versus Chinese wrought product), has shown that the potential for commercial viability exists for thin gauge strip of less than 1 mm thickness, as this is where cost savings can be attained through direct route processing.

Based on the prospective profile of DPR product, the range of potential product applications is greatly limited. Aerospace and medical applications have been excluded as natural market entry points due to stringent expectations regarding the quality and tolerancing of mill product used for these applications. The industrial sector has been identified as a suitable entry point. Pure titanium is most commonly used in this industry. However, the inability to reliably meet the typical properties of the "workhorse", grade 2, excludes the largest proportion of applications for pure titanium in strip form (i.e. heat exchangers and tubing). Furthermore, the prospect of producing a weldable product is poor, given the lack of evidence of weldable PM product made from low-cost sponge derived powders such as HDH powder. An unweldable product limits fabricability, and further restricts the usage of DPR product to applications where welding is not a critical requirement.

11 In Conclusion

The most critical commercialization barrier for DPR is the limited range of potential applications suitable for the DPR product profile identified in this research. For this reason, it is concluded that DPR is not a commercially viable process. The product profile that has been identified is: unweldable strip, of up to 2-3.2 mm thickness, but probably only up to 1 mm thickness, matching the typical performance of grade 3 or 4 wrought product. Ultimately, the range of potential product applications is limited because of the following:

1. The lack of availability of low-cost powders. This limits the product thickness to thin gauge strip (<1mm) as this is the range in which a profit margin is more likely to be secured relative to the current market price of wrought product of similar thickness.
2. The lack of availability of low-cost **quality** powders. The chlorine content of low-cost non-melt powders (typically >0.02 wt%) weakens the prospect of producing a weldable product.
3. DPR processing limitations, particularly oxygen control. The final oxygen content, that is typically greater than 0.2 wt%, limits the elongation and tensile properties of the final product to typical grade 3 and 4.

12 Recommendations for Future Work

Although this research has concluded that DPR is not commercially viable, the following recommendations are made regarding further work to confirm the commercialization barriers identified or to refine the process and performance bounds identified.

- **Specific applications for pure titanium DPR product:** It has been established that pure titanium DPR product is unlikely to be suitable for applications in which the pure titanium grades are most commonly used (i.e. heat exchangers and tubing). Further work is required to identify if there are any specific applications suitable for the product profile identified, and whether the volume of production/market for these specific applications offers some commercial potential.
- **Replacement of alternative materials:** The focus has been predominantly on determining the applicability of DPR product for applications in which wrought titanium is used. The possibility of replacing a different metal with a DPR titanium product has not been investigated. The margin of cost reduction needed to justify the selection of titanium, in place of other materials, would need to be identified. This could improve the range of potential product applications.
- **Performance of Ti-6Al-4V DPR product:** Since the dataset for DPR Ti-6Al-4V strip is very small, additional research is required to confirm the performance of the final product, which has not yet demonstrated properties comparable to typical wrought product. Optimization of oxygen content, microstructure, homogenization and pore size in Ti-6Al-4V DPR strip may improve elongation, such that it achieves more than just the minimum ASTM specification, as currently seen in the small data set.
- **Weldability of PM product:** The body of work regarding the weldability of PM product is very limited. Du Pont's assertion that <0.005 wt% chlorine is required for adequate weldability needs to be confirmed, as the original research is not in the public domain (instead a report referencing the work has been extensively cited).
- **Oxygen control:** The cost implications of the measures required to minimize final oxygen content to within the lower limit of the PM range identified in this research (0.16 wt%) needs to be assessed. 0.16 wt% oxygen is closer to the middle of the range of typical oxygen values for grade 2 product. Achieving this, at reasonable cost, may improve the range of product applications for DPR strip.

References

[1] J. A. Ober, "Mineral Commodity Summaries 2017," *US Geological Survey & Orienteering*. p. 202, 2017.

[2] D. S. Van Vuuren, "Keynote address : Titanium — an opportunity and challenge for South Africa," *7th Int. heavy Miner. Conf. South. African Inst. Min. Metall.*, 2009.

[3] S. J. Oosthuizen, "Titanium: the innovators' metal -Historical case studies tracing titanium process and product innovation," *J. South African Inst. Min. Metall.*, vol. 111, no. 11, pp. 781–786, 2011.

[4] Department of Mineral Resources RSA, "A beneficiation strategy for the minerals industry of South Africa," no. June. pp. 1–23, 2011.

[5] D. S. Van Vuuren, S. J. Oosthuizen, and M. D. Heydenrych, "Titanium production via metallothermic reduction of TiCl4 in molten salt: problems and products," *J. South. African Inst. Min. Metall.*, vol. 111, no. 3, pp. 141–148, 2011.

[6] W. Du Preez, "Beneficiation of South Africa's Titanium Resource. A Long Term Vision is the Key to Success," *Presentation to the Portfolio Committee on Trade and Industry*, no. October. pp. 1–5, 2014.

[7] R. K. Dube, "Metal strip via roll compaction and related powder metallurgy routes," *Int. Mater. Rev.*, vol. 35, no. 1, pp. 253–292, 1990.

[8] V. A. Duz and V. S. Moxson, "The direct powder rolling process for producing titanium and titanium alloy foils, sheets and plates," *Mater. Sci. Technol. 2005*, no. March, pp. 45–53, 2005.

[9] A. D. Hartman, S. J. Gerdemann, and J. S. Hansen, "Producing lower-cost titanium for automotive applications," *JOM*, vol. 50, no. 9, pp. 16–19, 1998.

[10] W. H. Peter *et al.*, "Titanium sheet fabricated from powder for industrial applications," *Jom*, vol. 64, no. 5, pp. 566–571, 2012.

[11] D. Cantin *et al.*, "Direct Powder Rolling (DPR) of Titanium. Light Metals Flagship," in *Titanium 2010. Orlando, Florida*, 2010, no. October.

[12] V. S. Moxson and V. A. Duz, "Process of direct powder rolling of blended titanium alloys, titanium matrix composites, and titanium aluminides. U.S. Patent No. 7,311,873.," U.S. Patent 7,311,873, 2007.

[13] V. A. Duz, V. S. Moxson, and O. M. Ivasishin, "Powder Metallurgy of Titanium," in *Titanium 2009, Waikoloa, Hawaii, September 13-16*, 2009.

[14] R. Smith, M. Paliwal, and J. Capone, "Paper presented by Ametek-Reading Alloys," 2011. [Online]. Available: http://c.ymcdn.com/sites/www.titanium.org/resource/resmgr/2010_2014_papers/SmithRyan_2011.pdf. [Accessed: 22-Nov-2017].

[15] M. Qian, J. E. Barnes, M. Gibson, and B. Gabbitas, "Powder Metallurgy in Australasia.," *Int. J. Powder Metall.*, vol. 50, no. 2, pp. 39–43, 2014.

[16] G. M. D. Cantin *et al.*, "Innovative consolidation of titanium and titanium alloy powders by direct rolling," *Powder Metall.*, vol. 54, no. 3, pp. 188–192, 2011.

[17] "The TECenter Commercialization Model. Phases, Stages and Steps." [Online]. Available: https://research.boisestate.edu/uiv/files/2013/01/TEC-Commercialization-Process-Model.pdf. [Accessed: 19-Oct-2017].

[18] H. Wang, Z. Zak Fang, and P. Sun, "A critical review of mechanical properties of powder metallurgy titanium," *Int. J. Powder Metall.*, vol. 46, no. 5, pp. 45–57, 2010.

[19] T. Lecompte *et al.*, "Dry granulation of organic powders - Dependence of pressure 2D-distribution on different process parameters," *Chem. Eng. Sci.*, vol. 60, no. 14, pp. 3933–3940, 2005.

[20] G. S. Upadhyaya, *Powder Metallurgy Technology*. Cambridge International Science Publishing, 1997.

[21] O. A. Katrus, “Calculation of processing parameters of powder strip rolling from the apparent density of powders,” *Sov. Powder Metall. Met. Ceram.*, vol. 20, no. 2, pp. 89–94, 1981.

[22] K. Araci, D. Mangabhai, and K. Akhtar, “Production of titanium by the Armstrong Process®,” in *Titanium Powder Metallurgy, Science, Technology and Applications*, 2015, pp. 149–162.

[23] P. K. Samal, “Direct powder rolling of dispersion strengthened metals or metal alloys,” U.S. Patent No. 4,594,217, 1986.

[24] J. H. Tundermann and A. R. E. Singer, “Deformation and densification during the rolling of metal powders,” *Powder Metall.*, vol. 12, no. 23, pp. 219–242, 1969.

[25] J. K. Hong, C. H. Lee, J. H. Kim, J. T. Yeom, and N. K. Park, “Ti strip properties fabricated by powder rolling method,” *Surf. Rev. Lett.*, vol. 17, no. 2, pp. 229–234, 2010.

[26] A. M. Musikhin, “Cold and hot rolling of iron powder,” *Powder Metall. Met. Ceram.*, vol. 20, no. 10, pp. 677–681, 1981.

[27] S. Chikosha, T. C. Shabalala, and H. K. Chikwanda, “Effect of particle morphology and size on roll compaction of Ti-based powders,” *Powder Technol.*, vol. 264, pp. 310–319, 2014.

[28] W. L. Patton, “Metal powder rolling process. U.S. Patent 3,530,210.,” US 3530210 A, 1970.

[29] N. A. Stone, R. Wilson, M. Yousuff, and M. Gibson, “Titanium flat product production. U.S. Patent No. 8,790,572.,” US 8790572 B2, 2014.

[30] K. A. Gogaev *et al.*, “Mechanical properties of powder titanium at different production stages . V . Properties of a titanium strip produced by powder rolling,” *Powder Metall. Met. Ceram.*, vol. 48, no. 11, pp. 652–658, 2009.

[31] D. H. Ro, M. W. Toaz, and V. S. Moxson, “The direct powder-rolling process for producing thin metal strip,” *JOM J. Miner. Met. Mater. Soc.*, vol. 35, no. 1, pp. 34–39, 1983.

[32] N. K. Park, C. H. Lee, J. H. Kim, and J. K. Hong, “Characteristics of powder-rolled and sintered sheets made from HDH Ti powders,” *Key Eng. Mater.*, vol. 520, no. March 2016, pp. 281–288, 2012.

[33] K. A. Gogaev, V. S. Voropaev, G. Y. Kalutskii, Y. N. Podrezov, D. G. Verbilo, and O. S. Koryak, “Production of titanium powder sheets by asymmetric rolling,” *Powder Metall. Met. Ceram.*, vol. 51, no. 9–10, pp. 509–517, 2013.

[34] G. M. D. Cantin *et al.*, “Production of Ti-6Al-4V Strip by Direct Rolling of Blended Elemental Powder.,” *Mater. Sci. Forum*, vol. 654, pp. 807–810, 2010.

[35] Y. Zhang, “A study of direct powder rolling route for CP-titanium,” Diss. University of Cape Town, 2015.

[36] C. Doblin, D. Cantin, and S. Gulizia, “Processing TiROTM powder for strip production and other powder metallurgy applications,” in *TiDA International Titanium Powder Processing Conference*, 2013.

[37] M. V. Mal’tsev, “Investigation of metal powder rolling,” *Powder Metall. Met. Ceram.*, vol. 10, no. 6, pp. 445–448, 1971.

[38] O. A. Katrus and A. I. Otrok, “Compactibility of metal powders in rolling,” *Sov. Powder Metall. Met. Ceram.*, vol. 10, no. 8, pp. 623–627, 1971.

[39] G. A. Vinogradov, “Method of calculating the density and thickness of porous rolled strip,” *Powder Metall. Met. Ceram.*, vol. 2, no. 3, pp. 356–360, 1963.

[40] V. P. Katashinskii, “Effect of roll diameter on the energy and force parameters of metal powder rolling,” *Powder Metall. Met. Ceram.*, vol. 19, no. 1, pp. 16–19, 1980.

[41] E. B. Lozhechnikov, L. A. Rapoport, A. P. Selemenev, S. S. Shumskii, and S. V. Yurkov, “Rolling of thin strip from powder,” *Powder Metall. Met. Ceram.*, vol. 24, no. 8, pp. 610–612, 1985.

[42] J. M. Rowe, J. R. Crison, T. J. Carragher, N. Vatsaraj, R. J. Mccann, and F. Nikfar, “Mechanistic insights

into the scale-up of the roller compaction process: A practical and dimensionless approach," *J. Pharm. Sci.*, vol. 102, no. 10, pp. 3586–3595, 2013.

[43] G. Reynolds, R. Ingale, R. Roberts, S. Kothari, and B. Gururajan, "Practical application of roller compaction process modeling," *Comput. Chem. Eng.*, vol. 34, no. 7, pp. 1049–1057, 2010.

[44] S. Yu, "Roll compaction of pharmaceutical excipients. Diss.," The University of Birmingham, 2013.

[45] M. Balicki, "Numerical Methods for Predicting Roll Press Powder Compaction Parameters," *Ec. Des Mines D'Albi-Carmaux.*, 2003.

[46] S. Yu, B. Gururajan, G. Reynolds, R. Roberts, M. J. Adams, and C. Y. Wu, "A comparative study of roll compaction of free-flowing and cohesive pharmaceutical powders," *Int. J. Pharm.*, vol. 428, no. 1–2, pp. 39–47, 2012.

[47] J. R. Johanson, "A Rolling Theory for Granular Solids," *Trans. ASME*, pp. 842–848, 1965.

[48] J. C and J. C. Cunningham, "Experimental studies and modeling of the roller compaction of pharmaceutical powders," Drexel University, 2005.

[49] G. Bindhumadhavan, J. P. K. Seville, M. J. Adams, R. W. Greenwood, and S. Fitzpatrick, "Roll compaction of a pharmaceutical excipient: Experimental validation of rolling theory for granular solids," *Chem. Eng. Sci.*, vol. 60, no. 14, pp. 3891–3897, 2005.

[50] K. Sommer and G. Hauser, "Flow and compression properties of feed solids for roll-type presses and extrusion presses," *Powder Technol.*, vol. 130, no. 1–3, pp. 272–276, 2003.

[51] J. C. Cunningham, D. Winstead, and A. Zavaliangos, "Understanding variation in roller compaction through finite element-based process modeling," *Comput. Chem. Eng.*, vol. 34, no. 7, pp. 1058–1071, 2010.

[52] M. Fayed and L. Otten, "Size enlargement by agglomeration," in *Handbook of Powder Science & Technology*, Springer Science & Business Media., 2013, p. 352.

[53] G. M. D. Cantin and M. A. Gibson, "Titanium sheet fabrication from powder," *Titan. Powder Metall. Sci. Technol. Appl.*, pp. 383–403, 2015.

[54] R. F. Mansa, "Roll Compaction of Pharmaceutical Excipients and Prediction Using Intelligent Software. July Issue," University of Birmingham 2007 PhD thesis, 2006.

[55] N. Souihi *et al.*, "Roll compaction process modeling: Transfer between equipment and impact of process parameters," *Int. J. Pharm.*, vol. 484, no. 1–2, pp. 192–206, 2015.

[56] M. Bi, F. Alvarez-Nunez, and F. Alvarez, "Evaluating and modifying Johanson's rolling model to improve its predictability," *J. Pharm. Sci.*, vol. 103, no. 7, pp. 2062–2071, 2014.

[57] B. A. Patel, M. J. Adams, N. Turnbull, A. C. Bentham, and C. Y. Wu, "Predicting the pressure distribution during roll compaction from uniaxial compaction measurements," *Chem. Eng. J.*, vol. 164, no. 2–3, pp. 410–417, 2010.

[58] A. M. Musikhin, "Elastic aftereffect in the cold rolling of porous metal strip," *Powder Metall. Met. Ceram.*, vol. 17, no. 7, pp. 503–506, 1978.

[59] A. Michrafy, H. Diarra, J. A. Dodds, M. Michrafy, and L. Penazzi, "Analysis of strain stress state in roller compaction process," *Powder Technol.*, vol. 208, no. 2, pp. 417–422, 2011.

[60] R. T. Dec, A. Zavaliangos, and J. C. Cunningham, "Comparison of various modeling methods for analysis of powder compaction in roller press," *Powder Technol.*, vol. 130, no. 1–3, pp. 265–271, 2003.

[61] P. Guigon and O. Simon, "Roll press design - Influence of force feed systems on compaction," *Powder Technol.*, vol. 130, no. 1–3, pp. 41–48, 2003.

[62] K. Schönert and U. Sander, "Shear stresses and material slip in high pressure roller mills," *Powder Technol.*, vol. 122, no. 2–3, pp. 136–144, 2002.

[63] M. G. Herting and P. Kleinebudde, “Studies on the reduction of tensile strength of tablets after roll compaction/dry granulation,” *Eur. J. Pharm. Biopharm.*, vol. 70, no. 1, pp. 372–379, 2008.

[64] A. R. Muliadi, J. D. Litster, and C. R. Wassgren, “Validation of 3-D finite element analysis for predicting the density distribution of roll compacted pharmaceutical powder,” *Powder Technol.*, vol. 237, no. February, pp. 386–399, 2013.

[65] Z. Liu, M. J. Bruwer, J. F. MacGregor, S. S. S. Rathore, D. E. Reed, and M. J. Champagne, “Scale-up of a pharmaceutical roller compaction process using a joint-Y partial least squares model,” *Ind. Eng. Chem. Res.*, vol. 50, no. 18, pp. 10696–10706, 2011.

[66] V. V. Nesarikar, C. Patel, W. Early, N. Vatsaraj, O. Sprockel, and R. Jerzweski, “Roller compaction process development and scale up using Johanson model calibrated with instrumented roll data,” *Int. J. Pharm.*, vol. 436, no. 1–2, pp. 486–507, 2012.

[67] A. R. Muliadi, J. D. Litster, and C. R. Wassgren, “Modeling the powder roll compaction process: Comparison of 2-D finite element method and the rolling theory for granular solids (Johanson’s model),” *Powder Technol.*, vol. 221, pp. 90–100, 2012.

[68] K. A. Gogaev, G. Y. Kalutskii, and V. S. Voropaev, “Asymmetric rolling of metal powders. I. Compactability of metal powders in asymmetric rolling,” *Powder Metall. Met. Ceram.*, vol. 48, no. 3–4, pp. 152–156, 2009.

[69] G. S. Upadhyaya, “Metal Powder Compaction,” in *Powder metallurgy technology*, Cambridge International Science Pub, 1997, p. 65.

[70] R. Angelo, P. C., & Subramanian, “Compaction of metal powders,” in *Powder Metallurgy: Science, Technology and Applications*, PHI Learning Pvt. Ltd., 2008.

[71] L. J. AH and V. Silins, “Process for producing elongated continuous bars and rods from metal powders,” U.S. Patent No. 3,389,993, 1965.

[72] P. Zhang, S. X. Li, and Z. F. Zhang, “General relationship between strength and hardness,” *Mater. Sci. Eng. A*, vol. 529, no. 1, pp. 62–73, 2011.

[73] P. T. J. Bex and L. Willem, “Method of manufacturing wires from compacted metal tapes,” U.S. Patent 3,324,541, 1967.

[74] C. R. Shakespeare, “The economics of stainless-steel strip production by roll compaction,” *Powder Metall.*, vol. 11, no. 22, pp. 379–399, 1968.

[75] I. Davies, W. M. Gibbon, and A. G. Harris, “Thin Steel Strip from Powder,” *Powder Metall.*, vol. 11, no. 22, pp. 295–313, 1968.

[76] M. Blore, V. Silins, S. Romanchuk, and T. Benz, “Pure nickel strip by powder rolling,” 1965.

[77] N. A. Stone, R. Wilson, M. Yousuff, and M. Gibson, “Titanium flat product production,” U.S. Patent No. 8,790,572., 2014.

[78] D. T. Marlowe *et al.*, “Method of manufacturing flat forms from metal powder and product formed therefrom,” U.S. Patent No. 4,743,512., 1987.

[79] P. E. Evans, “The Mechanism of the Compaction of Metal Powders by Rolling,” in *New Methods for the Consolidation of Metal Powders*, 1967, p. 99.

[80] “Titanium : Past, Present, and Future. National Research Council.” 1983.

[81] W. S. Wartel, R. J. Wasilewski, and W. I. Pollock, “Metal production,” U.S. Patent 3,084,042., 1963.

[82] D. Eylon, P. R. Smith, S. W. Schwenker, and F. H. Froes, “Status of titanium powder metallurgy,” *Ind. Appl. Titan. Zircon. Third Conf.*, pp. 48–65, 1984.

[83] I. M. Robertson and G. B. Schaffer, “Some effects of particle size on the sintering of titanium and a master sintering curve model,” *Metall. Mater. Trans. A Phys. Metall. Mater. Sci.*, vol. 40, no. 8, pp. 1968–1979,

2009.

[84] F. H. Froes, D. Eylon, G. E. Eichelman, and H. M. Burte, “Developments in titanium powder metallurgy,” *JOM*, vol. 32, no. 2, pp. 47–54, 1980.

[85] J. C. Withers, F. Cardarelli, J. P. Laughlin, and R. O. Loutfy, “Recent improvements for electrowinning titanium metal from composite anodes. International round table on titanium production in molten salts.,” 2008.

[86] I. Mellor and G. Doughty, “Novel and emerging routes for titanium powder production - an overview,” *Key Eng. Mater.*, vol. 704, no. August, p. 271, 2016.

[87] B. Dutta and F. H. Froes, *Additive manufacturing of titanium alloys : state of the art, challenges and opportunities*. Butterworth-Heinemann., 2016.

[88] S. Kosemura, E. Fukasawa, S. Ampo, T. Shiraki, and T. Sannohe, “Technology trend of titanium sponge and ingot production,” *Nippon Steel Technical Report.*, no. 85. pp. 31–35, 2002.

[89] M. Qian, “Cold compaction and sintering of titanium and its alloys for near-net-shape or preform fabrication,” *Int. J. powder Metall.*, vol. 46, no. 5, pp. 29–44, 2010.

[90] S. J. Gerdemann, “Titanium Process Technologies,” *Adv. Mater. Process.*, 2001.

[91] V. A. Duz, O. M. Ivasishin, V. S. Moxson, D. G. Savvakin, and V. V. Telin, “Cost-effective titanium alloy powder compositions and method for manufacturing flat or shaped articles from these powders,” US 20090252638 A1, 2007.

[92] F. Cardarelli, *Materials Handbook: A Concise Desktop Reference*. Springer Science & Business Media, 2008.

[93] Y. Liang and Y. Wu, “Methods To Prepare Spherical Titanium Powders and Investigation on on Spheroidization of HDH Titanium Powders,” in *Proceedings of the 13th World Conference on Titanium*, 2016.

[94] W. H. Peter *et al.*, “Current Status of Ti PM: Progress, Opportunities and Challenges,” *Key Eng. Mater.*, vol. 520, no. November 2015, pp. 1–7, 2012.

[95] R. Machaka and H. K. Chikwanda, “An experimental evaluation of the Gerdemann–Jablonski compaction equation,” *Metall. Mater. Trans. A Phys. Metall. Mater. Sci.*, vol. 46, no. 5, pp. 2194–2200, 2015.

[96] M. J. Donachie, “Titanium: A Technical Guide, 2nd Edition. Introduction to selection of titanium alloys,” *ASM Int.*, vol. 180, pp. 5–11, 2000.

[97] C. G. McCracken, C. Motchenbacher, and D. P. Barbis, “Review of titanium powder production methods,” *Int. J. Powder Metall.*, vol. 46, no. 5, 2010.

[98] I. A. Mwamba and L. H. Chown, “The use of titanium hydride in blending and mechanical alloying of Ti-Al alloys,” *J. South. African Inst. Min. Metall.*, vol. 111, no. 3, pp. 159–165, 2011.

[99] V. Duz, M. Matviychuk, A. Klevtsov, and V. Moxson, “Industrial application of titanium hydride powder,” *Met. Powder Rep.*, vol. 72, no. 1, pp. 30–38, 2017.

[100] O. Ivasishin and V. Moxson, “Low-cost titanium hydride powder metallurgy,” in *Titanium Powder Metallurgy, Science, Technology and Applications*, Butterworth-Heinemann, 2015, pp. 124–128.

[101] N. R. Moody, W. M. Garrison, J. E. Smugeresky, and J. E. Costa, “The role of inclusion and pore content on the fracture toughness of powder-processed blended elemental titanium alloys,” *Metall. Trans. A*, vol. 24, no. 1, pp. 161–174, 1993.

[102] R. J. Low, M. Qian, and G. B. Schaffer, “Chloride impurities in titanium powder metallurgy - A review,” in *Proc. 12th World Conf. on ‘Titanium*, 2012.

[103] Z. Z. Fang *et al.*, “Powder metallurgy of titanium – past, present, and future,” *Int. Mater. Rev.*, pp. 1–53, 2017.

[104] I. Weiss, D. Eylon, M. W. Toaz, and F. H. Froes, “Effect of isothermal forging on microstructure and fatigue behavior of blended elemental Ti-6Al-4V powder compacts,” *Metall. Trans. A*, vol. 17, no. 3, pp. 549–559, 1986.

[105] Z. Fan, H. J. Niu, B. Cantor, A. P. Miodownik, and T. Saito, “Effect of Cl on microstructure and mechanical properties of in situ Ti/TiB MMCs produced by a blended elemental powder metallurgy method,” *J. Microsc.*, vol. 185, no. 2, pp. 157–167, 1997.

[106] T. Horiya, T. Yamazaki, K. Takahashi, and H. Fujii, “Elimination of surface porosity in Ti-6Al-4V alloy powder compacts,” *Nippon Steel Tech. Rep.*, 1994.

[107] F. H. S. Froes, “A historical perspective of titanium powder metallurgy,” in *Titanium Powder Metallurgy, Science, Technology and Applications*, 2015.

[108] R. J. Low, M. Qian, and G. B. Schaffer, “Sintering of titanium with yttrium oxide additions for the scavenging of chlorine impurities,” *Metall. Mater. Trans. A Phys. Metall. Mater. Sci.*, vol. 43, no. 13, pp. 5271–5278, 2012.

[109] F. H. Sam Froes and M. Qian, “A perspective on the future of titanium powder metallurgy,” *Titan. Powder Metall. Sci. Technol. Appl.*, pp. 602–608, 2015.

[110] S. J. Oosthuizen, “In search of low cost titanium: The fray farthing chen (FFC) cambridge process,” *J. South. African Inst. Min. Metall.*, vol. 111, no. 3, pp. 199–202, 2011.

[111] V. Moxson, O. N. Senkov, and F. H. Froes, “Innovations in titanium powder processing,” *JOM*, vol. 52, no. 5, pp. 24–26, 2000.

[112] T. R. Muth *et al.*, “Causal factors of weld porosity in gas tungsten arc welding of powder-metallurgy-produced titanium alloys,” *JOM*, vol. 65, no. 5, pp. 643–651, 2013.

[113] M. Yan, H. P. Tang, and M. Qian, “Scavenging of oxygen and chlorine from powder metallurgy (PM) titanium and titanium alloys,” *Titan. Powder Metall. Sci. Technol. Appl.*, no. June, pp. 253–276, 2015.

[114] L. E. Jacobsen and A. J. Benish, “Titanium alloy. U.S. Patent No. 8,894,738.,” US 8894738 B2, 2014.

[115] P. Kumar, K. S. Ravi Chandran, F. Cao, M. Koopman, and Z. Z. Fang, “The nature of tensile ductility as controlled by extreme-sized pores in powder metallurgy Ti-6Al-4V alloy,” *Metall. Mater. Trans. A Phys. Metall. Mater. Sci.*, vol. 47, no. 5, pp. 2150–2161, 2016.

[116] A. I. Dekhtyar, O. M. Ivasishin, I. V. Moiseeva, V. K. Prokudina, D. G. Savvakin, and A. E. Sychev, “The mechanical properties of compact titanium produced from titanium hydride powders using self-propagating high-temperature synthesis,” *Powder Metall. Met. Ceram.*, vol. 53, no. 9–10, pp. 549–556, 2015.

[117] E. Baril, L. P. Lefebvre, and Y. Thomas, “Interstitial elements in titanium powder metallurgy: sources and control,” *Powder Metall.*, vol. 54, no. 3, pp. 183–186, 2011.

[118] International Titanium Association, “Titanium — The Infinite Choice,” *International Titanium Association*, 2011. [Online]. Available: http://c.ymcdn.com/sites/www.titanium.org/resource/resmgr/Docs/TiUltimate.pdf.

[119] O. M. Ivasishin, D. G. Savvakin, M. M. Gumenyak, and O. B. Bondarchuk, “Role of surface contamination in titanium PM,” *Key Eng. Mater.*, vol. 520, no. August, pp. 121–132, 2012.

[120] D. P. Barbis, R. M. Gasior, G. P. Walker, J. A. Capone, and T. S. Schaeffer, “Titanium powders from the hydride-dehydride process,” in *Titanium Powder Metallurgy, Science, Technology and Applications*, Elsevier, Waltham, 2015.

[121] W. Chen *et al.*, “Cold compaction study of Armstrong Process® Ti–6Al–4V powders,” *Powder Technol.*, vol. 214, no. 2, pp. 194–199, 2011.

[122] S. El-Soudani, J. Fanning, and M. Harper, “Rolled Product Form Development and Optimization Using Blended-Elemental Powder-Based Billets of Ti-6AL-4V Alloy,” *Proc. Aeromat*, pp. 1–23, 2012.

[123] D. H. Savvakin, M. M. Humenyak, M. V. Matviichuk, and O. H. Molyar, “Role of hydrogen in the process of sintering of titanium powders,” *Mater. Sci.*, vol. 47, no. 5, pp. 651–661, 2012.

[124] S. L. G. Petroni, E. T. Galvani, C. A. A. Cairo, C. C. Girotto, and V. A. R. Henriques, “PM Non-Ferrous and Special Materials: Compaction and Densification Behaviour of Titanium Hydride Powder,” in *European Congress and Exhibition on Powder Metallurgy. European PM Conference Proceedings*, 2014, pp. 1–6.

[125] C. Wang, Y. Zhang, S. Xiao, and Y. Chen, “Sintering densification of titanium hydride powders,” *Mater. Manuf. Process.*, vol. 32, no. 5, pp. 517–522, 2017.

[126] O. M. Ivasishin, D. Eylon, V. I. Bondarchuk, and D. G. Savvakin, “Diffusion during Powder Metallurgy Synthesis of Titanium Alloys,” *Defect Diffus. Forum*, vol. 277, no. July 2015, pp. 177–185, 2008.

[127] A. K. Sachdev, K. Kulkarni, Z. Z. Fang, R. Yang, and V. Girshov, “Titanium for automotive applications: Challenges and opportunities in materials and processing,” *Jom*, vol. 64, no. 5, pp. 553–565, 2012.

[128] C. Cui, B. Hu, L. Zhao, and S. Liu, “Titanium alloy production technology, market prospects and industry development,” *Mater. Des.*, vol. 32, no. 3, pp. 1684–1691, 2010.

[129] I. M. Robertson and G. B. Schaffer, “Review of densification of titanium based powder systems in press and sinter processing,” *Powder Metall.*, vol. 53, no. 2, pp. 146–162, 2010.

[130] D. W. Lee, H. S. Lee, J. H. Park, S. M. Shin, and J. P. Wang, “Sintering of Titanium Hydride Powder Compaction,” *Procedia Manuf.*, vol. 2, no. February, pp. 550–557, 2015.

[131] J. M. Oh, K. H. Heo, W. B. Kim, G. S. Choi, and J. W. Lim, “Sintering Properties of Ti–6Al–4V Alloys Prepared Using Ti/TiH2 Powders,” *Mater. Trans.*, vol. 54, no. 1, pp. 119–121, 2013.

[132] Y. F. Yang and D. K. Mu, “Rapid dehydrogenation of TiH2 and its effect on formation mechanism of TiC during self-propagation high-temperature synthesis from TiH2-C system,” *Powder Technol.*, vol. 249, pp. 208–211, 2013.

[133] Y. Zheng, X. Yao, J. Liang, and D. Zhang, “Microstructures and Tensile Mechanical Properties of Titanium Rods Made by Powder Compact Extrusion of a Titanium Hydride Powder,” *Metall. Mater. Trans. A Phys. Metall. Mater. Sci.*, vol. 47, no. 4, pp. 1842–1853, 2016.

[134] Y. Zhang, C. Wang, Y. Liu, S. Liu, S. Xiao, and Y. Chen, “Surface characterizations of TiH2 powders before and after dehydrogenation,” *Appl. Surf. Sci.*, vol. 410, pp. 177–185, 2017.

[135] O. M. Ivasishin, D. G. Savvakin, V. S. Moxson, and M. M. Gumenyak, “Manufacture of near-net shape titanium alloy articles from metal powders by sintering with presence of atomic hydrogen. U.S. Patent Application No. 14/584,176.,” US 20150328684 A1, 2015.

[136] O. M. Ivasishin, D. G. Savvakin, V. A. Duz, M. V. Matviychuk, and V. S. Moxson, “Extra low impurity content powder metallurgy titanium and titanium alloys,” *Titan. 2012*, no. 1, 2012.

[137] “Hamilton Precision Metals. Technical data Titanium CP Gr 1 and 2.” [Online]. Available: http://www.hpmetals.com/documentlibrary/titanium. [Accessed: 20-Oct-2017].

[138] W. F. Gale and T. C. Totemeier, “Mechanical properties of titanium and titanium alloys,” in *Smithells Metals Reference Book*, Butterworth-Heinemann, 2003.

[139] P. Paramore, J. D., Fang, Z. Z., & Sun, “Hydrogen sintering of titanium and its alloys,” in *Titanium Powder Metallurgy, Science, Technology and Applications*, 2015.

[140] M. Yan, M. S. Dargusch, T. Ebel, and M. Qian, “A transmission electron microscopy and three-dimensional atom probe study of the oxygen-induced fine microstructural features in as-sintered Ti-6Al-4V and their impacts on ductility,” *Acta Mater.*, vol. 68, pp. 196–206, 2014.

[141] H. Miura, T. Osada, and Y. Itoh, “Metal Injection Molding (MIM) Processing,” in *Advances in Metallic Biomaterials*, Springer Berlin Heidelberg, 2015, pp. 27–56.

[142] T. Ebel, O. Milagres Ferri, W. Limberg, M. Oehring, F. Pyczak, and F. P. Schimansky, “Metal injection

moulding of titanium and titanium-aluminides," *Key Eng. Mater.*, vol. 520, pp. 153–160, 2012.

[143] Y. Fan, P. H. Shipway, G. D. Tansley, and J. Xu, "The Effect of Heat Treatment on Mechanical Properties of Pulsed Nd:YAG Welded Thin Ti6Al4V," *Adv. Mater. Res.*, vol. 189, pp. 3672–3677, 2011.

[144] "Properties and Processing of TIMET 6-4 Titanium - Technical Manual." [Online]. Available: http://www.timet.com/assets/local/documents/technicalmanuals/TIMETAL_6-4_Properties.pdf. [Accessed: 12-Nov-2017].

[145] R. M. Buacom, "Strain-rate sensitivity of three titanium-alloy sheet materials after prolonged exposure at 550 degrees F (561 degrees K)," 1969.

[146] W. Huiqiang, F. Jicai, and H. Jingshan, "Microstructure evolution and fracture behaviour for electron beam welding of Ti-6Al-4V," *Bull. Mater. Sci.*, vol. 27, no. 4, pp. 387–392, 2004.

[147] G. Salishchev, O. Valiakhmetov, W. Beck, and S. Froes, "Production of Ti-6Al-4V Sheets for Low Temperature Superplastic Forming," *Mater. Sci. forum*, vol. 551, pp. 31–36, 2007.

[148] C. Köse and E. Karaca, "Robotic Nd:YAG Fiber Laser Welding of Ti-6Al-4V Alloy," *Metals (Basel).*, vol. 7, no. 6, p. 221, 2017.

[149] L. S. Smith, M. Gittos, and P. Threadgill, *Guide to Best Practice, Welding Titanium, A Designers and Users Handbook.* Titanium Information Group, 1999.

[150] "MatWeb Material Property Data -TIMET TIMETAL® 6-4 Titanium Alloy (Ti-6Al-4V; ASTM Grade 5) Sheet." [Online]. Available: http://www.matweb.com/search/datasheet.aspx?matguid=2b38b0d17e284ffcb41a7188f37f2d4e&n=1&ckck=1. [Accessed: 21-Oct-2017].

[151] "Rolled Alloys Inc.- 6Al-4V." [Online]. Available: https://www.rolledalloys.com/alloys/titanium-alloys/6al-4v/en/. [Accessed: 21-Oct-2017].

[152] G. I. Abakumov, V. S. Moxson, V. Duz, M. Matviychuk, and V. Sukhoplyuyev, "Powder Metallurgy Titanium and Titanium Alloy Components Manufactured from Hydrogenated Titanium Powders," in *Titanium 2012 Atlanta, Georgia, USA*, 2012.

[153] P. Lundall, J. Maree, and S. Godfrey, "Research Report Industrial Structure and Skills in the Metals Beneficiation Sector of South Africa," *March Issue.*, p. 14, 2008.

[154] "Metal Suppliers Online." [Online]. Available: http://www.suppliersonline.com/propertypages/6-4.asp#mechanical. [Accessed: 20-Oct-2017].

[155] L. E. Brownell and E. H. Young, "Factors Influencing the Design of Vessels - Economic Considerations," in *Process equipment design : vessel design*, Wiley, 1959.

[156] "BIBUS Metals AG: supplier and problem solver," 2001. [Online]. Available: http://www.stainless-steel-world.net/pdf/ssw0105.pdf. [Accessed: 21-Oct-2017].

[157] W. Knorr and J. Budde, "Influence of processing and heat treatment on the anisotropic properties of sheet and strip of commercially pure titanium," in *Titanium and Titanium Alloys: Scientific and Technological Aspects*, Springer US, Ed. 1982, pp. 1959–1967.

[158] K. Kimura and T. Katayama, "Manufacturing Technologies for Products of Titanium and its Alloys," 2014.

[159] "Jinshan Titanium Sheet Plate Manufacturers, Suppliers and Factory." [Online]. Available: http://www.js-titanium.com/titanium/titanium-sheet-plate.html. [Accessed: 23-Oct-2017].

[160] "Siddhagiri Metals and Tubes. Grade 2 Titanium Sheet." [Online]. Available: http://www.siddhagirimetals.com/titanium-grade-2-sheet-plate-supplier-astm-b265-ti-cp-gr-2-uns-r50400.html. [Accessed: 23-Oct-2017].

[161] J. Beddoes and M. Bibby, *Principles of metal manufacturing processes.* Butterworth-Heinemann, 1999.

[162] F. H. Froes, "Primary Working," in *Titanium: Physical Metallurgy, Processing, and Applications*, ASM

International, 2015.

[163] K. S. Dragolich and N. D. DiMatteo, “Commercially Pure and Modified Titanium,” in *Fatigue Data Book: Light Structural Alloys - ASM International*, 1994, p. 207.

[164] F. H. Froes, H. Friedrich, J. Kiese, and D. Bergoint, “Titanium in the family automobile: The cost challenge,” *Jom*, vol. 56, no. 2, pp. 40–44, 2004.

[165] “V2 CONSULTING LIMITED Titanium and Titanium Alloy Products Catalogue.” [Online]. Available: http://v2cl.com/uploads/3/4/9/3/3493043/v2_consulting_limited_-_titanium_and_alloy_products.pdf. [Accessed: 23-Oct-2017].

[166] M. Ashraf Imam, “The 13th World Conference on Titanium (Ti-2015),” *JOM*, vol. 68, no. 9, pp. 2492–2501, 2016.

[167] D. Mccoy, “The global titanium sponge market review,” in *International Titanium Association; Orlando; USA*, 2015.

[168] M. C. Gabriele, “Structural Changes, Tepid Energy Industry Sector Cause Titanium Scrap Market to Lose its Balance,” *Titanium Today. Aerospace Edition. 3 Qtr. Issue 13. No. 4*, p. 43, 2016.

[169] “An unparalleled investor behind changes in US titanium metal industry | MIRU (Metal-Information-Resources-Universe),” *Metal Information Resources Universe*, 2015. [Online]. Available: https://iru-miru.com/en/article/269. [Accessed: 22-Oct-2017].

[170] “MetalPrices.com.” [Online]. Available: https://www.metalprices.com/index.html. [Accessed: 23-Oct-2017].

[171] AMM staff, “Double trouble for titanium market | American Metal Market,” 2013. [Online]. Available: http://www.amm.com/Article/3266122/Double-trouble-for-titanium-market.html. [Accessed: 23-Oct-2017].

[172] V. Chan and H. Kwong, “Tiangong International (826 HK) - Equity Research,” 2014.

[173] Q. Liu, P. Baker, and H. Zhao, “Titanium Sponge Production Technology in China,” in *Proceedings of the 13th World Conference on Titanium*, 2015, pp. 177–182.

[174] “Argus Minor Metals. Global market prices, news and analysis,” no. 15–34, 2015.

[175] “New Antidumping and Countervailing Duty Petitions on Titanium Sponge from Japan and Kazakhstan | The National Law Review,” 2017. [Online]. Available: https://www.natlawreview.com/article/new-antidumping-and-countervailing-duty-petitions-titanium-sponge-japan-and. [Accessed: 23-Oct-2017].

[176] “World Titanium Industry Supply and Demand Overview - International Titanium Association,” 2016. [Online]. Available: http://www.titanium.org/news/314739/World-Titanium-Industry-Supply--Demand-Overview.htm. [Accessed: 23-Oct-2017].

[177] P. Dewhurst, “Titanium sponge supply: past , present and future,” in *Titanium 2013 October - Las Vegas - Nevada*, 2013.

[178] “Titanium Metal Market Emerges From Past Excesses with More Changes Anticipated - Roskill Information Services,” *Roskill Information Services*, 2017. [Online]. Available: https://roskill.com/news/titanium-metal-market-emerges-past-excesses-changes-anticipated/. [Accessed: 23-Oct-2017].

[179] M. Holz and G. P. Walker, “Ti Facts. International Titanium Association Education Committee.,” 2011.

[180] “Titanium Metal. Global Industry, Markets and Outlook — Market Report — Roskill.” [Online]. Available: https://roskill.com/market-report/titanium-metal/. [Accessed: 23-Oct-2017].

[181] G. M. Bedinger, “Titanium and titanium dioxide,” *USGS Miner. Commod. Summ.*, no. 703, 2016.

[182] “Titanium producers poised for growth,” *Adv. Mater. Process. ASM Int. Oct. Issue.*

[183] “Mineral Commodity Summaries 2005,” *United States Geological Survey*. 2005.

[184] Roskill, *Titanium metal: Market Outlook to 2018*. Roskill Information Services, 2013.

[185] S. Seong, O. Younossi, and B. W. Goldsmith, *Titanium Industrial Base, Price Trends, and Technology Initiatives*. 2009.

[186] W. Xiangdong and L. Fusheng, “Chinese Titanium Industry 2010. Jiahong, Haobin. CTA,” 2010.

[187] “Tiangong International Company. Announcement of the interim results for the six months ended 30 June 2015,” 2015. [Online]. Available: http://www.hkexnews.hk/listedco/listconews/SEHK/2015/0826/LTN201508261219.pdf. [Accessed: 23-May-2017].

[188] D. Chan, W. Li, and H. Ji, “China updates high and new technology enterprise tax rules : 5 key implications. Intellectual Property and Technology Alert,” 2016.

[189] Z. Wuzhuang, “Titanium in China – a rapid rising industry,” 2011. [Online]. Available: http://c.ymcdn.com/sites/www.titanium.org/resource/resmgr/2010_2014_papers/ZouWuzhuang_2011.pdf.

[190] J. Huang, “Baoji Titanium Industry Co., Ltd: Continuous investment = influence,” *StainlessSteelWorld*, 2012.

[191] “Zaporozhye Titanium and Magnesium Combine - ZTMC Got a Right To Supply Titanium Sponge To The Largest Chinese Producer Of Aerospace Products - Company Baoji.” [Online]. Available: http://ztmc.zp.ua/en/press-center/news-ztmk/466-ztmc-got-a-right-to-supply-with-a-titanium-sponge-to-the-largest-chinese-producer-of-aerospace-products-company-baoji. [Accessed: 24-Oct-2017].

[192] R. Cliff, C. J. R. Ohlandt, and D. Yang, “Ready for Takeoff: China’s Advancing Aerospace Industry,” 2011.

[193] Airbus, “Airbus and China to enhance cooperation in aviation and aerospace,” 2017. [Online]. Available: http://www.airbus.com/newsroom/press-releases/en/2017/06/airbus-and-china-to-enhance-cooperation-in-aviation-and-aerospace.html. [Accessed: 24-Oct-2017].

[194] Z. Xin, “Baoji high tech Zone to build a new Chinese titanium Valley,” 2015. [Online]. Available: http://www.yunchtitanium.com/news/baoji-high-tech-zone-to-build-a-new-chinese-ti-792810.html. [Accessed: 29-Nov-2017].

[195] A. Dehghan-Manshadi, M. J. Bermingham, M. S. Dargusch, D. H. StJohn, and M. Qian, “Metal injection moulding of titanium and titanium alloys: Challenges and recent development,” *Powder Technol.*, vol. 319, pp. 289–301, 2017.

[196] D. Whittaker and F. H. S. Froes, “Future prospects for titanium powder metallurgy markets,” in *Titanium Powder Metallurgy, Science, Technology and Applications*, 2015.

[197] “Mineral Commodity Summaries 2009,” *US Geological Survey & Orienteering*. p. 176, 2009.

[198] F. H. Froes, “Titanium Powder Metallurgy: A Review - Part 1,” *Adv. Mater. Process.*, vol. 170, no. 9, pp. 16–23, 2012.

[199] J. Dawes, R. Bowerman, and R. Trepleton, “Introduction to the Additive Manufacturing Powder Metallurgy Supply Chain,” *Johnson Matthey Technol. Rev.*, vol. 59, no. 3, pp. 243–256, 2015.

[200] “Titanium Europe 2016 - Executive Summary Report,” in *Titanium Europe 2016 April 18-20*, 2016.

[201] “Powder Metallurgy Review,” *Inovar Communications Ltd*, vol. Autumn, p. 49, 2016.

[202] “Establishment of Titanium Powder Technology for Additive Manufacturing. OSAKA Titanium technologies Co., Ltd. August 18th.” 2016.

[203] “Flying High - End Use Markets,” *Metal Bulletin Magazine*, vol. May, pp. 52–53, 2016.

[204] “Ames team wins award for development of titanium powder manufacturing process,” *Powder Metallurgy Review*. [Online]. Available: http://www.pm-review.com/ames-team-wins-award-development-titanium-powder-manufacturing-process/. [Accessed: 30-Nov-2017].

[205] P. Sun, Z. Z. Fang, Y. Zhang, and Y. Xia, “Review of the Methods for Production of Spherical Ti and Ti Alloy Powder,” *JOM*, vol. 69, no. 10, pp. 1853–1860, 2017.

[206] X. Xu, P. Nash, and D. Mangabhai, “Characterization and Sintering of Armstrong Process Titanium Powder,” *JOM*, vol. 69, no. 4, pp. 770–775, 2017.

[207] Y. Yamamoto, W. H. Peter, and A. S. Sabau, “Low Cost Titanium Near-Net-Shape Manufacturing Using Armstrong Process CP-Ti and Ti-6Al-4V Powders,” *Adv. Powder Met. Part. Mater*, pp. 3–24, 2010.

[208] W. Chen, Y. Yamamoto, and W. H. Peter, “Investigation of Pressing and Sintering Processes of CP-Ti Powder Made by Armstrong Process,” *Key Eng. Mater.*, vol. 436, pp. 123–130, 2010.

[209] Y. Yamamoto, J. O. Kiggans, M. B. Clark, S. D. Nunn, A. S. Sabau, and W. H. Peter, “Consolidation process in near net shape manufacturing of armstrong CP-Ti/Ti-6Al-4V powders,” *Key Eng. Mater.*, vol. 436, pp. 103–111, 2010.

[210] X. Xu and P. Nash, “Sintering mechanisms of Armstrong prealloyed Ti-6Al-4V powders,” *Mater. Sci. Eng. A*, vol. 607, pp. 409–416, 2014.

[211] K. S. Weil, Y. Hovanski, and C. A. Lavender, “Effects of TiCl4 purity on the sinterability of Armstrong-processed Ti powder,” *J. Alloys Compd.*, vol. 473, no. 1–2, 2009.

[212] M. Qian, Y. F. Yang, M. Yan, and S. D. Luo, “Design of Low Cost High Performance Powder Metallurgy Titanium Alloys: Some Basic Considerations,” *Key Eng. Mater.*, vol. 520, pp. 24–29, 2012.

[213] X. Goso and A. Kale, “Production of titanium metal powder by the HDH process,” *J. South. African Inst. Min. Metall.*, vol. 111, no. 3, pp. 203–210, 2011.

[214] M. Qian and G. B. Schaffer, “Sintering of titanium and its alloys.” 2010.

[215] R. M. German, “Progress in titanium metal powder injection molding,” *Materials (Basel).*, vol. 6, no. 8, pp. 3641–3662, 2013.

[216] E. Carreño-Morelli, J.-E. Bidaux, M. Rodríguez-Arbaizar, H. Girard, and H. Hamdan, “Production of titanium grade 4 components by powder injection moulding of titanium hydride,” *Powder Metall.*, vol. 57, no. 2, pp. 89–92, 2014.

[217] B. Bannon and E. Mild, “Titanium Alloys for Biomaterial Application: An Overview,” in *Titanium Alloys in Surgical Implants*, ASTM International, 1983.

[218] “Saetra - Titanium Alloy Ti 6Al-4V Data,” 2000. [Online]. Available: www.cartech.com. [Accessed: 29-Nov-2017].

[219] “Allegheny Ludlum Technical Data Sheet - Corrosion-Resistant Titanium Alloys.” [Online]. Available: http://www.titanmf.com/wp-content/uploads/docs/Titanium-Brochure-ATI.pdf. [Accessed: 12-Nov-2017].

[220] G. Lütjering and J. C. Williams, *Titanium*. Springer Science & Business Media., 2007.

[221] G. Welsch, R. Boyer, and E. W. Collings, *Materials Properties Handbook: Titanium Alloys*. ASM international, 1993.

[222] R. Thomas, “Titanium in the geothermal industry,” *Geothermics*, vol. 32, no. 4, pp. 679–687, 2003.

[223] Y. Zong, P. Liu, B. Guo, and D. Shan, “Springback evaluation in hot v-bending of Ti-6Al-4V alloy sheets,” *Int. J. Adv. Manuf. Technol.*, vol. 76, no. 1–4, pp. 577–585, 2015.

[224] W. Beck, “Superplastic forming and diffusion bonding of titanium and titanium alloys,” in *Titanium and Titanium Alloys: Fundamentals and Applications*, Wiley-VCH, 2003, pp. 273–288.

[225] M. Peters, J. Hemptenmacher, J. Kumpfert, and C. Leyens, “Structure and properties of titanium and titanium alloys,” in *Titanium and titanium alloys : fundamentals and applications*, Wiley-VCH, 2003, pp. 1–36.

[226] “Supra Alloys - Titanium Grades Information - Properties and Applications for all Titanium Alloys & Pure Grades.” [Online]. Available: http://www.supraalloys.com/titanium-grades.php. [Accessed: 13-Nov-2017].

[227] “Alcobra Metals - Titanium Product Guide.” [Online]. Available: https://alcobrametals.com/guides/titanium. [Accessed: 13-Nov-2017].

[228] C. N. Elias, J. H. C. Lima, R. Valiev, and M. A. Meyers, “Biomedical applications of titanium and its alloys,” *JOM*, vol. 60, no. 3, pp. 46–49, 2008.

[229] S. L. Chawla, *Materials Selection for Corrosion Control*. ASM international, 1993.

[230] “AMERICAN ELEMENTS. Titanium Foil.” [Online]. Available: https://www.americanelements.com/titanium-foil-7440-32-6. [Accessed: 15-Nov-2017].

[231] T. Harilal, “Titanium & its Alloys in Aviation,” *Metalword*, no. April, pp. 26–28, 2017.

[232] “Elgiloy Specialty Metals - Strip Products - CP Titanium Grade 1.” [Online]. Available: http://www.elgiloy.com/assets/1/6/Strip_-_Titanium_Grade_1_Ti25.pdf. [Accessed: 12-Nov-2017].

[233] “Nippon Steel and Sumitomo Metal Corporation Catalog - Titanium Products.” [Online]. Available: http://www.nssmc.com/. [Accessed: 12-Nov-2017].

[234] “VAHTERUS Plate & Shell Heat Exchangers.” [Online]. Available: http://www.vahterus.com/Vahterus_esite_EN.pdf. [Accessed: 15-Nov-2017].

[235] J. Mountford, “Titanium – Properties, Advantages and Applications Solving the Corrosion Problems in Marine Service,” *Corros. Pap.*, 2002.

[236] M. Bauccio, *ASM Metals Reference Book, 3rd Edition*. 1993.

[237] “TOAKS Titanium 450ml Cup – TOAKS OUTDOOR.” [Online]. Available: https://www.toaksoutdoor.com/products/cup-450. [Accessed: 15-Nov-2017].

[238] “US Titanium Industry Inc. - Machining, Forming and Welding Technology.” [Online]. Available: http://usa-titanium.com/cp-titanium-tube-for-exhaust-pipe-muffler/. [Accessed: 15-Nov-2017].

[239] “Dedicated Motorsports - Titanium Slip Joint Connector - Aftermarket Performance Upgrades.” [Online]. Available: https://www.dedicatedmotorsports.com/in-titanium-slip-joint-connector-mm-wall-p/105-10203-0000.htm. [Accessed: 14-Nov-2017].

[240] “Uniti Titanium: Seamless Titanium Pipe and Titanium Tubing.” [Online]. Available: http://www.uniti-titanium.com/products/seamless-titanium-tube/. [Accessed: 14-Nov-2017].

[241] “FINE TUBES - Cooling tubes for heat exchangers and condensers for the nuclear, chemical processing and aerospace industry.” [Online]. Available: http://www.finetubes.co.uk/products/applications/cooling-tubes/. [Accessed: 15-Nov-2017].

[242] H. Richaud-Minier, P. Gerard, H. El-Alami, and H. Marchebois, “Super Stainless Steel Welded Tubing Solutions: An Alternative To Titanium Welded Tubing For Seawater-Cooled Heat Exchangers?,” *CORROSION*, 2009.

[243] R. Heidersbach, *Metallurgy and corrosion control in oil and gas production*. John Wiley & Sons, 2013.

[244] “SECTION II ASME Boiler and Pressure Vessel Code An International Code,” no. 1 July. ASME, 2015.

[245] “Mersen Brochure - Pressure Vessels.” [Online]. Available: https://tr.mersen.com/uploads/tx_mersen/B05_3_E_Brochure_Pressure_vessels_05.pdf. [Accessed: 15-Nov-2017].

[246] D. J. Schumerth, “Thin-Wall Titanium Condenser Tubing: The Next Plateau,” in *2002 International Joint Power Generation Conference*, pp. 129–137.

[247] K. S. Dragolich and N. D. DiMatteo, *Fatigue Data Book: Light Structural Alloys - ASM International*. 1994.

[248] “Flexitallic Gasket Design Criteria.” [Online]. Available: http://www.flexitallic.com/uploads/files/broDesignCriteria.pdf. [Accessed: 13-Nov-2017].

[249] AspenTech, “Aspen Icarus Reference Guide - Icarus Evaluation Engine (IEE) V7.2.” 2010.

[250] C. Leyens and M. Peters, “Non-Aerospace Applications of Titanium and Titanium Alloys,” in *Titanium and titanium alloys : fundamentals and applications*, Wiley-VCH, 2003, pp. 393–422.

[251] C. Gioka, C. Bourauel, S. Zinelis, T. Eliades, N. Silikas, and G. Eliades, “Titanium orthodontic brackets: structure, composition, hardness and ionic release,” *Dent. Mater.*, vol. 20, pp. 693–700, 2004.

[252] C. Veiga, J. P. Devim, and A. J. R. Loureiro, “Properties and applications of titanium alloys: a brief review,” *Rev. Adv. Mater. Sci.*, vol. 32, no. 2, pp. 133–148, 2012.

[253] “Specialty Metals - Titanium - Stainless - Exotic Catalogue,” 2015. [Online]. Available: http://www.specialtymetals.com.au/uploads/5/3/6/6/53662743/specialty-metals-brochure-hd-2015-v5.pdf. [Accessed: 13-Nov-2017].

[254] D. Southall and S. J. Dewson, “Innovative Compact Heat Exchangers,” *Group*. 2010.

[255] “Ti-TEK (UK) Limited - Titanium Grades, Aluminium Alloys and Titanium Grading.” [Online]. Available: https://titek.co.uk/grades-of-titanium/. [Accessed: 15-Nov-2017].

[256] Sandvik, “Sandvik Datasheet - Ti Grade 3 (Tube and pipe, seamless).”

[257] K. Thulukkanam, *Heat Exchanger Design Handbook*. CRC Press, 2013.

[258] M. Zhan, K. Guo, and H. Yang, “Advances and trends in plastic forming technologies for welded tubes,” *Chinese J. Aeronaut.*, vol. 29, no. 2, pp. 305–315, 2016.

[259] I. Polmear, D. StJohn, J. F. Nie, and M. Qian, *Light alloys : metallurgy of the light metals*. Butterworth-Heineman, 2017.

[260] V. Burt, “Designing for Corrosion Control and Prevention,” in *Corrosion in the Petrochemical Industry, Second Edition*, ASM International, 2015.

[261] “VSMPO Tirus - Titanium Supplier - Titanium Products.” [Online]. Available: http://www.vsmpo-tirus.co.uk/products_custom_manufacturing.php. [Accessed: 15-Nov-2017].

[262] “Lytron Total Thermal Solutions. Lightweight Titanium Heat Exchangers.” [Online]. Available: http://www.lytron.com/Tools-and-Technical-Reference/Application-Notes/Lightweight-Titanium-Heat-Exchangers. [Accessed: 15-Nov-2017].

[263] R. Smith, B. Fichera, and J. O’Leary, “The fabrication of brazed, lightweight titanium plate-fin heat exchangers for aircraft application.,” in *Proceedings of the 3rd International Brazing and Soldering Conference*, 2006, pp. 310–316.

[264] M. Navarro, A. Michiardi, O. Castaño, and J. A. Planell, “Biomaterials in orthopaedics,” *J. R. Soc. Interface*, vol. 5, no. 27, pp. 1137–1158, 2008.

[265] “Professional Plastics - Titanium Products.” [Online]. Available: https://www.professionalplastics.com/TITANIUM. [Accessed: 15-Nov-2017].

[266] A. Fink, B. Kolesnikov, and H. Wilmes, “Hybrid Titanium Composite Material Improving Composite Structure Coupling,” *20th AAAF Colloq.*, no. January, pp. 1–12, 2003.

[267] V. Venkatesh and R. R. Boyer, “Recent Advances in Titanium Technology in the USA,” in *Proceedings of the 13th World Conference on Titanium*, 2016, pp. 13–18.

[268] W. A. Gooch and M. Burkins, “The Design and Application of Titanium Alloys to US Army Platforms.” The Design and Application of Titanium Alloys to US Army Platforms, 2008.

[269] “Ametek - Technical Data Sheet - Ti-6Al-4V ELI.” [Online]. Available: http://www.ametek-ct.com/-/media/ametekct/pdf/technical literature/ti 6al 4v eli.pdf. [Accessed: 15-Nov-2017].

[270] “United performance metals - Data sheet - Ti-6Al-4V ELI.” [Online]. Available: https://www.upmet.com/sites/default/files/datasheets/ti-6al-4v-eli.pdf. [Accessed: 12-Nov-2017].

[271] I. Inagaki, T. Takechi, Y. Shirai, and N. Ariyasu, “Application and features of titanium for the aerospace industry,” *Nippon steel & sumitomo metal technical report*. pp. 22–27, 2014.

[272] A. Fujita, Y. ItsumiI, T. Nakamoto, and K. Yamamoto, “Pre-coated titanium sheet with excellent press formability,” *Featur. - Ⅰ Mater. Process. Technol.*, p. 19.

[273] T. Cassagne, P. Houlle, D. Zuili, P. Bluzat, J. M. Corrieu, and N. Larché, “Replacing Titanium In Sea Water Plate Heat Exchangers,” *Corrosion*. NACE International, 2010.

[274] “Installation And Operation Manual SUPERCHANGER - Plate & Frame Heat Exchanger.” [Online]. Available: www.tranter.com. [Accessed: 15-Nov-2017].

[275] “Vallourec - Brochure: Heat Exchanger Tubes.” [Online]. Available: http://www.vallourec.com/HEATEXCHANGERTUBES/EN/Documents/General Brochure VHET 2014.pdf. [Accessed: 16-Nov-2017].

[276] M. Bloodworth, “HASKEL - Tube expansion issues and methods.” [Online]. Available: http://www.haskel.com/wp-content/uploads/Tube-Expansion-Issues-and-Methods-copy.pdf. [Accessed: 16-Nov-2017].

[277] “Vishal Steel - Heat Exchanger Tube, Boiler Tube, U Bent Tube.” [Online]. Available: http://www.vishalsteelindia.com/seamlesstube-heatexchangertube-ubendtube/pipestubestubing-type-inconel-seamless-heat-exchanger-tube.html. [Accessed: 17-Nov-2017].

[278] “Tube Rolling Motors from Thomas C. Wilson.” [Online]. Available: http://www.tcwilson.com/tube-rolling-motors/. [Accessed: 17-Nov-2017].

[279] “SUGINO. FB Type Tube Expander: Tube Expansion Tool with Curling Function.” [Online]. Available: http://www.sugino.com/site/tube-expanding-tube-end-facing-tool-e/exp-type-fb.html. [Accessed: 17-Nov-2017].

[280] P. Kapranos and R. Priestner, “Review: Overview of metallic materials for heat exchangers for ocean thermal energy conversion systems,” *J. Mater. Sci.*, vol. 22, pp. 1141–1149, 1987.

[281] L. Lunde and M. Seiersten, “Offshore Applications for Titanium Alloys,” in *Titanium and Titanium Alloys: Fundamentals and Applications*, Weinheim, FRG: Wiley-VCH Verlag GmbH & Co. KGaA, 2005, pp. 483–497.

[282] M. A. Greenfield, R. F. Geisendorfer, D. K. Haggard, and L. P. Clark, “Weldability of hot isostatically pressed prealloyed titanium 6AI-4V powder,” *Balance*, vol. 6, no. 4.2, pp. 0–3, 1977.

[283] “Fenn-Torin Laboratory Rolling Mills - Brochure.” [Online]. Available: http://www.fenn-torin.com/wp-content/uploads/115-001-Fenn-Laboratory-Brochure.pdf. [Accessed: 26-Nov-2017].

[284] “Applied measurement technology at MEFOS - Brochure.” [Online]. Available: http://ivf.se/Global/Swerea_MEFOS/Dokument/Publikationer/Broschyrer/applied_measurement_technology.pdf. [Accessed: 26-Nov-2017].

[285] M. Asadi, “Influence of the Hot Rolling Process on the Mechanical Behavior of Dual Phase Steels,” Universitatsbibliothek Clausthal, 2010.

[286] Y. J. Liu, A. K. Tieu, D. D. Wang, and W. Y. D. Yuen, “Friction measurement in cold rolling,” *J. Mater. Process. Technol.*, vol. 111, no. 1, pp. 142–145, 2001.

[287] “Swerea Mefos - Pilot plant equipment.” [Online]. Available: https://www.swerea.se/sites/default/files/publications/pilot_plant_equipment.pdf. [Accessed: 26-Nov-2017].

[288] “FAG OEM und Handel AG - The Design of Rolling Bearing Mountings.” [Online]. Available: http://www.m3.tuc.gr/ANAGNWSTHRIO/STOIXEIA MHXANWN/PDF APO FAG/WL_00200_5_T6-8_de_en.pdf. [Accessed: 26-Nov-2017].

[289] “Sherman International - Machinery Suppliers, Project Coordinators and Engineers - Hot Rolling Mills.” [Online]. Available: http://www.shermanusa.com/Inventory/HRM_-_Hot_Rolling_Mills/HRM_-_Stacked/hrm_-_stacked_40.htm. [Accessed: 26-Nov-2017].

[290] “National Machinery Exchange.” [Online]. Available: http://inv.nationalmachy.com/q/webinv/005700=p,4662,,,b,,,20073391. [Accessed: 26-Nov-2017].

[291] “Cold Rolling Mill | Hero Way.” [Online]. Available: http://hwroller.com/2-3-cold-rolling-mill. [Accessed: 26-Nov-2017].

[292] “Rolling Mill - Quarrell laboratory - Research Centres - Materials Science and Engineering - The University of Sheffield.” [Online]. Available: https://www.sheffield.ac.uk/materials/centresandfacilities/quarrell/rollingmill. [Accessed: 26-Nov-2017].

Appendix A

Patents relating to titanium or titanium alloys are highlighted in colour.

Table 13: Direct powder rolling patents filed to date.

Filing date	Details	Original Assignee	Patent Number
1952	Rolling mill adaptation to control the flow of metal powder for the manufacturing of endless strip and plate.	Hermann Franssen	US 2758336
1955	Production of strips or bands from metal powder (copper)	Friedrich Heck	US 2882554
1956	Direct rolling of non-porous thin strip of 0.1 to 0.2 mm thickness from carbonyl nickel powder.	Int. Nickel Co	US 2889224
1957	Rolling mill adaptation to enable the rolling of nickel strip, with a width greater than 1 inch. Seeks to prevent the forming of frills on the strip edge in subsequent cold rolling.	Int. Nickel Co	US 2922189
1963	Direct rolling of nickel powder to produce strip and sheet of low hardness.	Sherritt Gordon Mines Ltd	US 3268368
1967	The rolling of aluminum strips from powders of different sizes depending on the required thickness of the sheet.	Schloemann Ag	US 3493368
1967	Process for roll-compacting of metal powder with flange lubrication	Aluminum Co Of America, Du Pont	US 3478136
1968	Rolling mill adaptation to minimize metal powder leakage and improve consistency of density and thickness from the middle to the edge of the sheet/strip product. Applied to titanium, aluminum, zinc, lead, stainless steel, tool steel and copper powder.	Du Pont	US 3530210
1970	Controlled and continuous feeding of water-atomized ferrous powders into a powder rolling mill via a vibrating feeder.	Metal Innovations Inc	US 3686376
1985	Manufacturing of dispersion strengthened metal or dispersion strengthened metal alloy.	Scm Corporation	US 4594217
1987	Method of manufacturing flat forms from metal powder and product formed therefrom	Carpenter Technology Corporation	US 4743512
1989	Manufacturing of titanium aluminide foil.	Secretary of the Air Force	US 4917858
2004	Manufacturing of fully dense strips, plates, sheets, and foils from titanium alloys, titanium metal matrix composites, titanium aluminides, and flat multilayer composites.	ADMA Products, Inc.	US 7311873 B2
2008	The feeding of pre-sintered titanium/titanium alloy DPR green product into a pre-heating station, with a protective atmosphere, followed by hot rolling, also under a protective atmosphere.	CSIRO	WO 2008122075 A1
2013	Roll compaction of a molybdenum-based powder followed by sintering and a combination of warm rolling, annealing, and cold rolling.	Ametek, Inc.	US 9238852

Appendix B

Table 14: Sources and dates for titanium DPR data

Source	Authors/Institution	Date
[27]	CSIR – Chikosha et al.	2014
[28]	Du Pont Patent	1970
[25]	South Korea - Jeoung et al.	2010
[32]	South Korea – Park et al.	2012
[30]	Ukraine – Gogaev et al.	2009
[33]	Ukraine – Gogaev et al.	2012
[39]	Ukraine – Vinogradov	1962
[31]	Imperial Clevite	1983
[29]	CSIRO Patent	2014
[34]	CSIRO – Cantin et al.	2010
[35]	UCT – Zhang	2015
Ongoing experimental work	UCT – Naicker	2016
[10]	ORNL – Peter et al.	2012
[12]	ADMA Patent	2006
[22]	CSIRO	2015
[36]	CSIRO	2013
[37]	Ukraine - Mal'tsev	1969
[38]	Ukraine – Katrus et al.	1969

Table 15: 2-high rolling mill specifications used in the mill capability assessment (section 4.2)

Mill details	Roll diameter (mm)	Source
Fenn-torin model: 103 reversing mill	254	[283]
Fenn-torin model: 082 2hi reversing hot & cold rolling mill	200	[283]
2-high mill	240	[284]
12”-2-high laboratory rolling mill	304	[285]
2-high rolling mill	225	[286]
Reversible rolling mill	600	[287]
Three-stand continuous rolling mill	228	[287]
Two-high rolling mill	690	[288]
Mill Type: 2 HI Make Devy united	610	[289]
Carl Wezel combination 2-hi/4-hi reversing cold rolling mill	480	[290]
Cold rolling mills	Various	[291]
Laboratory's rolling mill - Hille 50 mill.	140	[292]